Delft University of Technology

Master Thesis

THE INFLUENCE OF URBAN DESIGN ON MICRO-CLIMATE OF THE FLOATING COMMUNITIES IN THE HOT-TROPICAL REGION OF HAGONOY IN THE PHILIPPINES

Author:
Vaishnavi Yerram
5261619

Graduation committee:
Ir. P. Ham
Dr. Ir. H.R.Schipper
Dr. Ir. M.M.E.van Esch
Dr. Ir. W.H. van der Spoel

A thesis submitted in fulfillment of the requirements for the degree of Master of Sciences

in

Civil Engineering
Building Engineering Track

To be publicly defended on September 13, 2022.

Declaration of Authorship

I, Vaishnavi Yerram
5261619, declare that this thesis titled, "THE INFLUENCE OF URBAN DESIGN ON MICRO-CLIMATE OF THE FLOATING COMMUNITIES IN THE HOT-TROPICAL REGION OF HAGONOY IN THE PHILIPPINES" and the work presented in it are my own. I confirm that:

- This work was done wholly or mainly while in candidature for a research degree at this University.
- Where any part of this thesis has previously been submitted for a degree or any other qualification at this University or any other institution, this has been clearly stated.
- Where I have consulted the published work of others, this is always clearly attributed.
- Where I have quoted from the work of others, the source is always given. With the exception of such quotations, this thesis is entirely my own work.
- I have acknowledged all main sources of help.
- Where the thesis is based on work done by myself jointly with others, I have made clear exactly what was done by others and what I have contributed myself.

Signed: Vaishnavi Yerram

Date: September 12, 2022

"Sometimes science is more art than science, Morty."

Rick Sanchez

Abstract

According to the Intergovernmental Panel on Climate Change (IPCC) 's 2021 report, the recent sea level rate has nearly tripled in the last few decades compared with 1901-1971 [80]. It estimates that the sea levels may rise by 20 cm in the next thirty years or up to 80 cm by the end of 2100. The increase in sea levels poses serious questions and challenges to the housing infrastructure in flood-prone areas. Two locations that have been severely affected by the tidal and fluvial floods and typhoons are the provinces of Bulacan and Pampanga in the Philippines region. There is a ground level subsidence of up to 5cm per year because of the uncontrolled ground-water level conditions prevalent worsening the floods [14]. The high levels of stagnant waters causes unsanitary conditions in these areas.

In 2017, Pieter Ham, co-founder of Finch Floating Homes, developed a floating house model suitable for the Philippines' climatic conditions. After the prototype construction was proven successful, they are now venturing into creating a floating neighborhood in Hagonany, located on the island of Luzon. My research topic aims to study the urban physics context of the floating homes neighborhood.

Alazne Enchaniz Jurado, as part of her master thesis in 2021 at Delft University of Technology, designed resilient coastal neighborhoods for the city of Hagonoy, Philippines [17]. After extensive research on the geographical, social, and cultural context, she designed floating neighborhood models suiting the needs and requirements of the people. However, the urban physics parameters of these concepts are to be further studied to determine the thermal and wind comfort of the occupants in the outdoor areas. This is because of the high-temperature tropical climate present in that region. Therefore, the primary focus of the present project, this MSc thesis, is to understand the role of urban physics in floating community development. It focuses on the influence of vegetation and urban form configurations on the outdoor thermal comfort and outdoor wind comfort of the open spaces, as they serve as the primary gathering locations for the residents. After analyzing the results, it concludes that increasing vegetation decreases the daytime temperatures, thereby improving the comfortability index. Additionally, the urban form also significantly plays a role in influencing the micro-climate of the region.

Acknowledgements

This report titled *"The influence of urban design on the micro-climate of the floating communities in the hot-tropical region of Hagonoy in The Philippines."* was written to complete the Building Engineering program's graduation requirements at the Delft University of Technology. This report presents the journey I have undertaken for the past nine months and is also the final step in completing my journey as a Masters's student. This project stems from my motivation to contribute to the disaster resilient and social housing sector, which has been my driving force since its inception. This was only possible with the support of several people, and I would like to express my deepest gratitude to all of them.

Firstly, I would like to express my sincere gratitude to all the members of my graduate committee. They have mentored me and supported me throughout the thesis. I want to thank my supervisor, **Ir. P. (Pieter) Ham**, who has been my guiding block from the very beginning. By consistently supporting me with his motivating words and reassurances, he has pushed me to work in the right direction. The passion that he shares for this project has resonated deeply within me as well. His mentorship was a truly valuable asset. Secondly, I would like to thank my graduation committee chair **Dr. Ir. H.R. (Roel) Schipper**. He was the first person to greet us into the Masters's program two years ago, has been prompt with all my problems throughout the years, and has also counseled me to create this project and throughout its journey till the very end. I am grateful for his constant support and eagerness to help, which immensely helped the project's smooth functioning. Thirdly, I would like to thank Dr. **Ir. M. M. E. (Marjolein) Pijpers-van Esch** for helping me crack down on the critical phase of the project: the modeling. Even though the entire process was a novice to me, she has mentored me from the basics to any problems I may have encountered along the way. She has truly helped me give shape and structure to this project, and I owe her my sincere thanks. Next, I would like to thank **Dr. Ir. W.H. (Willem) van der Spoel** for helping me understand the working principles of urban physics and for helping me transition from the building to the urban scale. His deep insights and asking the right questions helped me stay on the right track. I would also like to thank **A.A.A. (Abdullah) Aldakheelallah** for helping me kick-start the modeling and simulations and for always being prompt with my queries.

I express my deepest gratitude to my parents and sisters, **Vijay Kumar Yerram, Vanitha Yerram, Sowmya Chanda, and Divya Muriki**, for making this journey possible in the first place. They have constantly supported and encouraged me to pursue my dreams and education, even though it came at the cost of making sacrifices and tough decisions during the coronavirus pandemic. I will always be indebted to them for everything they gave me. I thank my cousin and friends from India, **Raga Anjani Chanda, Nikhila Srinivas, Pradeepthi Thimmapa, Sana Firdous, and Tarun Jairam**, for being the greatest cheerleaders anyone could have ever asked. I thank them for always believing in me and being my constant support system. Finally, the family I have created away from home, **Ajit Sagaram, Daniel Núñez, Dirk-Jan Rosenmuller, Pranathi Srikrishna, and Rathish Gupta**. I thank them for literally everything they have done and been for me in the past two years, for being there through all the ups and downs, and for helping me create beautiful memories. I could not have asked for a better set of people, and I owe many thanks to them all. . . .

Contents

List of Figures

List of Tables

List of Abbreviations

UMC	**U**rban **M**icro **C**limate
UHI	**U**rban **H**eat **I**sland
CFD	**C**omption **F**luid **D**ynamics
PAGASA	**P**hilippine **A**tmospheric, **G**eophysical and **A**stronomical **S**ervices **A**dministration
UBL	**U**rban **B**oundary **L**ayer
UTCI	**U**niversal **T**hermal **C**limate **I**ndex
PET	**P**hysiological **E**quivalent **T**emperature
SET	**S**tandard **E**ffective **T**emperature
RH	**R**elative Humidity **H**umidity
SVF	**S**ky **V**iew **F**actor
UWG	**U**rban **W**eather **G**enerator
MRT	**M**ean **R**adiant **T**emperature

Chapter 1

Introduction

1.1 Context Microclimate

We live in changing and pressing times in terms of climate change. We are witnessing an unprecedented increase in urbanization and industrialization, with a projected statistic of 2/3rd of the population living in urban areas by 2050 [4]. As per the current trends, the center of urbanization has moved to Asia due to its rapid economic growth [7], which can be seen in Figure 1. Such rapid urbanization has created built-environments that are high on energy consumption and deforestation, thereby creating urban micro-climates [81]. A micro-climate can be defined as an area where the climate differs from its surrounding areas in terms of temperatures, rainfall, snow, wind, and air pressure. The larger the micro-climate, the more we can witness its impact [1]. The urban-microclimates are dependent on the meteorological conditions and the morphological conditions, such as urban density, building form, vegetation, and building orientation [82]. They usually create urban heat islands, a type of microclimate that is warmer than its surrounding areas.

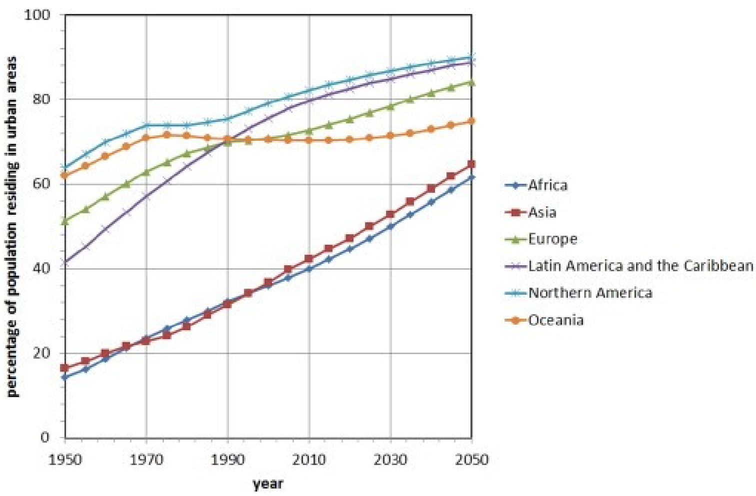

FIGURE 1.1: Population percentage residing in urban areas 1950-2050 [8]

The anthropogenic heat generated in the built environment is also attributed to various factors such as land cover changes, land use, and building performance. The heat increase affects the building energy performance and the inhabitants' comfort levels [2]. Many research studies thereon showed that the increased urban heat generation causes an energy penalty, thereby increasing the annual energy demand of the buildings [3]. It is predicted that global energy consumption will increase by 22 percent to 46 percent by 2060 [5]. Without effective countermeasures at an urban scale, the energy demand will increase over time.

The urban micro-climates, or UMCs, are primarily assessed by the urban thermal comfort, wind comfort, and urban energy demand. This depends on various factors, including natural, in-direct, and built environments, as shown in Figure 3, with the temperature being one of the most critical parameters in UMC research [9]. However, this research's scope is limited to available meteorological data, building characteristics, greenery, and the developed urban model by Alazne Jurado, as mentioned previously.

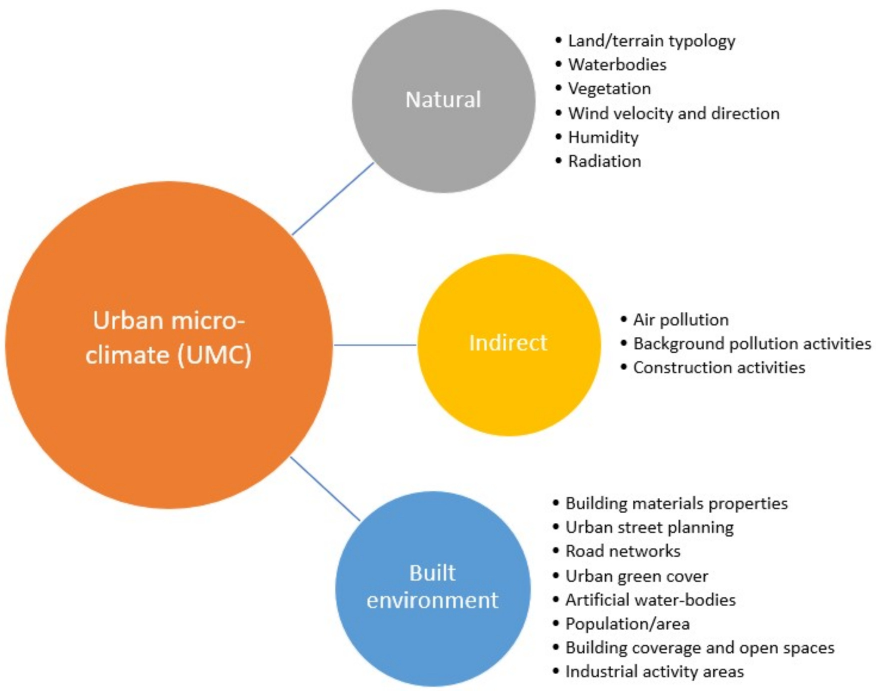

FIGURE 1.2: Factors affecting urban microclimate (Modified from [9])

There is an increasing need to study the climate principles to develop energy-efficient and sound urban models. However, despite the many advancements made in this sector, a communication gap exists between the climatologist and designers. This is because of the lack of awareness of the other fields. Most urban areas also lack the appropriate climate data for modeling and analysis [6]. The guidelines and tools for this purpose are also scarce and not readily available. There is a need for an integrated approach to studying the micro-climate and its influence on energy demand. This research aims to study the appropriate integrated micro-climate models and simulations and their application to the case study of the early urban design floating homes community model in Hagonoy in The Philippines.

FIGURE 1.3: Chart explaining why we need urban-microclimate research [Source: Author]

1.2 Context Philippines and Hagonoy

The Philippines, officially known as the Republic of the Philippines, is an archipelagic country in South-East Asia. According to National Mapping and Resource Information (NAMRIA) reports, it consists of 7641 islands. These are divided into three main classes or divisions: Luzon, Visayas, and Mindanao.

According to the forum organized by The Manila Times, the Department of Human Settlements and Urban Development (DHSUD), there is a reported 6.75 million units of housing shortage throughout the country [12]. It is estimated that this number may increase to 22 million units by the end of 2040 if the housing shortage is not addressed correctly [12]. Figure 1 shows an urbanization shift in Asian countries, with more and more people migrating to urban lands. This eventually leads to high housing demand with increased prices.

Owing to its geography and development, this region is acutely vulnerable to extreme weather and climatic conditions [10]. This nation suffers from violent typhoons and cyclones [10]. Due to climate change, there has been an increase in floods, heavy rainfalls, and sea level rises [11]. Its geographical location also makes it prone to earthquakes, volcanic eruptions, and other natural disasters [13].

The typhoon Haiyan, also known as Super Typhoon Yolanda, is one of the deadliest tropical cyclones on record and hit The Philippines in 2013, killing at least 6.300 people and displacing 2 million people. However, this nation has recently witnessed storms even deadlier than Typhoon Haiyan [10]. The high number of deaths and displacements is due to the migration of people searching for affordable housing, even if it means moving to a high-risk area [14]. Flood-resilient homes and typhoons are needed to prevent immense damage to livelihood [15].

Pieter Ham, a Ph.D. candidate at the Delft University of Technology, developed a floating house model in collaboration with Finch Floating Homes to combat this problem. After successfully building prototypes, they want to venture into developing a floating community neighborhood in the region of Hagonoy, as shown in Figure 1.4.

FIGURE 1.4: Geographical map showing Hagonoy and Bulacan in the context of The Philippines

Hagonoy is a coastal municipality located in the South-West corner of the Bulacan province and is part of the island group Luzon. It consists of 26 barangays, each with a smaller cluster unit called Purok [16]. Each barangay is considered a socio-economic unit [16] composed of different stakeholders.

A barangay called the 'Mercado' is divided into five main groups. They include aquaculture industry owners, fishing industry, commuters, and workers for group 1 and domestic/social workers who mainly comprise women [17].

FIGURE 1.5: Flooding conditions inside the housing in Hagonoy

FIGURE 1.6: Floating home model prototype

Much like the rest of The Philippines, Hagonoy too deals with the consequences of extreme climatic conditions and growing housing demand. To tackle this issue, Alazne Jurado, as part of her master thesis, under the guidance of Pieter Ham, developed an urban community model for the floating homes for the barangay 'Mercado' as mentioned above. This model is developed based on the neighborhood dynamics, living patterns, and essential and non-essential elements based on the local perspectives received [17]. As part of Horizon 1, 'Expansion of the city plan,' the model is developed to gather 39 families by the end of 2023. The Horizon 3 'Floating Barangay' plan aims to sustain 65 families by 2050 [17].

The micro-climate analysis will be performed for the Mercado Barangay.The climate in this region is characterized as hot, tropical, and maritime. It has a high temperature, high humidity, and high rainfall. The coming chapters will provide more information about the modeling, weather classification and comfort parameters.

This research project was carried out for the duration of nine months, starting from December 2021 to September 2022.

1.3 Problem statement

It is established that the living conditions of the people in the Hagonoy region are not suitable for the changing climactic conditions. To ensure the resilience and comfort of floating homes in this region, several studies and tests have to be conducted to understand the effect of microclimate in planning and construction. Various environmental parameters and characteristics of the location have to be studied. These parameters will be implemented in the proposed urban community model in outdoor thermal and wind comfort. The input parameters for these simulations are vastly collected from the meteorological rural weather data from the official websites, such as Philippine Atmospheric, Geophysical, and Astronomical Services Administration (PAGASA) and other relevant sources. Further improvisations and alternatives are provided based on the results.

1.4 Research objectives

This thesis aims to analyze the urban planning model's urban physics context, as mentioned in the Background. The following research objectives can be categorized based on the requirements:
a) To assess the urban physics context of the floating neighborhood in the hot-tropical climate of the Philippines. The sub-objectives include (Givoni, B., 1992):

- To provide sufficient thermal comfort in urban outdoor spaces
- To provide sufficient pedestrian wind comfort in urban outdoor spaces
- To minimize the heat stress

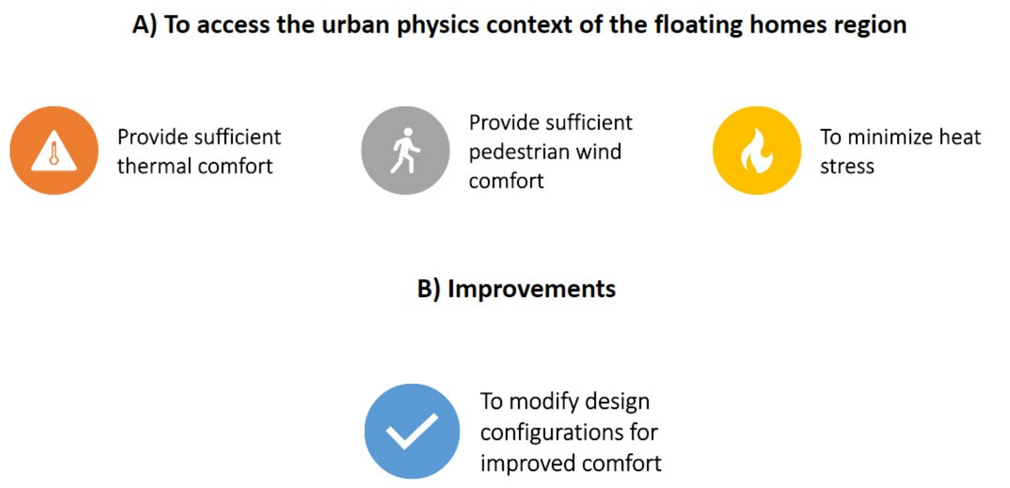

FIGURE 1.7: Research objectives of the thesis

b) To develop improvement strategies to the urban planning models to enhance the overall community efficiency

- To modify design configurations based on optimal comfort

1.5 Research Questions

1.5.1 Main Research Question

From the objectives mentioned earlier, the main research question can be formulated.

"How to provide outdoor thermal and wind comfort in the hot tropical climate of the Philippines for the floating homes community in the Mercado region based on the water-body effect, vegetation and urban design configurations?"

To answer the main research question, it is crucial to define the thermal and wind comfort, the comfort criteria indices, and the inputs required. The modeling requires material properties database for existing and floating home infrastructure. Therefore, site and pilot analyses are studied to obtain the necessary information. Additionally, the influencing parameters considered in this study are the water-body effect, vegetation, and urban form. These parameters significantly affect the surrounding micro-climate. It is essential to understand the relation between these parameters and comfort indices. This is because the alternative scenarios are adjusted based on this relationship to improve performance. Based on this, the following sub-questions are drafted.

1.5.2 Sub-questions

a) Site Analysis: What are the location parameters to be studied?

The urban planning of the existing infrastructure and the floating homes has to be studied in terms of materials, location, height, orientation, and vegetation. Additionally, the presence of water bodies significantly impacts the overall outdoor thermal comfort. This also has to be considered in the analyses to understand the difference in outdoor comfort with and without water bodies. The EPW (EnergyPlus Weather file) provides information regarding the urban air temperature, wind speed, wind direction, radiation, relative humidity, and total sky cover.

b) Thermal comfort: How do we define comfortability for the specific design parameters? How do we improve thermal comfort in outdoor spaces? What parameters need to be studied?

Urban design plays a major role in determining outdoor thermal comfort. This is analyzed from the inputs as mentioned above and tools.

c) Wind comfort: How to assess the pedestrian wind comfort and natural ventilation in the built environment?

Different urban configurations lead to different wind speed conditions. Design details such as the openness and shading spaces, height, and alignment of buildings are usually analyzed for understanding the wind conditions in the area. This research will perform a fundamental outdoor wind comfort analysis through ENVI-met simulations. This is run on computational fluid dynamics (CFD) and determines urban wind patterns.

d) Effect of urban form, water bodies, and vegetation: How is the micro-climate affected by the following parameters?

The urban density requirements keep increasing, and it is important to consider this aspect in urban planning, especially in hot and tropical climates [79]. It reduces the thermal comfort in outdoor spaces [80]. Whereas the waterbody and vegetation may positively impact reducing heat stress.

e) Modelling: How to set up the model and utilize simulation tools?

As mentioned earlier, several simulations are required to obtain the results from the set-ups. The simulations are set-up using the ENVI-met tools, whereas the initial modeling was drafted using Rhinoceros3D and Grasshopper packages. Both the modeling techniques are based on computational fluid dynamics tools.

f) Improvement Strategies: How can the planning be improved with the above-mentioned results? Furthermore, what strategies can be developed?

This analysis is conducted on the urban planning model developed by Alazne Enchaniz Jurado. After obtaining results, improvement strategies will be discussed to reach an optimal design configuration for enhanced comfort.

1.6 Research Methodology

Initially, the site context was studied through openstreetmaps and Google street view maps. The literature related to the pilot project of the floating homes was also extensively studied. Thereafter, the thermal comfort and wind comfort parameters and comfort indices were studied upon. The meteorological data to set-up these simulations is obtained from the Ladybug plug-in in Rhinoceros3D software. The weather data of the Manila region is collected as an EPW file. Since the Manila region is the most extensive database located 50 km away from the Mercado region, this weather data file is chosen. Thereafter, simulations have been set up in ENVI-met, with visualisation in the Leonardo sub-tool. These results were further analysed, and discussed to provide improvements and recommendations.

This workflow has been sub-divided into five steps which is provided below. This is also visually presented in Figure 1.8 :

Step 1: Context and Literature study

- Pilot project: Study the design of the pilot project of floating houses and communities
- Site context: Study the site conditions and attain any location information
- Comfort parameters: Study the various parameters required for establishing occupant comfort, select the parameters to be measured and the model required for simulations.

Step 2: Measurements and Modeling

- Measurements: Obtain all relevant initial information and set up models for the measurements.
- Modelling and Simulations: After setting up the models, various simulations are run to obtain the efficient results

Step 3: Analysis

- Documentation of all the information and simulations, and analysis of the results
- Performance discussions

Step 4: Improvements

- Qualitative and (Quantitative) Improvements: Description of improvement strategies to further optimize the urban design of the floating community

Step 5: Conclusions

- Conclusion: It is expected that after following the steps mentioned above, the main research question and the sub-questions will be answered. At the end of this thesis, it is expected to understand the urban occupant comfort for the floating communities, with improvements and recommendations.

FIGURE 1.8: Research Methodology

1.7 Relevance

This thesis contributes to a much larger plan to improve the housing and living standards of the people in Hagonoy, the Philippines, tackling the environmental and climatic conditions. By performing the urban-microclimate analysis, we can determine the outdoor occupant comfort concerning thermal and wind. This can further be used to provide information about the energy at urban scale and hypothesizes an average energy demand for the community. Based on this, future research can be carried forward to design an autonomous off-grid system for the community based on natural and renewable sources such as installing PV panels. This thesis can also be an application-based guideline for future relevant projects.

1.8 Report Outline

The report has been divided into five Chapters. The first section talks about the introduction and research framework as discussed in Chapter 1. The second Chapter provides a literature survey discussing thermal comfort and wind comfort at an urban scale. This forms the basis and foundation for the analysis to follow. The third Chapter discusses the model development, available and chosen software. Chapter 4 provides information about results and discussions. The final Chapter discusses the conclusions and recommendations for further studies.

Chapter 2

Literature Review

2.1 Outdoor Thermal Comfort

2.1.1 Defining Thermal Comfort

The definition of Thermal comfort is *"that condition of mind which expresses satisfaction with the thermal environment and is assessed by subjective evaluation"* [21][22]. The thermal comfort of an individual varies significantly from person to person depending on several personal and environmental factors, such as culture, acclimation, clothing, human metabolism, and thermal expectations. Since this is based on a person's subjective opinion of their psychological state, two individuals are unlikely to experience the same levels of comfort.

Since it is almost impossible to correctly determine the thermal comfort for everyone, an objective approach that considers the physiological aspects is preferred only. [18] The body must maintain a constant internal temperature performed by the thermoregulatory system. It allows the heat generated by the body's metabolism to dissipate to maintain thermal comfort. This system is quite complex and involves mechanisms such as sweating, vasodilation, vasoconstriction, and thermogenesis to cool the body down or warm it up. They can exchange this heat with the external environment through conduction, radiation, convection, and evaporation [18].

According to the law of conservation of energy, an energy balance can be written, which equates the heat storage to the heat production in the body with a subtraction of the heat loss, as shown in Equation 2.1

$$\delta Q_s = Q_m - (\pm Q^* \pm Q_h + Q_e + Q_g)$$

Equation 2.1

In this equation, the terms are represented as below:

δQ_s ***- Heat storage in the body***

The heat storage must maintain a constant temperature of 37 degrees Celsius. Therefore, this term must constantly be approaching zero [23].

Q_m ***– Heat production in the body***

This value depends on the metabolism generated in the human body. When there is a metabolism increase, additional heat is generated [24]. When metabolism activity reduces, there is a loss of heat. This value is a subtraction of the metabolic rate with the amount of external work done [25].

Q^* - Radiative heat exchange

Radiative heat exchange can be defined as the transfer of heat energy in the form of electromagnetic waves. This transfer occurs through solids, gases, and fluids and does not need matter to travel through. This factor depends on the surface temperature, opposing surface temperature, and emissivity. The emissivity factor is the amount of heat emitted from a material and is 0.9 for most materials. However, this factor comes down to 0.05 for shiny objects [26].

In outdoor situations, radiative heat exchange occurs in both shortwave and longwave radiation with the surroundings. According to Planck's law, objects at high temperatures exhibit more radiation at shorter wavelengths [27].

$$Q^* = \epsilon \sigma T^4$$

Equation 2.2

where,

Q*	radiative heat transfer rate	W
ϵ	emissivity factor	-
σ	Stefan-Boltzmann constant	$5.6x10^-8J/sm^2K^4$
T	absolute temperature	K

h - Convection or sensible heat exchange

Convection can be defined as the heat transfer along the flow of matter. The most significant attribution to the convective heat transfer is due to the convective heat loss from the skin to the external temperature and environment. This can be caused due to internal or external processes like buoyancy forces. Convective heat loss is increased when the speed of the air movement increases; there is a decrease in air temperature and high skin temperature.

$$Q_h = F_{cl} h_{cl} (T_{cl} - t_a)$$

Equation 2.3

where,

Q_h	convective heat exchange	W
F_{cl}	clothing area factor	-
h_{cl}	convective heat transfer coefficient	W/m^2K
T_{cl}	clothed body temperature	K
T_a	ambient temperature	K

***Q_e* - Evaporative heat exchange**

This heat loss can occur through breathing or at the skin surface. The largest share of latent heat transfer is through the heat transfer with the skin surface. The higher the wind speeds, the greater the evaporative heat flux [28]. This is also dependent on the humidity of the air. The more moisture in the air, the slower the evaporation [29].

$$Q_e = \frac{w(p_{sk,s} - p_a)}{R_{cl} + \frac{1}{f_{cl} * h_e}}$$

Equation 2.4

where,

Q_e	evaporative heat exchange	W
w	skin wettedness	percentage
$p_{sk,s}$	skin vapor pressure	kPa
p_a	ambient air vapor pressure	kPa
R_{cl}	evaporative heat transfer resistance of clothing	Km^2/W
f_{cl}	clothing area factor	-
h_e	evaporative heat transfer coefficient	$W/(kPa.m^2)$

***Q_g* - Conductive heat exchange**

Conduction, also known as thermal diffusion, transfers heat energy through microscopic collisions of particles and electron movement inside the body. This occurs between the bodies or boundaries of two different systems. This is negligible or insignificant to the thermal comfort and is usually not considered in the thermal balance equations.

2.1.2 Outdoor thermal comfort parameters

The heat storage in the body tending to zero is largely dependent on convective, radiative, and evaporative heat transfer along with internal heat production. Conductive heat exchange is ignored in this case. This thermal equilibrium primarily depends on four environmental or meteorological parameters: air temperature, mean radiant temperature, relative humidity, and wind speed [30]. It also depends on two personal parameters: metabolic rate and clothing coefficient of the occupants [31]. The meteorological and personal parameters can be described as follows:

- *Potential air temperature:* Potential air temperature can be defined as, *"the temperature that a sample of air would have if it were brought dry-adiabatically to a pressure of 1000 hPa" [83].* It is useful to study this parameter as it remains constant under changing adiabatic pressure.
- *Mean radiant temperature:* Shortwave and longwave radiation are fitted into one single parameter, which can be defined as the average temperature of the surfaces that radiates heat at the point of measurement in a steady condition. This can be derived from the operative and air temperature. This has a significant influence on thermal comfort.
- *Relative Humidity:* This can be defined as the amount of moisture present in the air expressing as percentage of its maximum saturation capacity (also known as saturation point). This affects the evaporative heat loss from the body. This is dependent on air temperature and the vapor content of the urban atmosphere.
- *Wind speed:* This affects both the convective and evaporative heat transfer from the body. An increase in the wind speed or the air velocity increases the convective, evaporative, and conductive heat transfer rate. This is an important factor to consider for natural ventilation, more strictly for tropical and humid climatic zones.
- *Metabolic rate:* This is associated with the person's activities. The more the metabolic rate, the higher the heat generated.
- *Clothing insulation:* This affects the person's thermal comfort by restricting the heat transfer to and from the body and the surrounding external environment.

TABLE 2.1: Clothing resistance values for different types of clothing. (1 clo = 0.11 $m^2 K/W$)($Adaptedfrom$[45])

Type of clothing	**Value (clo)**
None	0
Normal tropical clothing	0.3
Light summer clothing	0.3
Summer suit	0.8
Normal suit	1
Clothing for polar regions	3-4

TABLE 2.2: Metabolic rate per activity category assuming a body surface area of 1.8 m^2 (Adapted from [45])

Category	Activity	Metabolism (W)
I	Resting	85
II	Sitting, reading, general office work	105
III	Drawing, typing, laboratory work	130
IV	Teaching, light assembly	160
V	House working, washing up	200

TABLE 2.3: Parameters required for PET calculation (Adapted from [18])

Parameter needed	Unit	Heat transfer mechanism
Air temperature	degree celsius	convection, evaporation
Mean radiant temperature	degree celsius	radiation
Relative humidity	percentage	evaporation
Wind speed	m^2/s	convection, evaporation
Metabolic rate	W	-
Clothing insulation	clo	-

2.1.3 Thermal comfort index

The thermal comfort index can be described as, *"how the human body experiences atmospheric conditions, specifically air temperature, humidity, wind, and radiation."* [32]. There are different types of thermal indices, as mentioned below:

- *Universal Thermal Climate Index (UTCI):* It is a bioclimatic index to describe the thermo-physiological comfort of the occupant [33]. It considers humidity, wind, radiation, and all other factors that affect the physiological reaction of the human body to its immediate environment [34].

- *Physiological Equivalent Temperature (PET):* It is defined as the, *"air temperature at which, in a typical indoor setting (without wind and solar radiation), the energy budget of the human body is balanced with the same core and skin temperature as under the complex outdoor conditions to be assessed."*[35]. It is a good thermal index for different climatic zones [36], and it is most commonly used in Europe because of its accuracy and reliability [18]. The PET comparison with the perceived heat stress for hot tropical regions is given in 2.5

TABLE 2.4: Indoor environment reference values for PET (Source: [87])

Indoor meteorological parameter	**Value**
Air temperature	20 °C
MRT	20 °C
Relative humidity	50 percent
Wind speed	0.1 m/s

- *Standard Equivalent Temperature (SET):* As per the latest ASHRAE standards, SET can be defined as, *"the temperature of an imaginary environment at 50 percent [relative humidity], less than 0.1 meters per second airspeed, and [the mean radiant temperature equals the air temperature], in which the total heat loss from the skin of an imaginary occupant with an activity level of 1.0 met and a clothing level of 0.6 clo is the same as that from a person in the actual environment, with actual clothing and activity level"*[37]. This thermal comfort index considers the four meteorological and two personal factors during its calculations.

Physiological Equivalent Temperature (PET) is an energy balance model based on the 2 node model created by Gagge et. al. in 1971 [84]. This was further extended by Hoppe [85] in 1984. To calculate PET, the first step is to determine the thermal conditions of the body with respect to Munich Energy Balance Model for Individuals (MEMI) [86]. The energy balance model is provided in Equation 2.1 determining the thermal environment. The energy gains or losses determined here are compared to an indoor environment settings. This virtual environment data is provided in Table 2.1.3. The air temperature (T_a) of the indoor environment is then modified till the point where the indoor environment and the actual environment are expressing the same thermal load. The (T_a) value at which both are equal is expressed as PET of the environment [87].

For this thesis, the ENVI-met modeling tool is taken into consideration. It is coded in the Object Pascal programming language, using DELPHI [2]. It is a CFD and thermodynamics-based model for holistic micro-climate simulations of the urban environment. It provides detailed information about urban surfaces, vegetation, soil, and air properties. It calculates the mean radiant temperature, which can be visualized using their tool, Leonardo. It also provides thermal comfort human indices such as PET and PMV, using the four meteorological variables with their post-processing tool BIO-met.

TABLE 2.5: PET comparison with the perceived heat stress in tropical regions (Adapted from [38])

PET (degree celsius)	Thermal perception	Perceived heat stress
<14	very cold	extreme cold stress
14 - 18	cold	strong cold stress
18 - 22	cool	cold stress
22 - 26	slightly cool	slightly cold stress
26 - 30	comfortable	no thermal stress
30 - 34	slightly warm	slightly heat stress
34 - 38	warm	heat stress
38 - 42	hot	strong heat stress
>42	very hot	extreme heat stress

2.1.4 Heat stress

Heat stress can be defined as the heat load sustained *"under the combined effect of metabolic heat production, environmental factors ((i.e., air temperature, humidity, airflow, and heat radiation), and clothing requirements"* [39]. PET values concern the thermal state of the body. In a tropical climate, a temperature range of 26 to 30 degrees Celsius is considered comfortable. When people cannot maintain the inner core body temperature, they may develop heat disorders.

The thermal sensation depends on the geographical location's climatic zone, in this case, the Philippines, which falls under the hot and tropical region category. The thermal perception and physiological stress are given in Table 2.5. The neutral range for a Cold climate is 18.1 - 23 degrees Celsius. For the Mediterranean climate, it is 20 - 25 degrees Celsius [40].

The UTCI values compared to the perceived thermal stress are given in Table 2.1.4. The albedo values for common materials are given in Table 2.7

TABLE 2.6: UTCI values and its comparison with the perceived heat stress (Adapted from [31])

UTCI (degree celsius)	Perceived thermal stress
>= 45	Extreme heat stress
38 - 46	Very strong heat stress
32 - 38	Strong heat stress
26 - 32	Moderate heat stress
9 - 26	No thermal stress
0 - 9	Slight cold stress
-13 - 0	Moderate cold stress
-27 - -13	Strong cold stress
-40 - -27	Very strong cold stress
<40	Extreme cold stress

TABLE 2.7: Albedo values for different components

Material	Albedo
Asphalt	0.125
Grass and Trees	0.205 - 0.25
Brick	0.3
Concrete	0.225
Wood	0.15
Glass	0.305
Metal roof unpainted	0.3 - 0.5
Playground	0.45
Path	0.1
Corrugated iron for facade/roof	0.13

2.1.5 Philippines Climate

The average weather data is collected from the Ladybug plugin in Rhino 3D, taken from the EnergyPlus website. An EPW file of the Manila region is taken as an input file for obtaining meteorological data. The distance between Hagonoy and Manila is 55km; both cities are situated at the coastal line. This is the most viable and complete information provided nearest to the interest location. Therefore, it is assumed that the data is admissible for the region of Hagonoy. Climate Consultant 6.0 software is used to extract and visualize the data. This is based on the ASHRAE Standard 55 and the Current Handbook of Fundamentals Model. All the additional data is provided in Appendix A.

Climate:

The Philippines' climatic zone is considered to be tropical and maritime. It can be characterized by high temperatures, high humidity, and excessive rainfall. Hagonoy falls under the Type 1 category according to the Climate Map of The Philippines. It is characterized by two prominent seasons *"dry* *from November to April and wet during the rest of the year. The maximum rainfall period is from June to September."*(Source: PAGASA)

Temperature:

In general, the mean annual temperature is 27.5 degrees Celsius. The Manila region's highest hourly temperature is recorded as 38 degrees in June, followed by 36 degrees in May. We consider 8th May for simulation, representing a more typical day in that region. For this month, the lowest temperature recorded is 25 degrees. The highest, lowest, and average recorded dry bulb temperatures for each month can be seen in Figure 2.1

FIGURE 2.1: Average monthly temperature graph (degree celsius) for Manila in 2021(Source: EPW file from the Climate Consultant software - Adapted by Author)

Humidity:

Due to high temperatures and being surrounded by water on all sides, the Philippines records high relative humidity. Overall, the average recorded relative humidity varies from 71 percent to 85 percent in March and September, respectively. It is extremely uncomfortable in the summer, March to May when temperatures and relative humidity are at their highest levels. For 8th May, the highest recorded Relative Humidity is 79 percent, with the lowest being 44 percent. This can be seen in Figure 2.2

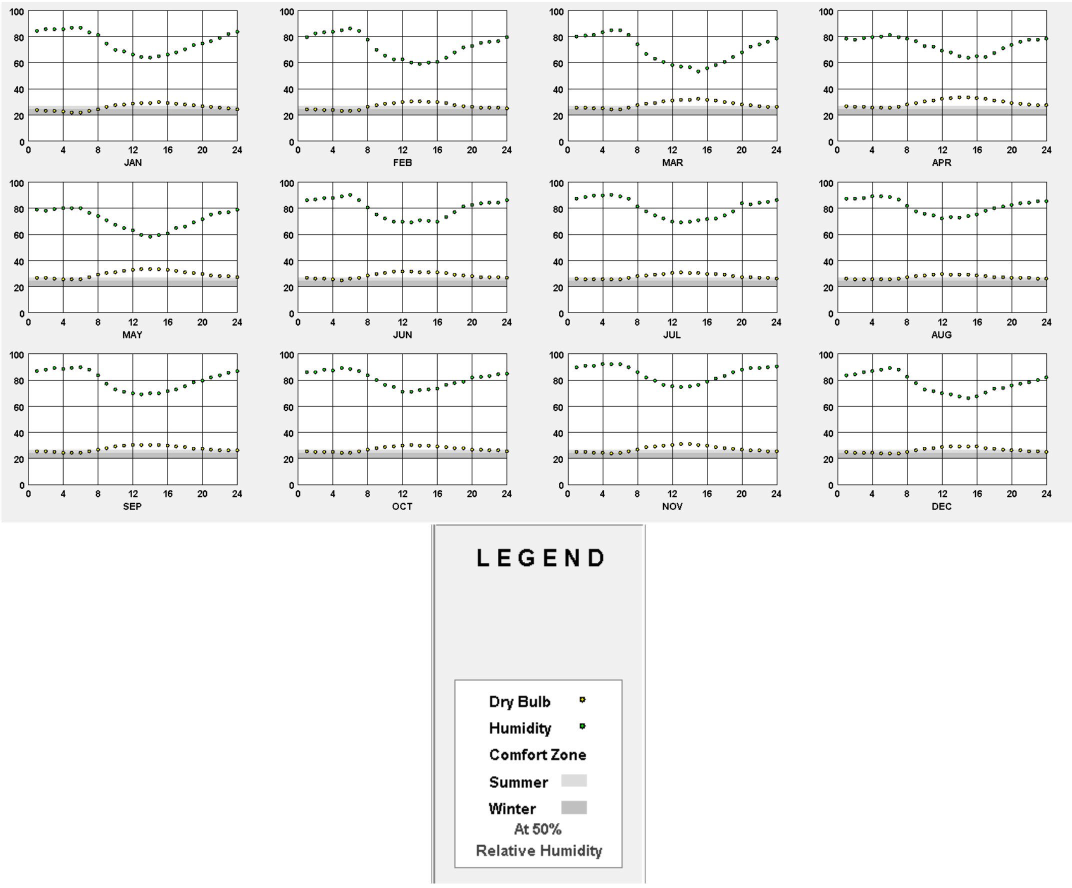

FIGURE 2.2: Dry bulb x Relative Humidity for Manila region (Source: EPW file from the Climate Consultant software - Adapted by Author)

Wind speed: The prevailing wind system can be divided into three categories (Source: www.fao.org, 2019)

- November to February: N-E monsoon
- July to September: S-W monsoon
- Rest of the year: From east

According to the chart, the windiest month is usually December. On 8th May, the maximum wind speed was recorded as 8.2 kmph, with the lowest being 0 kmph. The wind direction varies throughout the year. However, most of the wind comes from the west and east direction. This is also similar to the day of interest. These representations can be seen in Figure 2.3, 2.4 and Figure 2.5.

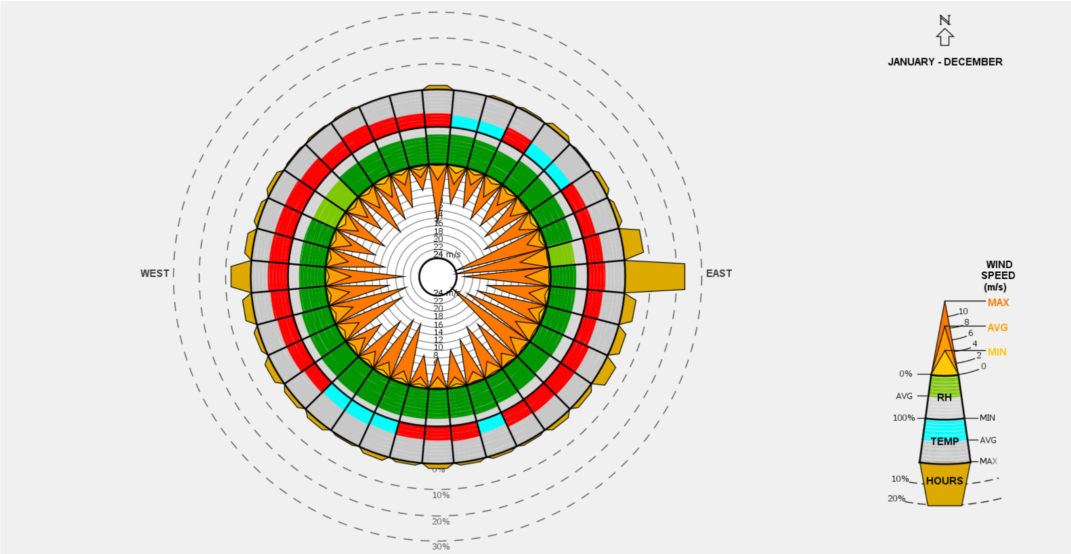

FIGURE 2.3: Wind wheel at Manila region throughout the year.

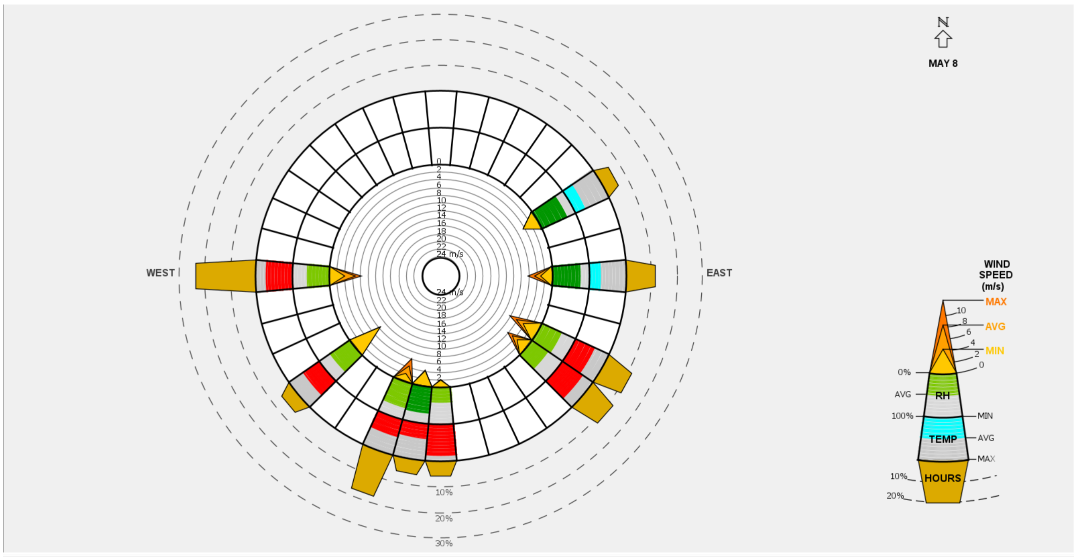

FIGURE 2.4: Wind wheel at Manila region on 8th May

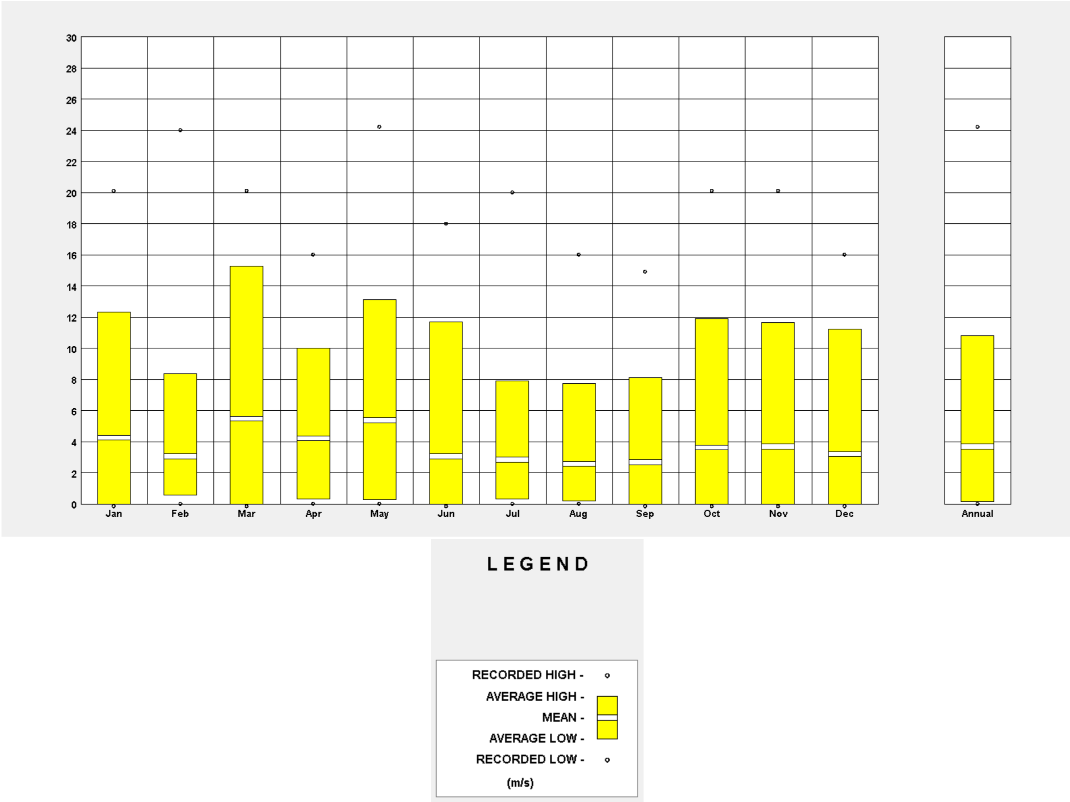

FIGURE 2.5: Wind speeds in Manila region throughout the year(Source: EPW file from the Climate Consultant software - Adapted by Author)

Typhoons:

The Philippines is highly vulnerable to cyclones and typhoons due to its location. It witnesses heavy rainfall, winds, and flooding. The country witnesses cyclones usually between May and November; however, strong winds are relevant throughout the year. The latest typhoon map and the predicted frequency are given in Appendix A.

2.1.6 Simulations

Some of the existing software packages to calculate PET are ENVI-met and Rayman. ENVI-met is a computational fluid dynamics model, whereas the latter is a three-dimensional radiation model. Even though the computationally heavy CFD approach takes an immense amount of time for each simulation, this is also one of the most verifiable and complete simulation tools available for microclimate analysis. Therefore, ENVI-met is chosen for simulations.

The initial model was drafted in Grasshopper and Rhinoceros3D, a software developed by McNeel and Associates. This is because of its simple user interface and functionality in developing a model. This software is either built-in in the primary package or is readily available online for free download. It is an open-source platform with easy to grasp user interface. It also is less time-consuming compared to the other mentioned software. Additional plugins were used for initial radiation studies, which include Ladybug and Honeybee. Dragonfly plugin was further used to convert the model from Rhino 3D to ENVI-met area input (.inx) file.

The calculations of the microclimate model in ENVI-met include (which is relevant in this case): short and long wave radiation fluxes, which consider shading and reflections from buildings, soil, surfaces, and vegetation. It determines biometeorological metrics such as MRT, PET, and UTCI, along with wind speeds and flow patterns. Additionally, it provides information about the simulation of water and heat exchange.

2.2 Outdoor Wind Comfort

2.2.1 Defining outdoor wind comfort

The interactions between the buildings and the environment are complex. Urban infrastructure significantly changes the wind dynamics and the thermodynamics field [2], albeit creating safety issues and discomfort for pedestrians [47]. Buildings can create dangerous wind patterns, creating an uninhabitable environment and leaving the spaces unoccupied. Therefore, urban wind comfort can be defined as the branch of wind engineering that studies wind effects at an urban scale, ensuring the safety and comfort of pedestrians and cyclists. High winds are prevalent in the standing vortex and corner streams [48].This is of particular interest for high-rise buildings, because the wind speeds are deflected from the higher altitudes to the ground level. Also for the low-rise buildings or rural areas, the building masses affect the local wind velocities.

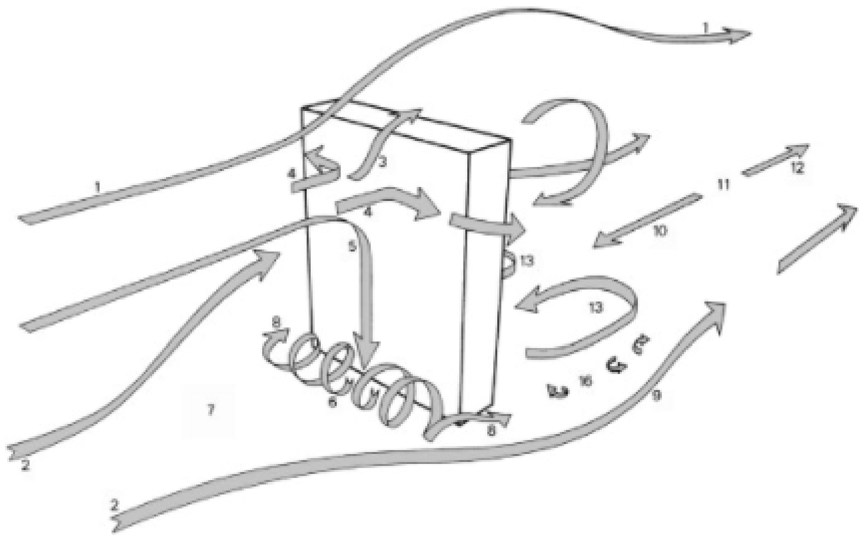

FIGURE 2.6: Wind profile above the urban area (Source: [52])

Solar radiation and local wind speeds are the only urban micro-climactic factors primarily dependent on urban planning, such as the site location, building form, configuration, and geometry of open spaces [48]. Therefore, urban planners have power over designing the spaces to improve climate interaction and ensure safety and comfort in public spaces. However, wind planning is usually ignored in micro-climactic studies, even though it is considered one of the most important factors for user satisfaction [49].

The urban boundary layer, in this case, is defined as the portion of the atmospheric boundary layer (ABL) between the surface and the height at which the city no longer influences the wind flow. [2] The vertical profile of the average wind speed is:

$$U = \frac{u_*}{k}\left[ln(\frac{z}{z_o}) + \psi(\frac{z}{L})\right]$$

Equation 2.5

where,

U	average wind speed	m/s
u_*	friction velocity	m/s
z	height	m
k	von Karman constant (0.45)	-
L	Obukhov length	m
z_o	aerodynamics roughness	m

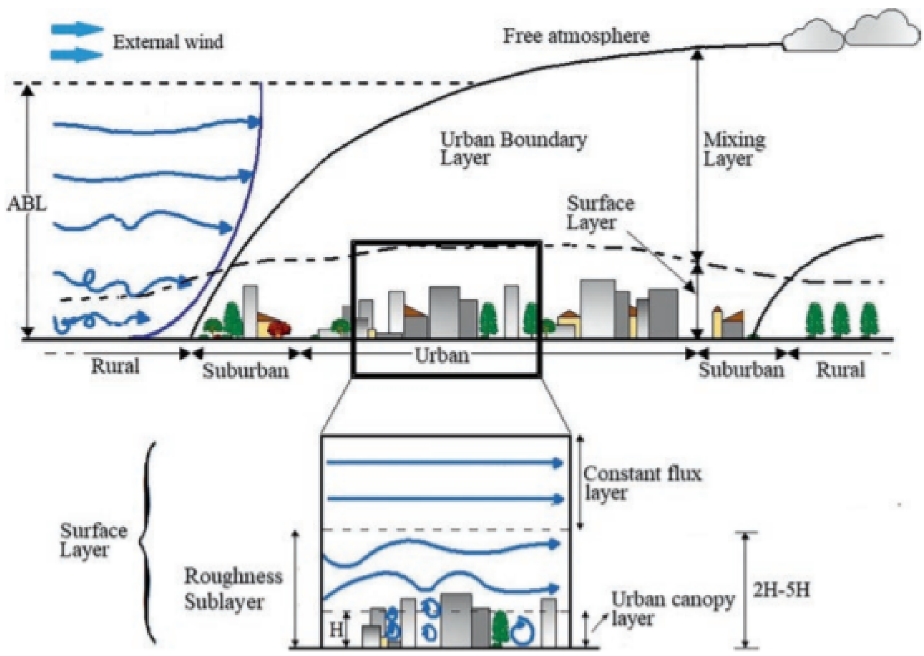

FIGURE 2.7: Urban Boundary Layer structure (Source: [2], Modified from [50])

The wind profile above the urban areas and vegetation canopies usually assume a constant and is in neutral conditions.

$$U = \frac{u*}{k}\left[ln(\frac{z-do}{zo}) + \psi(\frac{z}{L})\right]$$

Equation 2.6

where,

U	average wind speed	m/s
u_*	friction velocity	m/s
z	height	m
d_o	displacement height	m
L	Obukhov length	m
z_o	aerodynamics roughness	m

Here, they represent the displacement height which is the effective height from the ground level due to the vertical flow displacement. The parameters z_o and d_o are associated with the surface roughness coefficient.

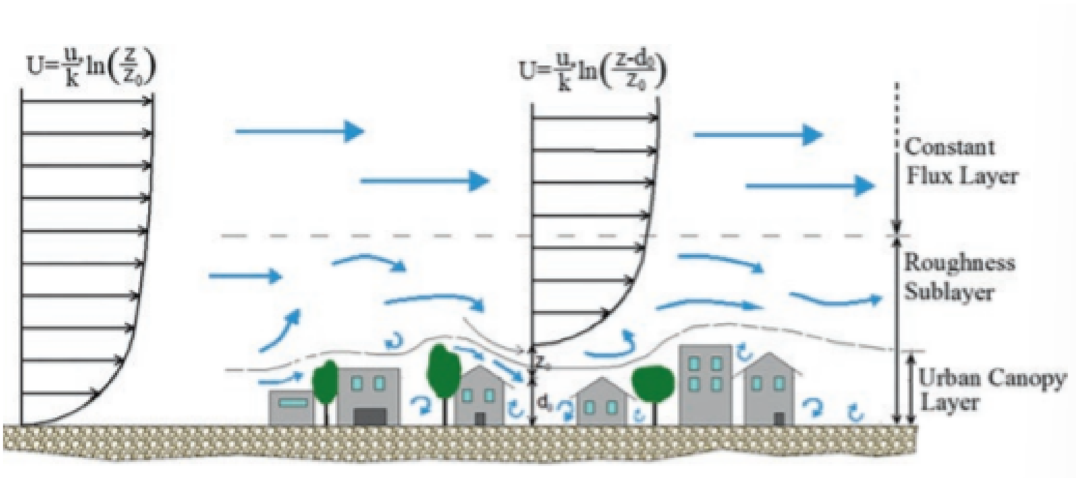

FIGURE 2.8: Wind profile above the urban area (Source: [2], adapted from [51])

2.2.2 Urban wind comfort context

The urban topography plays a major role in the wind speed patterns. Some of its examples are described below [47] [48].

- *Corners of the building:* The building corners are considered the most uncomfortable areas in urban spaces. This is due to the pressure differences created by the side vortices between the front of the building and the sides, high- and low-pressure zones, respectively. In order to maintain the safety of the pedestrians, it is preferable not to design any public or open spaces near the high-speed flows, in this case, the corners of the building.

- *Venturi effect:* This is a reduction in the fluid pressure. In this case, the wind pressure, when it has to pass through narrow and constricted regions. This thereby increases the acceleration of the wind. This can be a common occurrence in urban areas if restricted access between two portions is restricted, thereby leading to uncomfortable spaces. For buildings less than 50m in height, there exists a protection zone upwind of the building.

- *Passages:* They can create uncomfortable spaces when the *"flow with high pressure from the stagnation side tries to escape through the passage."* [47]. This creates wind with high velocity and acceleration.

2.2.3 Wind comfort criteria

To accurately estimate pedestrian wind comfort, the following parameters need to be determined [53]:

- *Local wind conditions:* influenced by the urban environment and surroundings.

- *Typical wind data:* The wind conditions close to the location of the building represent typical wind patterns.

- *Specific comfort criteria:* Criteria which co-relate the local wind speeds with the perceived wind comfort by the pedestrians.

The average wind speed can be calculated using the local meteorological data from Equation 2.7. This is taken from [54].

$$U = U_{10,m}(U_0/U_{10,m})(U/U_0)$$

Equation 2.7

where U_0 can be calculated from the Equation 2.8

$$U_0 = Kz^{\alpha}U_{10,m}$$

Equation 2.8

where,

U	average wind speed at pedestrian level	m/s
$U_{10,m}$	average wind speed at pedestrian level including roughness but not built form	m/s
Z	height of wind speed evaluation. Taken at 1m for pedestrian level	m
K, α	related to terrain toughness. From Table	-

TABLE 2.8: Terrain roughness parameters (Source: [48])

Terrain	**K**	α
Sea	0.7	0.14
Meteorological station: free open space	0.68	0.17
Rural zone with windbreaks	0.52	0.2
Suburban zone	0.4	0.235
Urban zone (continuous blocks of buildings)	0.35	0.25
Dense urban zone with many tall buildings	0.21	*0.33*

There are several comfort criteria to assess pedestrian comfort levels. Some of them discussed include Davenport, Lawson, and NEN 8100. These criteria assess varied conditions such as sitting, standing, walking, and strolling. The acceptable comfort classes for various location types are given in Table 2.9.

TABLE 2.9: Acceptable pedestrian wind comfort categories for different location types

Comfort classes	**Wind**	**Occurance**	**Location types**
Sitting	<=3.9 m/s	>70%	Outdoor cafes, patios, terraces, beaches, gardens, fountains, monuments
Standing, strolling	<=6.1 m/s	>80%	Building entrances, exits, childrens play area
Walking, rigorous activities	<= 8.3 m/s	>80%	public/private sidewalks, pathways, public/private vehicular drop-off zones
Uncomfortable, unacceptable for walking	>8.3 m/s	>20%	
Dangerous to walk	>25 m/s	>0.01%	

Lawson:

Even though wind comfort perception is mainly subjective, there are general models and guidelines developed by Lawson. These are presented in Table 2.10.

TABLE 2.10: Lawson comfort criteria (Source: [55]

Color	Class	Velocity m/s	Exceedence
	Class A: Sitting/Standing - Long	>4.0	<5.0%
	Class B: Sitting/Standing - Short	>6.0	<5.0%
	Class C: Leisurely Walking	>8.0	<5.0%
	Class D: Fast Walking	>10.0	<5.0%
	Class Safety: Distress	>15.0	>0.0002%

NEN8100:

It is a comfort criterion developed by the Dutch, and it applies a threshold value to the hourly mean wind speed of 5m/s for all the categories of activities. The comfort criteria are given in Table 2.11.

TABLE 2.11: NEN8100 comfort criteria (Source: [55])

Color	Class	Velocity m/s	Exceedence
	Class A: Sitting/Standing - Long	>5.0	<2.5%
	Class B: Sitting/Standing - Short	>5.0	<5.0%
	Class C: Leisurely Walking	>5.0	<10.0%
	Class D: Fast Walking	>5.0	<20.0%
	Class E: Uncomfortable	>5.0	>20.0%
	Class Safety 1: Limit Risk	>15.0	<0.30%
	Class Safety 2: Dangerous	>15.0	>0.30%

Davenport:

Published in 1975, this criterion is the oldest in the group. The maximum exceedance probability is 1 per week for tolerability for certain activities. *"The longer the average wind speeds exceed this limit, the more uncomfortable the activity is assumed to be."* This can be seen in Table 2.12 [53].

TABLE 2.12: Davenport comfort criteria (Source: [53])

Color	Class	Velocity m/s	Exceedence
	Class A: Sitting/Standing - Long	3.6	<1.5%
	Class B: Sitting/Standing - Short	5.3	<1.5%
	Class C: Leisurely Walking	7.6	<1.5%
	Class D: Fast Walking	9.8	<1.5%
	Class E: Uncomfortable	9.8	>= 1.5%
	Class Safety: Dangerous	15.1	>= 0.01%

These wind comfort indices are primarily created for non-tropical climatic zones. However, there is no specific criteria drawn for tropical climates from the investigated literature. In the above mentioned categories, Lawson is the most widely recognized comfort criteria, thereby choosing this. The wind comfort criteria is calculated for all the days in the year, and is not directly expressed as in thermal comfort. Therefore, the velocity mentioned in the Tables is the maximum acceptable value for that category. And exceedance can be defined as the number of days the wind speed exceeds the acceptable velocity mentioned expressed as the ratio to the number of days in the year. This percentage should be within the range mentioned for acceptability.

From the literature, there was wind comfort criteria drawn for calm climates. The wind comfort is briefly calculated using this tool as well, and is provided in the Appendix B. This was not fully explored due to the time limitations of the project.

2.2.4 Simulations

There are two methods to model and obtain results for wind analysis. They are wind tunnel tests and computational fluid dynamics simulations.

Wind tunnel tests:

They are om-site point measurements performed with Laser Doppler Anemometry (LDA) or Hot Wire Anemometry (HWA) [7]. These tests are conducted to obtain the average wind speed and turbulence intensity at the pedestrian level. However, this method is expensive and highly time-consuming. This is also not adaptable because the whole geometry needs to be redesigned and rebuilt in case of any changes.

Computational Fluid Dynamics:

It is a time-saving, cost-effective design tool that provides quantitative and qualitative wind pattern presentations. It is a computer-aided tool, and several software exists for the assessment like SimScale, ENVI-met, Rhino 3D with Grasshopper, Butterfly, Openfoam, Swift, and Eddy 3D as some additional plugins that may be combined for use. They are often used to determine wind flow, pedestrian comfort, wind-driven rain, pollutant dispersion, and snow drift [2].

Several parameters must be chosen carefully for successful assessments: volume dimensions, boundary conditions, turbulence model, and grid resolution. [48] Most of these models follow the RANS equations method using the k- model.

For this thesis, wind comfort is determined from ENVI-met simulations which are based on CFD analysis. The Philippines climate data is mentioned in Section 2.1, and the daily rural and urban meteorological data is collected from the Ladybug plugin.

The winding history of Manila, i.e., the wind-rose diagram of the region in the year 2020, is given in Figure 2.9.

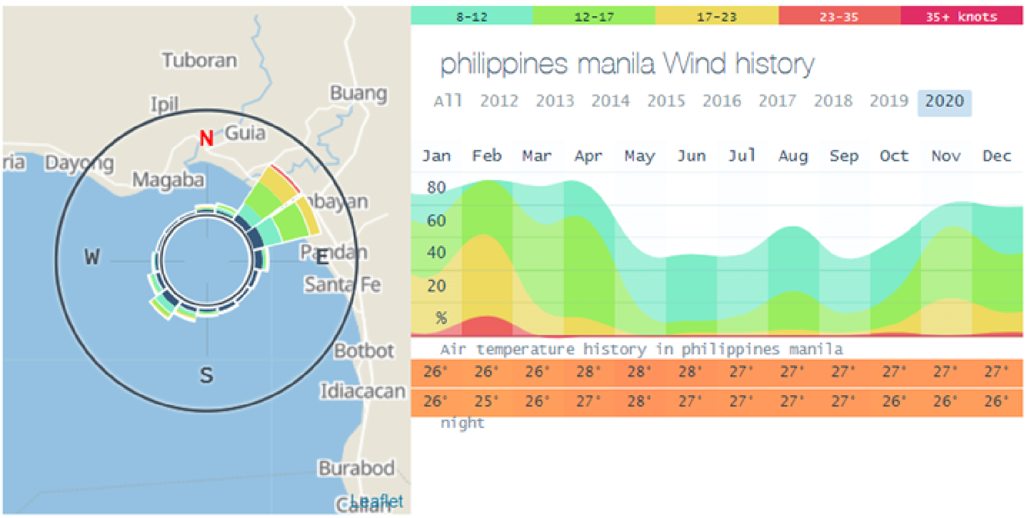

FIGURE 2.9: Philippines manila wind history 2020thermrl-www,windy.app

2.3 Influencing Parameters

2.3.1 Waterbodies

Waterbodies can positively influence the microclimate of the surrounding areas as they provide natural cooling. It acts as an urban cooling island. Waterbodies have low reflectivity, leading to absorption of solar radiation and decreasing mean radiant temperature.

Water has a high thermal capacity and evaporation effect, which lowers the surface and air temperature. However, this creates a sea breeze phenomenon. This phenomenon usually occurs during hot summer days due to the temperature difference between land and water. During day time, the land surface heats up more than the water surface.Thereby, creating warmer air over the land than the water surface [68]. This wind may, however, be obstructed by building obstacles. Overall, waterbodies have the potential to reduce energy consumption and improve outdoor thermal comfort and reduce the urban heat island effect.

They have the ability to maintain the temperatures at night because of the thermal inertia and high heat capacity [70]. Therefore, it is known to be pretty stable. According to the [70] study, water's cooling effect is more prevalent during the day, and there is a warming influence during the night. Wind turbulence, wind velocity, humidity, temperature, and wind direction affect the cooling influence of waterbodies [70] [71] [72] [73] [74] [75]. Other parameters that influence the cooling effect are the size of the water body, evaporation rate, and water albedo [76].

The typical value of the ocean albedo is approximately 0.06, which indicates that the ocean reflects 6 percent of the solar radiation coming onto its surface and absorbs the remaining [77].

Since the location is surrounded by water, it may act as a cooling effect on the heat island created. For this thesis, the simulations are run with the existing landscape typology. The floating homes are surrounded by shallow water, which can absorb high heat absorption capacity. As an alternative scenario, the water body is replaced by pavement material properties to understand the degree of its influence on the total outdoor comfort. These simulations are run as two different test scenarios in ENVI-met. The material properties of water are represented in Table 2.13.

TABLE 2.13: Properties of water

Property	**Value**
Heat Capacity (J/m^3K)	4.18
Thermal Conductivity (W/mK)	0.57
Albedo	0
Emissivity	0.92-0.97

2.3.2 Vegetation

The traditional way to provide shading in outdoor spaces is through trees. They lower the daytime temperature around the tree canopy. However, they also reduce the sky view factor and obstruct night-time surface cooling and radiation losses [20]. The air that passes through the trees has its speed reduced, temperature reduced, and humidity increased.

In an urban landscape, trees are mostly found in parks, gardens, and sometimes at the side and center of the streets. Each location can serve a different purpose for the microclimate. If trees are present in the streets or next to buildings, they can be used as shading devices to reduce the UHI. If the trees are present in parks and gardens, they provide cool daytime spaces for pedestrians. They also lower the MRT and the radiative load on pedestrians. The impact of tree shading depends on the species composition and leaf canopy. The main parameters include [20]:

- Tree line distance (this is the distance between buildings and line of trees)
- Tree line length (length of the line of the trees)
- Tree species (canopy width, height, and transparency)

Because of its various benefits, trees can help reduce energy consumption and the cooling demand of the buildings. Clustered trees are more effective than scattered trees [65]. Artificial sun shading devices can also be used for this purpose. Some outdoor shading types include tarps, garages, and building shadows. Trees are the most effective of all of them. Some green building devices are lawns, green roofs, and green walls.

A shade benefit analysis provides information about the decreased cooling load and increased cooling load by adding shade in different regions. Hardwood forests are the most predominant in tropical climates, along with fruit-bearing trees. The most common tree in the Philippines is Gmelina (Gmelina Arborea). There is especially demand for mangrove plantations and nipa palm. [66] The best orientation for tree planting in the Northern Hemisphere is west, followed by east.

In 2000, Hagonoy had about 6.6 percent of natural forest cover. From the year 2001 to 2020, Hagonoy lost over 15ha of tree cover with an estimated 2.5 percent decrease [64]. In Alazne's report, the urban spatial design is such that it promotes tree plantations and gardens. Vegetable gardens are attached to each home. For the given location in the thesis, there are mangrove plantations next to the main Barangay road, which will be the main focus for input parameters. Assuming that the urban density will increase, vegetation can facilitate the cooling effect, especially during the daytime.

An ideal scenario of tree plantations for a building layout in the southern hemisphere is given in Figure 2.11.

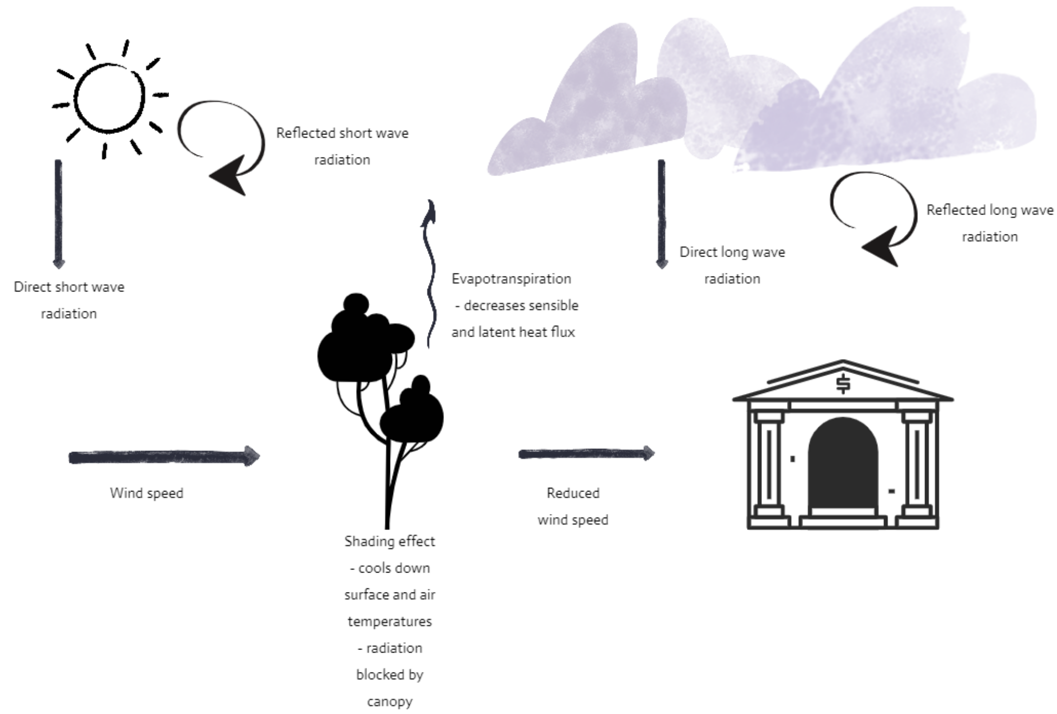

FIGURE 2.10: Effect of trees on the building energy balance (Source: Author)

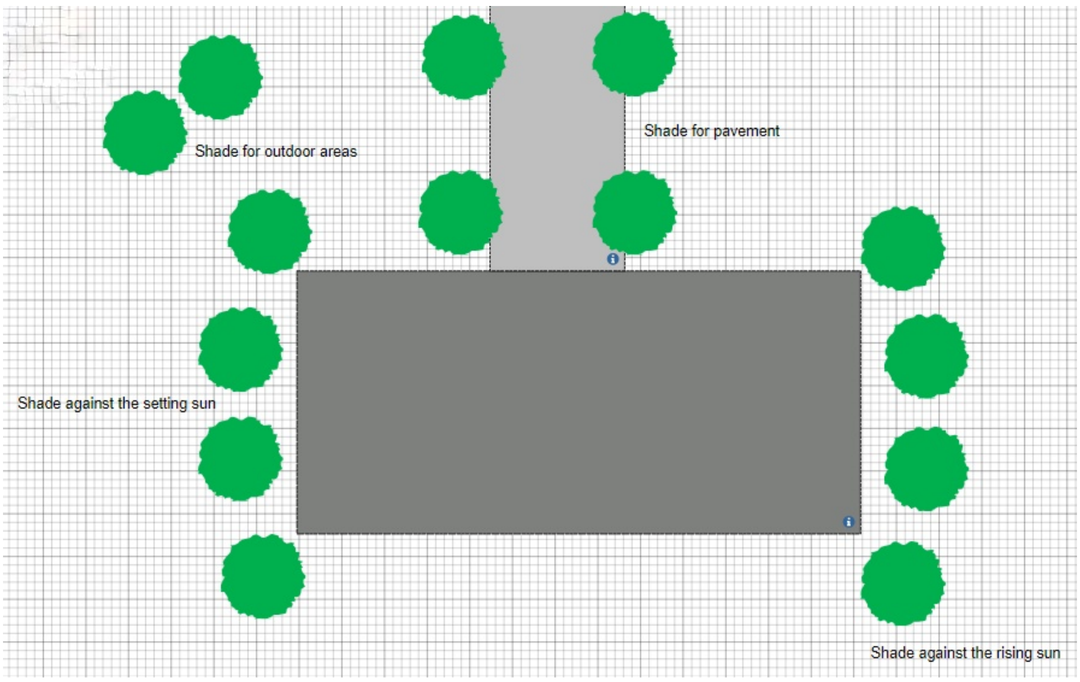

FIGURE 2.11: Ideal building layout plan with trees (Modified from [20])

2.3.3 Urban Morphology

The relationship between urban form and the thermal environment is attributed to building density, building height, and degree of openness [81].

Building Density is the ratio of the total volume of the buildings to the parcel area. A parcel area is a unit containing a cluster of blocks. Understandably, the higher the value higher the urban densification. This parameter directly affects the sun-shading, shadow distribution, and ventilation [81]. As per a study conducted by [67], they have divided the landscape typologies into 17 categories, of which ten are artificial, and the remaining are natural. These categories are known as the zone types or LCZ types. The correlation between LCZ and the urban parameters is given in Figure 2.12.

LCZ type	Mean building height (m)	Building surface fraction (%)	Impervious surface fraction (%)	Pervious surface fraction (%)	Sky view factor	Q_F Wm^{-2}
Compact high-rise	>25	40–60	40–60	<10	0.2–0.4	50–300
Compact mid-rise	10–25	40–70	30–50	<20	0.3–0.6	<75
Compact low-rise	3–10	40–70	20–50	<30	0.2–0.6	<75
Open high-rise	>25	20–40	30–40	30–40	0.5–0.7	<50
Open mid-rise	10–25	20–40	30–50	20–40	0.5–0.8	<25
Open low-rise	3–10	20–40	20–50	30–60	0.6–0.9	<25
Lightweight low-rise	2–4	60–90	<20	<30	0.2–0.5	<35
Large low-rise	3–10	30–50	40–50	<20	>0.7	<50
Sparsely built	3–10	10–20	<20	60–80	>0.8	<10
Heavy industry	5–15	20–30	20–40	40–50	0.6–0.9	>300
Dense trees	3–30	<10	<10	>90	<0.4	0
Scattered trees	3–15	<10	<10	>90	0.5–0.8	0
Bush/scrub	<2	<10	<10	>90	0.7–0.9	0
Low plants	1	<10	<10	>90	>0.9	0
Bare rock or paved	<0.25	<10	>90	<10	>0.9	0
Bare soil or sand	<0.25	<10	<10	>90	>0.9	0
Water	N/A	<10	<10	>90	>0.9	0

FIGURE 2.12: Local climate zone types and the associated urban parameters (Source: [62])

The *average building height* can be defined as the sum of all the heights of the buildings by the total number of buildings present in the coverage area. Increasing building height can block the sunlight and affect the visibility and shadow entering the streets. This directly impacts the wind patterns and the urban surface temperatures [82].

Building coverage area can be defined as the ratio of the built area to the total parcel area. This influences air transmission and mobility, affecting thermal and wind comfort. If the street pattern has a high degree of openness, it decreases the air temperature and heat island effect. Different forms of urban morphology indicate the openness of the street blocks. Some examples include linear arrays, street canyons, courtyards, and open spaces.

In the urban plan designed by Alazne, she follows the courtyard street pattern where floating homes are branched in three with a common realm of open space between them. This was designed based on the requirements of the local people encouraging face-to-face interaction. This is represented in Figure 2.13.

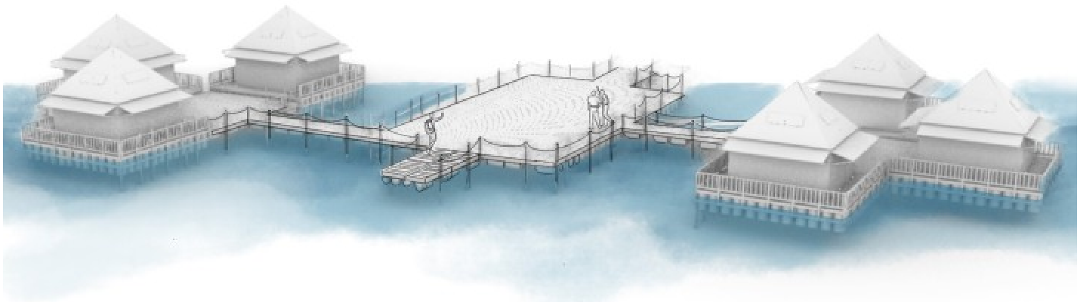

FIGURE 2.13: Courtyard style urban depiction of the original model(Source: [16])

The different urban configurations are assessed using the ENVI-met software as different test runs. They are based on the openness of the buildings, enclosing courtyard typology, and the coverage area.

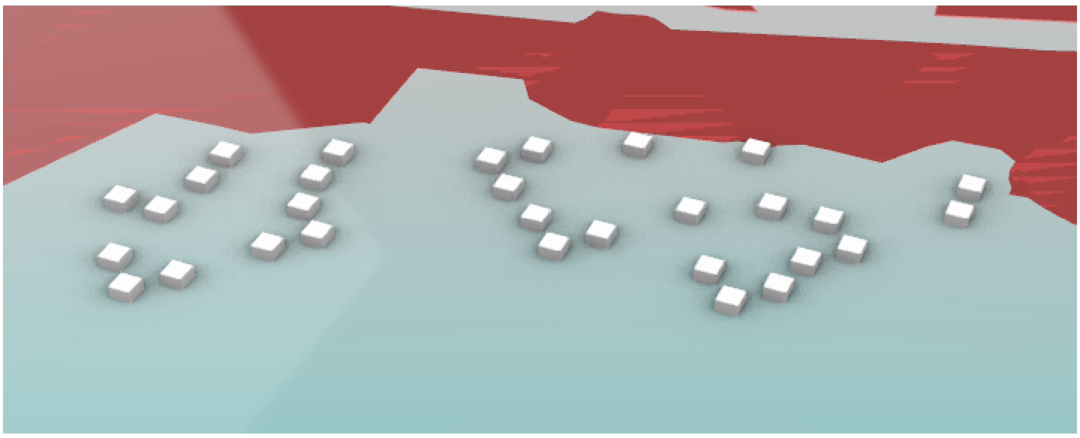

FIGURE 2.14: Original Floating homes model (Source: By Author (Adapted from [16]))

Chapter 3

Modeling

3.1 Rhino model set-up

The model geometry is divided into existing infrastructure and floating homes. Overall, this has been initially designed in Rhino 3D.

3.1.1 Existing Infrastructure

The geographical context of the Mercado region is provided in Figure 3.3 using Google satellite maps.

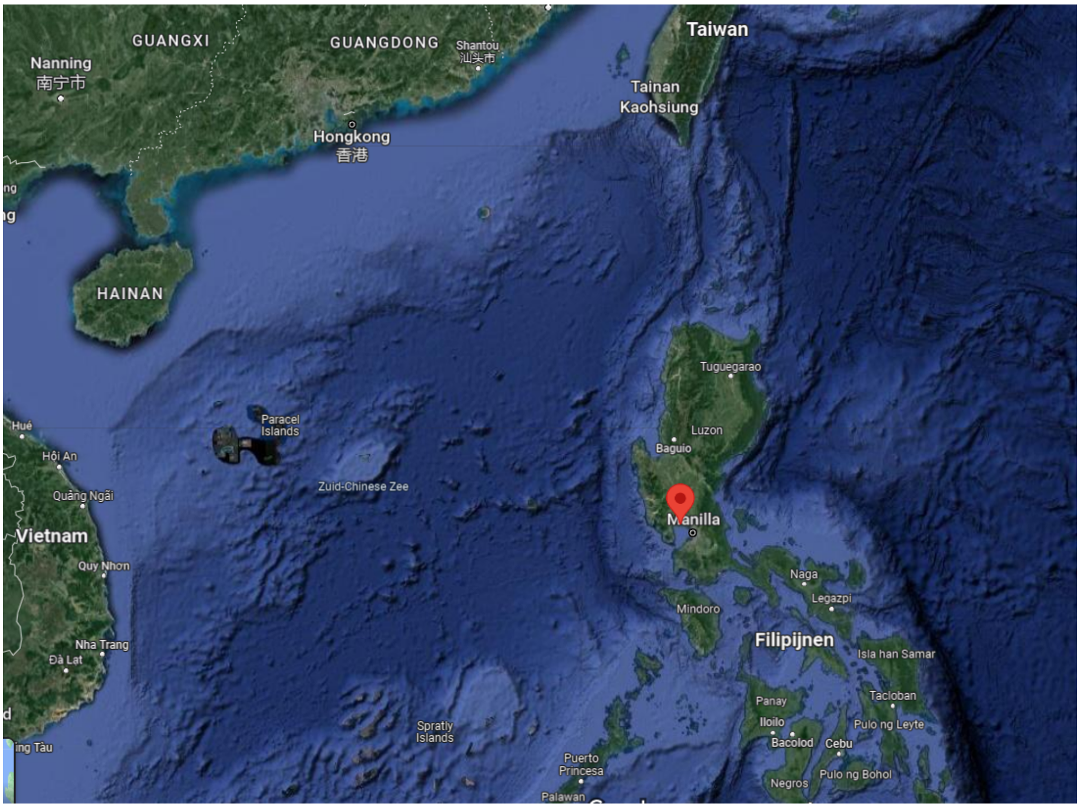

FIGURE 3.1: Geographical context of the Mercado region using Google maps

FIGURE 3.2: Geographical context of the Mercado region using Google maps

FIGURE 3.3: Geographical context of the Mercado region using Google maps

The existing infrastructure of the Mercado region has been modeled using the Openstreetmap information from their website. This file is saved as an Open studio model type (.osm). The Java Script Reader converts this to an Object (.obj) file. This file includes the buildings, vegetation, roads, and waterways. However, since the Mercado region is not under good surveillance, the data available was scarce, as we can see in Figure 3.4. Therefore, the rest of the existing buildings and soil had to be manually drawn using the digitized bitmap files as a surface layout. This can be seen in Figure 3.5. The soil and roads are drawn as polysurfaces, the buildings as boxes, and the vegetation as meshes. All the components are closed geometries and are referenced to a singular object plane.

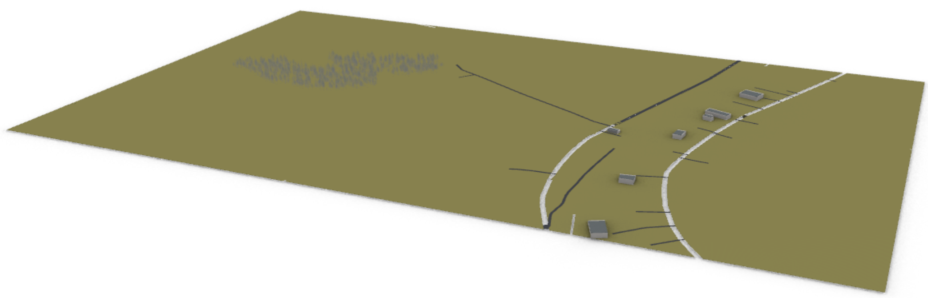

FIGURE 3.4: Open street map data on Rhino 3D

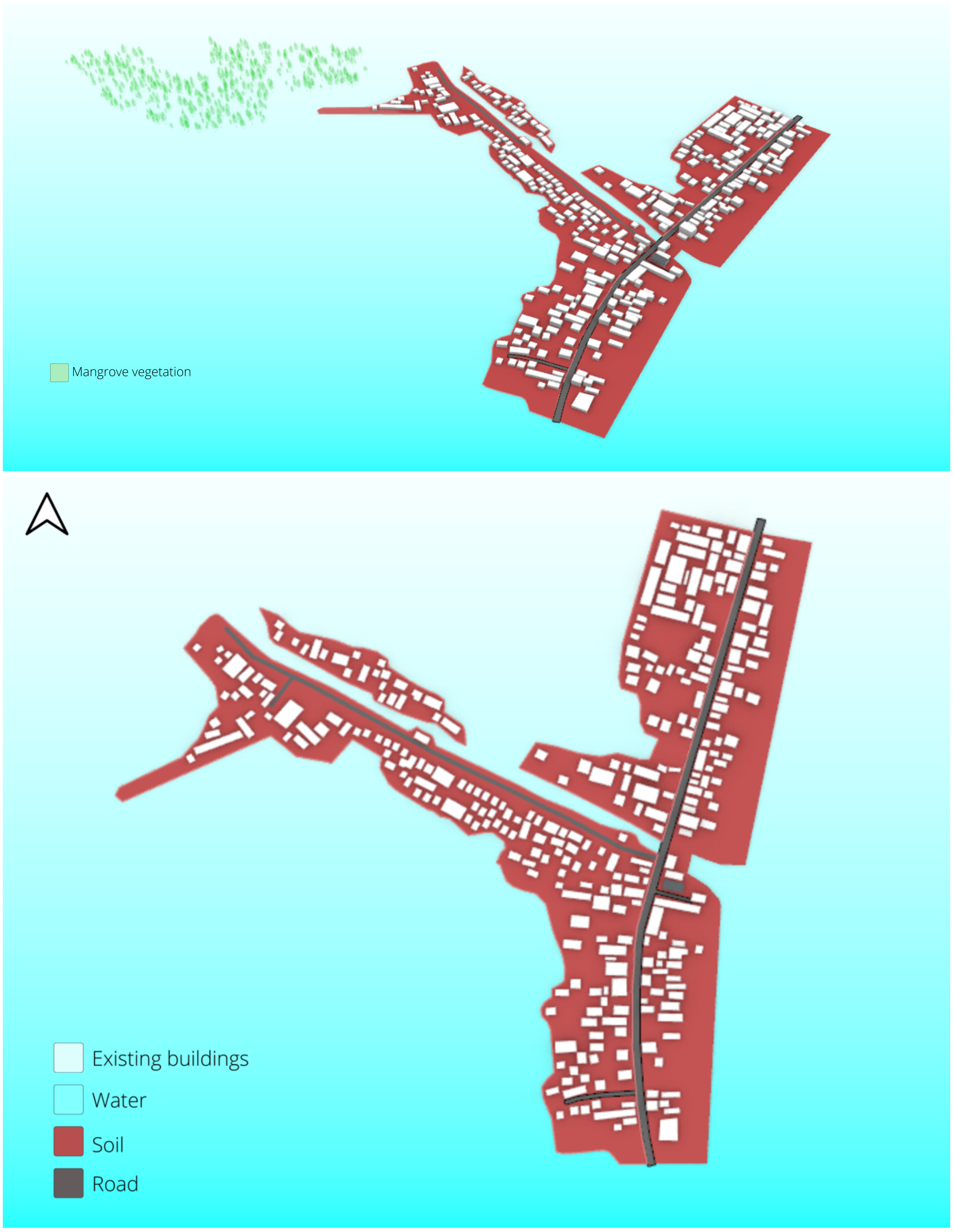

FIGURE 3.5: Existing infrastructure in Rhino 3D including buildings, roads, soil, and vegetation

3.1.2 Floating Homes

The urban model of the floating homes has been designed in Rhino 3D by Alazne for her thesis project [17]. This is represented in Figure 3.6

The level of detail of the buildings is Level 1, which is simple box-shaped geometries as mentioned in Figure 3.7. This model had to be simplified based on the ENVI-met requirements. ENVI-met cannot take sloped surfaces in its model geometry. Therefore, the overhangs in the original model had to be eliminated.

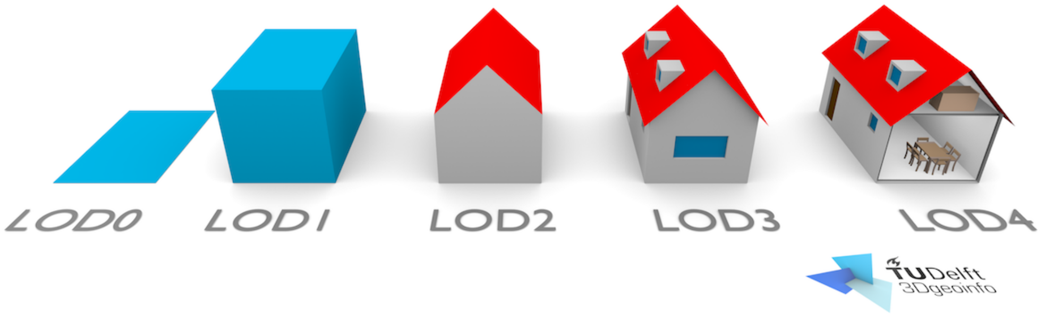

FIGURE 3.7: Level of Details

The sloping roof has been converted to a rectangular box with a 30 percent height of the initial component. This height was chosen based on the radiation analysis of the building concerning the Manila climate data in the local context, in this case, the ground surface. This analysis was performed using a simplified radiation script on Rhino 3D. The results are provided in the Figure 3.8 and Table 3.1.

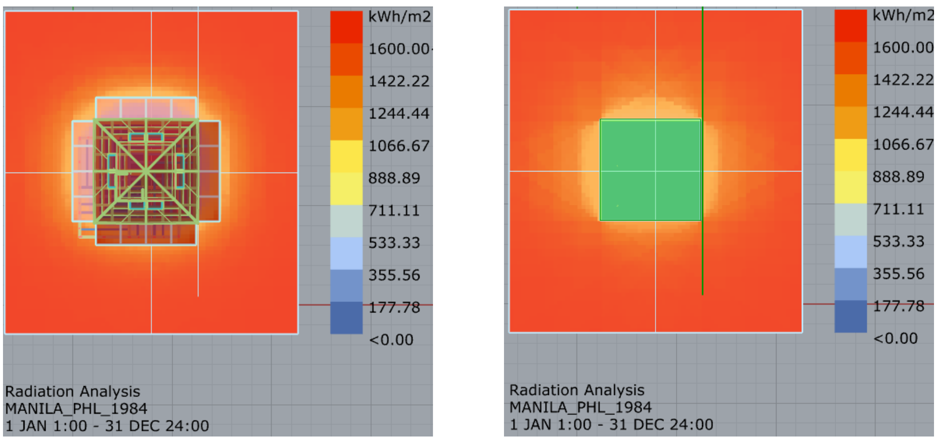

FIGURE 3.8: Radiation analysis of the original model and the simplified model

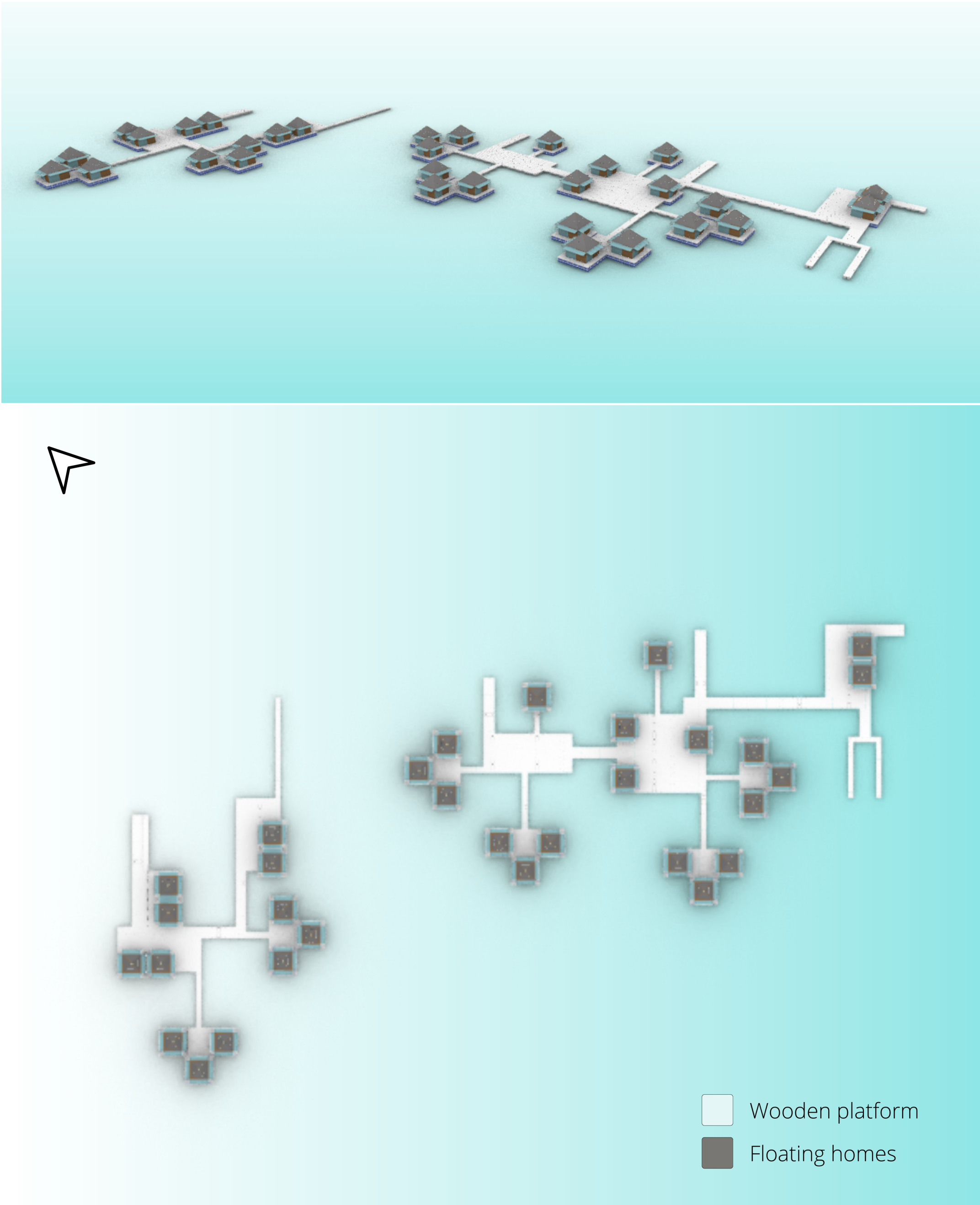

FIGURE 3.6: Floating homes model as per the original plan

TABLE 3.1: Radiation analysis to determine building height

Model	Total radiation (kWh/m2)
Original	711.27
100% roof height	688.63
50% roof height	705.27
30 % roof height	712.08

The model has been converted to a simple 3D box geometry with 6m x 6m dimensions. The dimensions had to be altered to suit the 3m x 3m grid size of the ENVI-met, thereby making that its resolution. Otherwise, the dimensions of floating homes would be non-uniform. The window-to-wall ratio of the facades is 0.4 with unglazed material properties. However, this was also not considered in the final ENVI-met model as it would heavily increase the computational time. Since the primary focus is on outdoor comfort, this simplification does not pose much difference in the results. For the initial base simulation, the geometry does not consider sun-shading devices. This is because ENVI-met would treat these surfaces as walls instead of planar composition.

Overall, the model had to be shortened to a base surface of 145 m x 115 m from an initial grid of 700 x 600 m. This was done to reduce the computational time of the model from approximately 15 days to 4 days. The final model in Rhino 3D is provided in Figure 3.10.

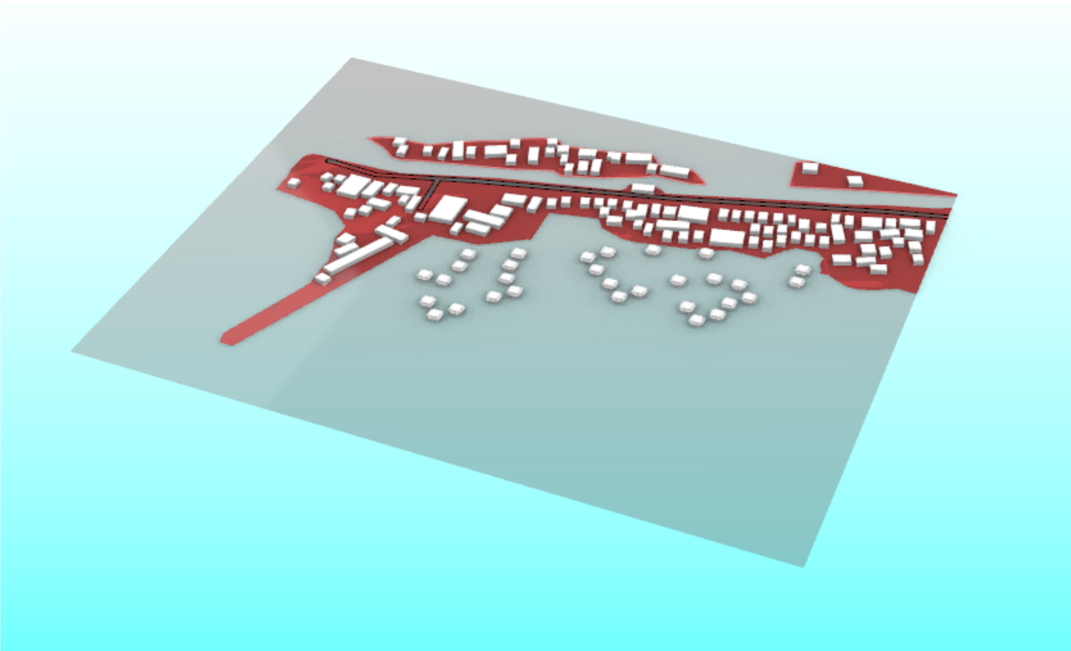

FIGURE 3.9: Final model to be used for ENVI-met simulations

FIGURE 3.10: Final model to be used for ENVI-met simulations

After the final model had been prepared in Rhino, it was converted to a .inx area input file using the Dragonfly-Legacy plug-in along with Honeybee and Ladybug-Legacy. The wall and roof properties for the buildings are concrete hollow blocks and steel roofing, respectively for existing infrastructure. The type of soil is loamy and the roads used/dirty concrete pavements. The wooden platforms and water surfaces are digitized in the final ENVI-met model.

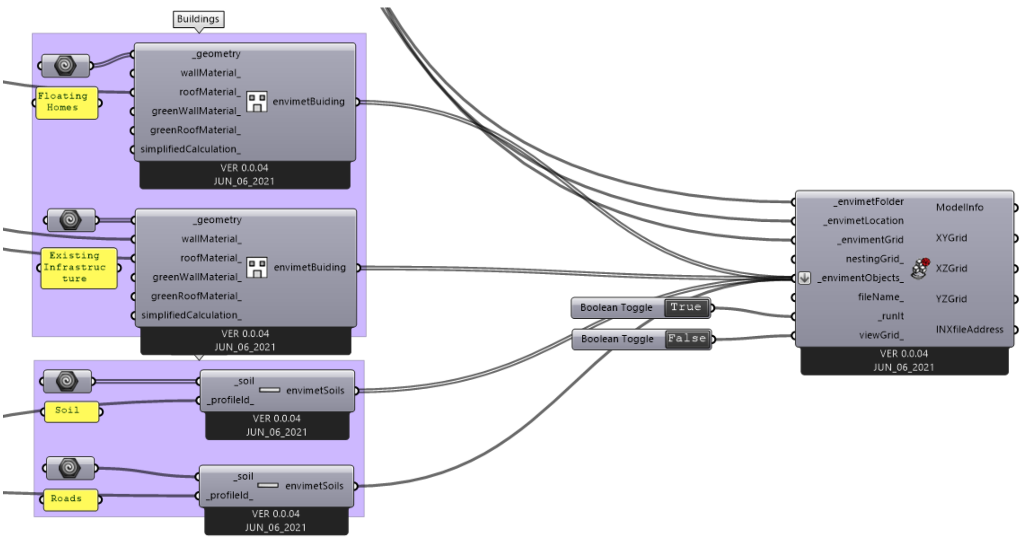

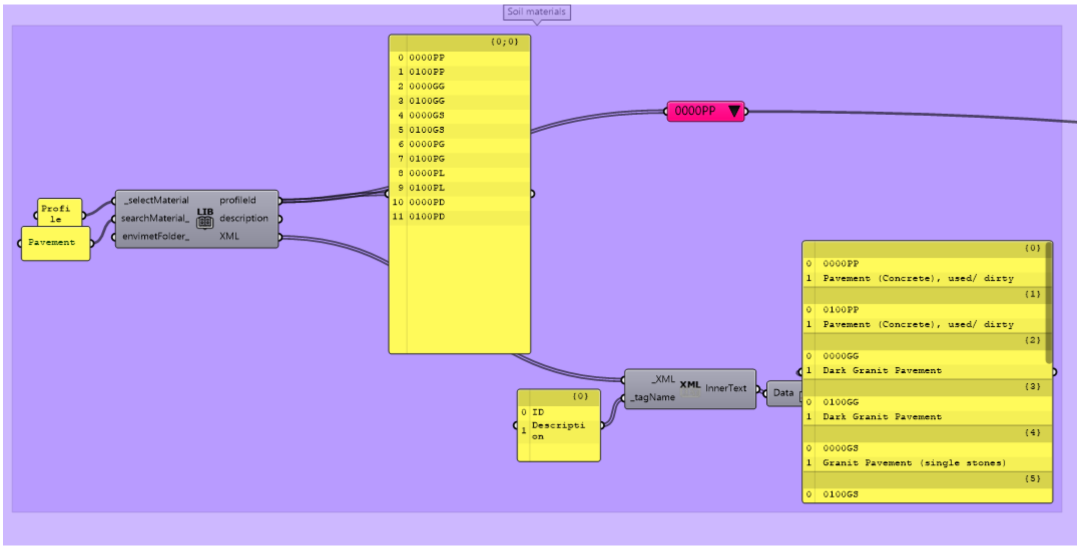

FIGURE 3.11: Grasshopper script for Rhino to ENVI-met model conversion

3.2 ENVI-met model set-up

Table 3.2 provides the input files required for ENVI-met. These files contain information regarding the buildings, vegetation, non-building surfaces, and weather data. Detailed information about input parameters can be found in Table 3.3. The numerical values are tabulated in the coming sub-sections in Chapter 3.

TABLE 3.2: Input files for ENVI-met simulation

File	Format	Description
Area input file	.inx	contains information regarding buildings, vegetation, soil, ground surfaces, model rotation, location and resolution
Simulation file	.simx	contains information regarding the boundary conditions, meteorology data, simulation data, time and duration, and other computing options
Database	.edb	contains information regarding soils, profiles, wall materials, facade greening, and simple plants

TABLE 3.3: Input parameters per category type

Category	**Input parameters**
Buildings	Location
	Roof and facade material
	Material properties, reflectance, albedo, conductivity
Vegetation	Location
	Type (deciduous, coniferous, grass)
	Height
	Leaf density area
Non-building surfaces	Pavement - Location, material, properties
	Soil - Location, properties
	Water - Location, properties
Weather	Temperature
	Wind speed and directions
	Date, sun dawn, sun set
	Relative humidity and cloud coverage

3.2.1 Area File

After the finalized Rhino geometry, the model has been converted to an ENVI-met area file. The buildings with the vegetation are given in Figure 3.12, and the final soil surfaces are portrayed in Figure 3.12. This data is provided in the plug-in ENVI-met Spaces.

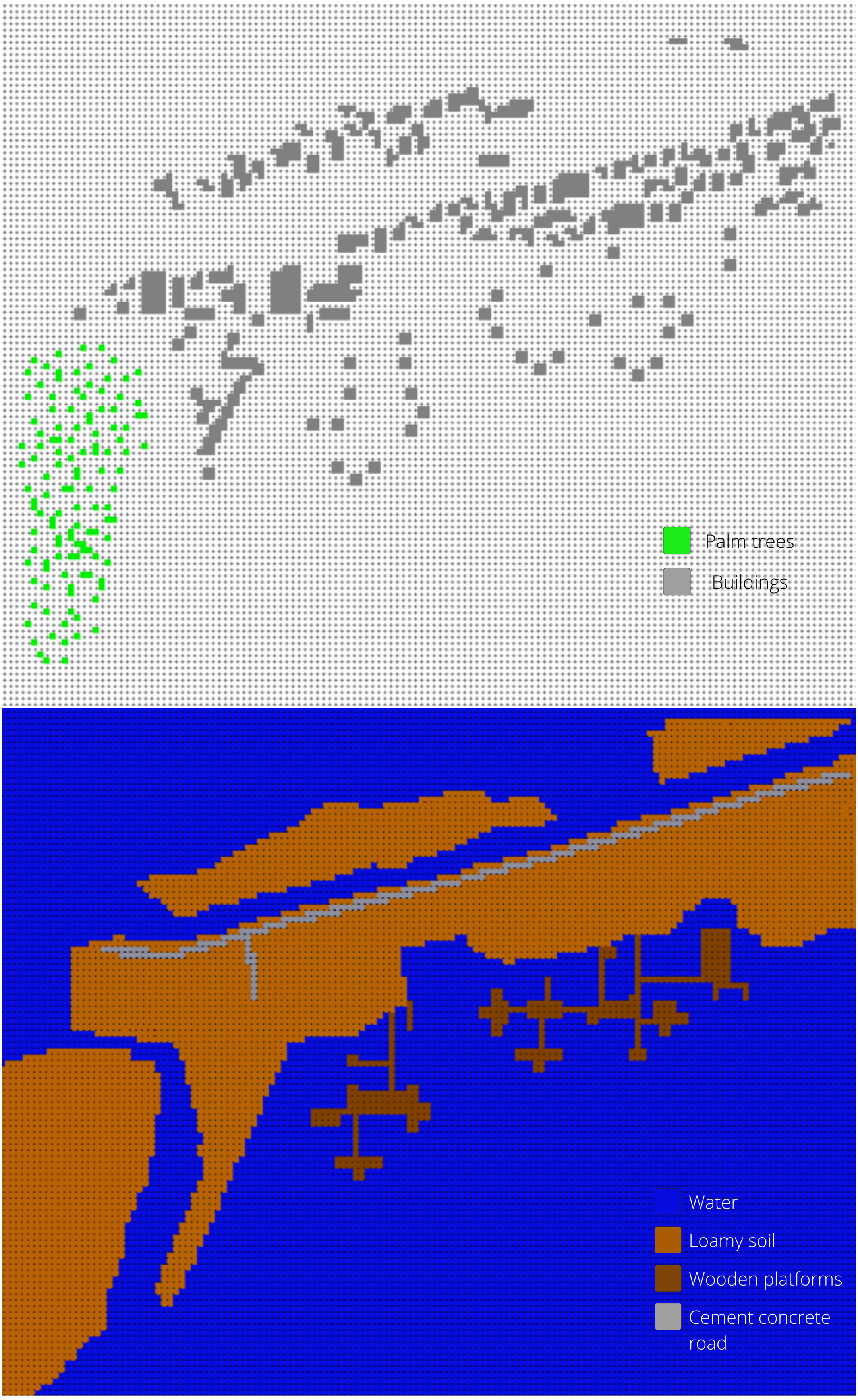

FIGURE 3.12: Building and soil profiles of the model in ENVI-met Spaces

3.2.2 Simulation File

The simulation is performed for 8th May 2021 from 0000 hrs to 2400 hrs. The meteorological boundary conditions use the forcing method, where wind, air temperature, radiation, and relative humidity are forced. This is a lateral boundary condition forcing type which allows the values of the 1D model to be copied to the border. It takes an EPW file as a FOX input format to obtain the meteorological data. The minimum interval for updating the wind inflow is 30 seconds. This data is provided in the plug-in ENVI guide.

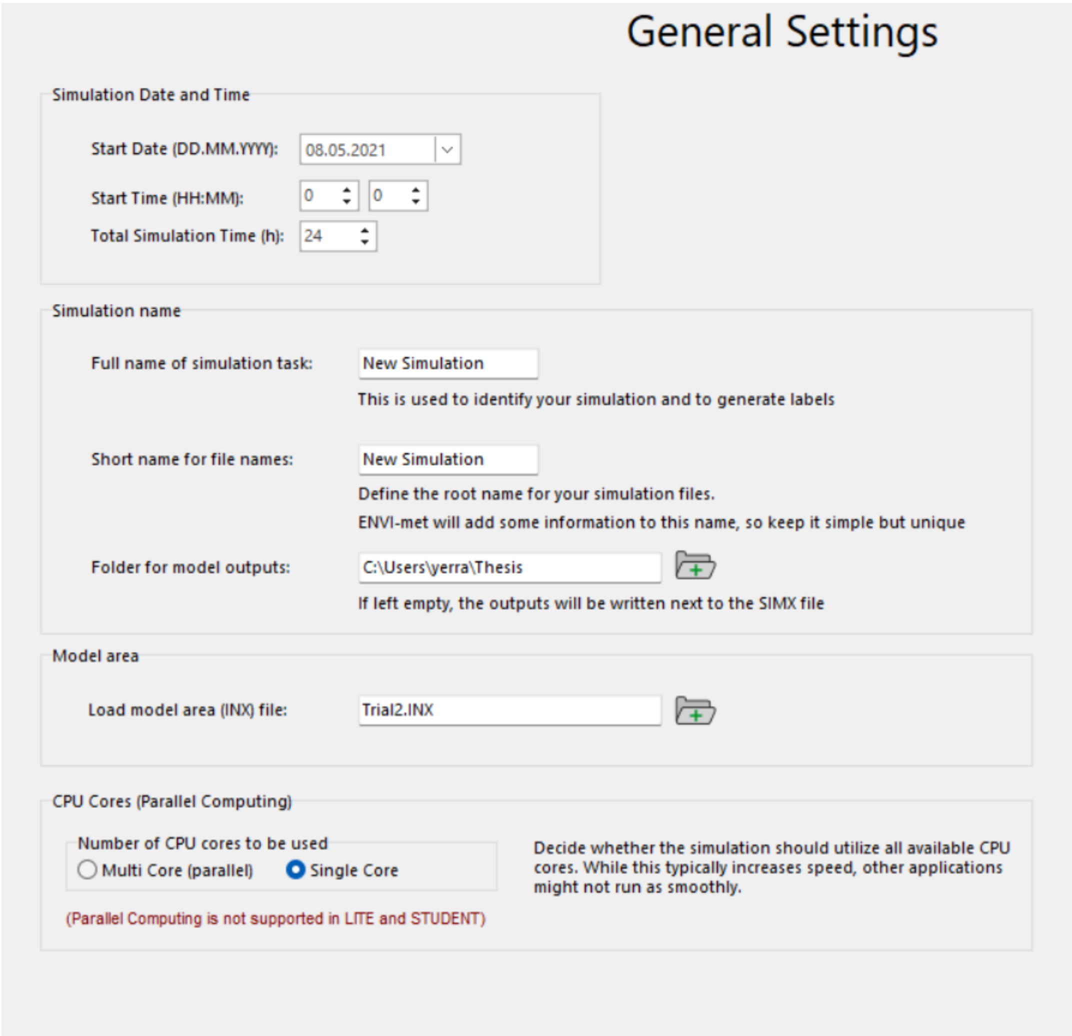

FIGURE 3.13: General settings of the simulation file in ENVI-guide

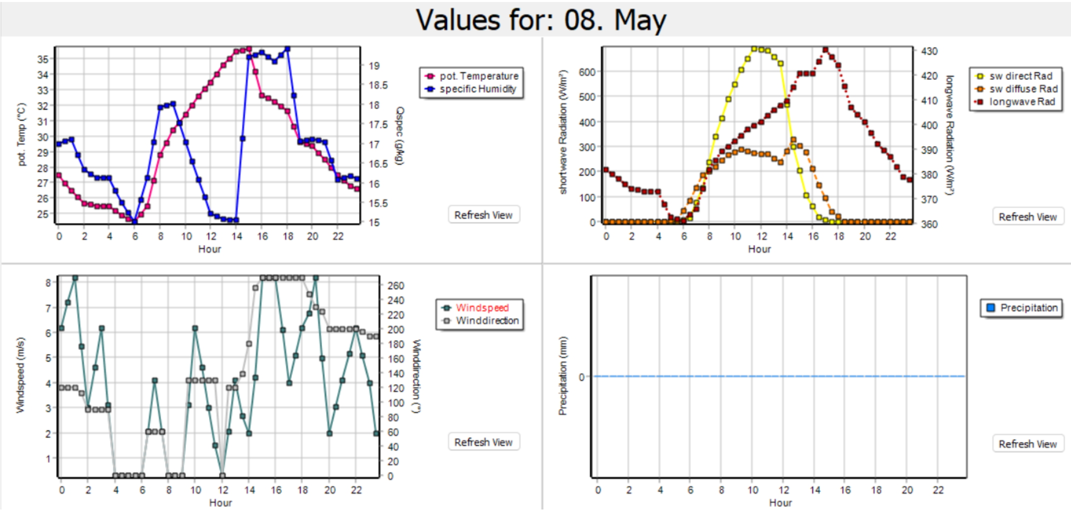

FIGURE 3.14: Fox file manager for 8th May in ENVI-guide

3.2.3 Database File

For the ENVI-met simulation, the model requires additional information about the materials, soils, and vegetation. The plug-in Database Manager is a global system with predetermined values for various frequently used components. Each component has a unique ID which is a six-sign alphanumerical code. The database is divided into two categories: the System database and the User database. Only the User database can be edited by the user. It is stored in an EML format. The material properties for the components of interest are provided in the Table 3.5 and 3.4.

	Concrete walls (existing buildings)	**Gypsum board panels (floating homes)**	**Steel metal roof**
Default thickness (m)	0.3	0.127	0.02
Absorption(frac)	0.7	0.4	0.2
Transmission(frac)	0	0	0
Reflection(frac)	0.3	0.6	0.8
Emissivity(frac)	0.9	0.9	0.1
Specific heat(J/kgK)	840	880	420
Thermal conductivity(W/mK)	0.86	0.17	45
Density(kg/m^3)	930	1000	8000

TABLE 3.4: Database material properties for surfaces and soil

	Loamy soil	Deep water	water	Wooden planks	Cement concrete
Type of material	Natural soil	0	0	Artificial material	Artificial material
Water content at saturation (m^3 water/ m^3 soil)	0.451	0	0	0	0
Water content at field capacity (m^3 water/ m^3 soil)	0.24	0	0	0	0
Water content at wilting point (m^3 water/ m^3 soil)	0.155	0	0	0	0
Matrix potential (m)	-0.478	0	0	0	0
Hydraulic conductivity (m/s)	7.000	0	0	0	0
Volumetric heat capacity (J/m^3K)	1.212	0	4.18	0.454	2.083
Clapp and Hornberger constant	5.39	0	0	0	0
Heat Conductivity (W/mK)	0	0	0.57	0.900	1.630

For the vegetation, the most commonly present plants in the Mercado region are Mangroves and Palm trees. Mangrove trees are not present in the ENVI-met database. Because of the lack of online information, palm trees are used instead in their location because of their everyday presence. Palm trees with the description LAD medium, large trunk, dense, 15m have been chosen for the simulations. The wooden platforms with green plantations have been incorporated into the model.

In the ENVI-met, initial water and soil temperatures are assumed by the software itself, and the CFD analysis is conducted per hour.

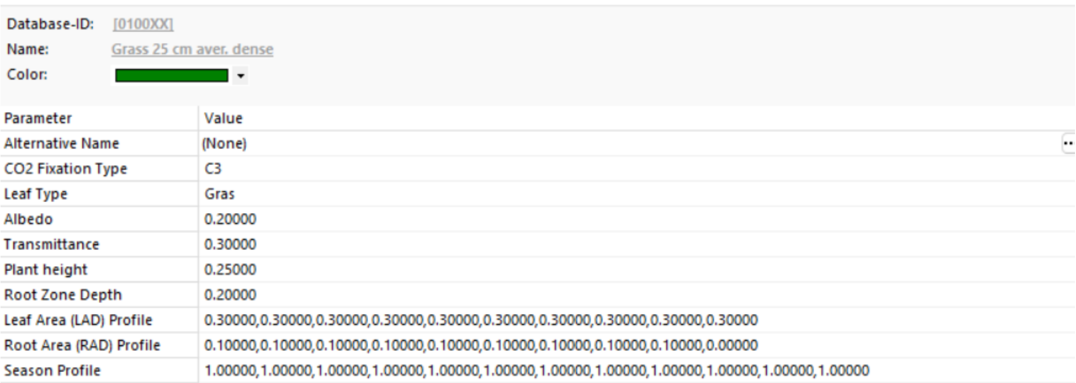

Database-ID: [0100XX]
Name: Grass 25 cm aver. dense
Color:

Parameter	Value
Alternative Name	(None)
CO2 Fixation Type	C3
Leaf Type	Gras
Albedo	0.20000
Transmittance	0.30000
Plant height	0.25000
Root Zone Depth	0.20000
Leaf Area (LAD) Profile	0.30000,0.30000,0.30000,0.30000,0.30000,0.30000,0.30000,0.30000,0.30000,0.30000
Root Area (RAD) Profile	0.10000,0.10000,0.10000,0.10000,0.10000,0.10000,0.10000,0.10000,0.10000,0.00000
Season Profile	1.00000,1.00000,1.00000,1.00000,1.00000,1.00000,1.00000,1.00000,1.00000,1.00000,1.00000,1.00000

FIGURE 3.15: Database material properties for vegetation

3.2.4 .edx file for BIO-met

BIO-met is a post-processing tool to calculate the human thermal comfort indices based on the output files obtained from the simulations. These output files are in the .edx format. It calculates the PET, UTCI, SET, and PMV based on simulation files and personal human parameters. The personal parameters are defined in Figure 3.16. The height, weight and clothing insulation are characteristic to the people of The Philippines.

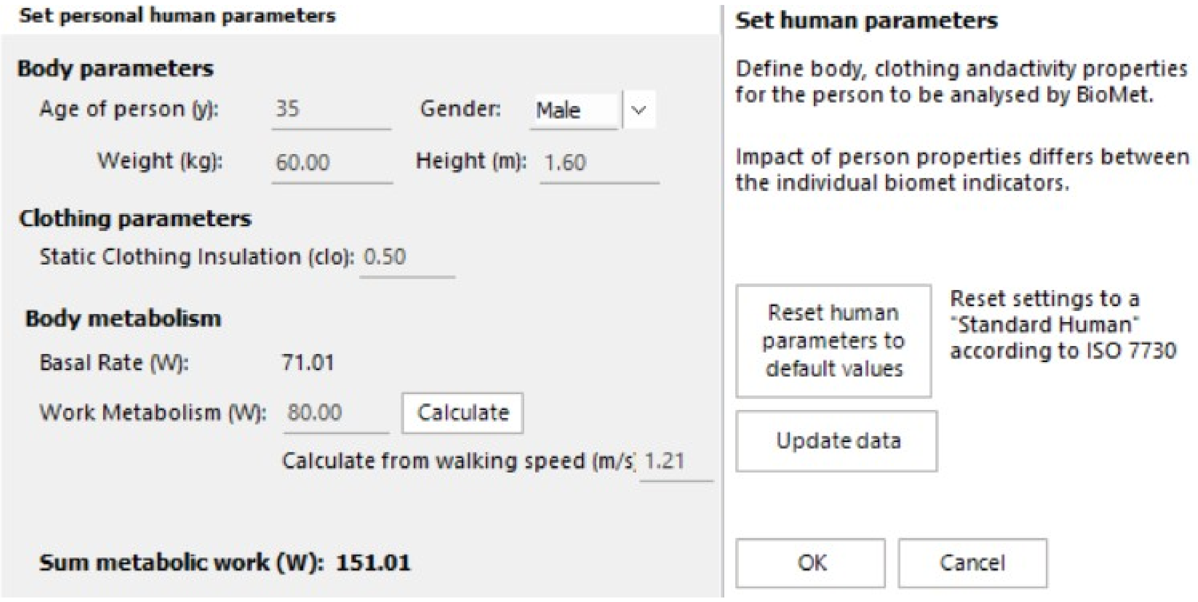

FIGURE 3.16: Personal Human Parameters for the study

3.3 Scenarios

Several scenarios based on the influencing parameters are tested in the ENVI-met software. The categories include urban morphology, water body effect, vegetation, and the original model. The general assumptions which pertain to all the models have been discussed in the previous sections, whereas further details are presented in each scenario section. The different scenarios are tabulated in Table 3.5.

TABLE 3.5: Model scenarios with abbreviations

Model Scenario	**Abbreviation**
Original	O1
Urban Forms with vegetation	U1, U2V, U3V
Original + Vegetation	O2
Replacing waterbody with pavement	O3
Urban forms without vegetation	U2, U3

The different scenarios considered are elaborated in the following subsections.

3.3.1 Original Model (O1)

The building and soil profiles of the original model are given in Fig 3.12. All the following scenarios are compared with this to determine its comfortability, and improvements. Therefore, this can be considered as the baseline.

3.3.2 Original Model with Vegetation (O2):

In this model, 12.5 percent vegetation is added to the original typology. The vegetation is scattered across the open areas on the wooden platforms, reducing the overall vegetative density. Extra wooden platforms were added to incorporate the added vegetation. The types of vegetation used are given in Table 3.6. The building and soil profiles are given in Figure 3.18.

TABLE 3.6: Vegetation data for U1, U2, and U3

Vegetation	Albedo	Transmittance
Grass 50 cm avg dense	0.2	0.3
Soja 63 cm	0.2	0.3
Funkia (Hosta) 40 cm	0.2	0.3
Hedges 1-2m	0.2	0.3

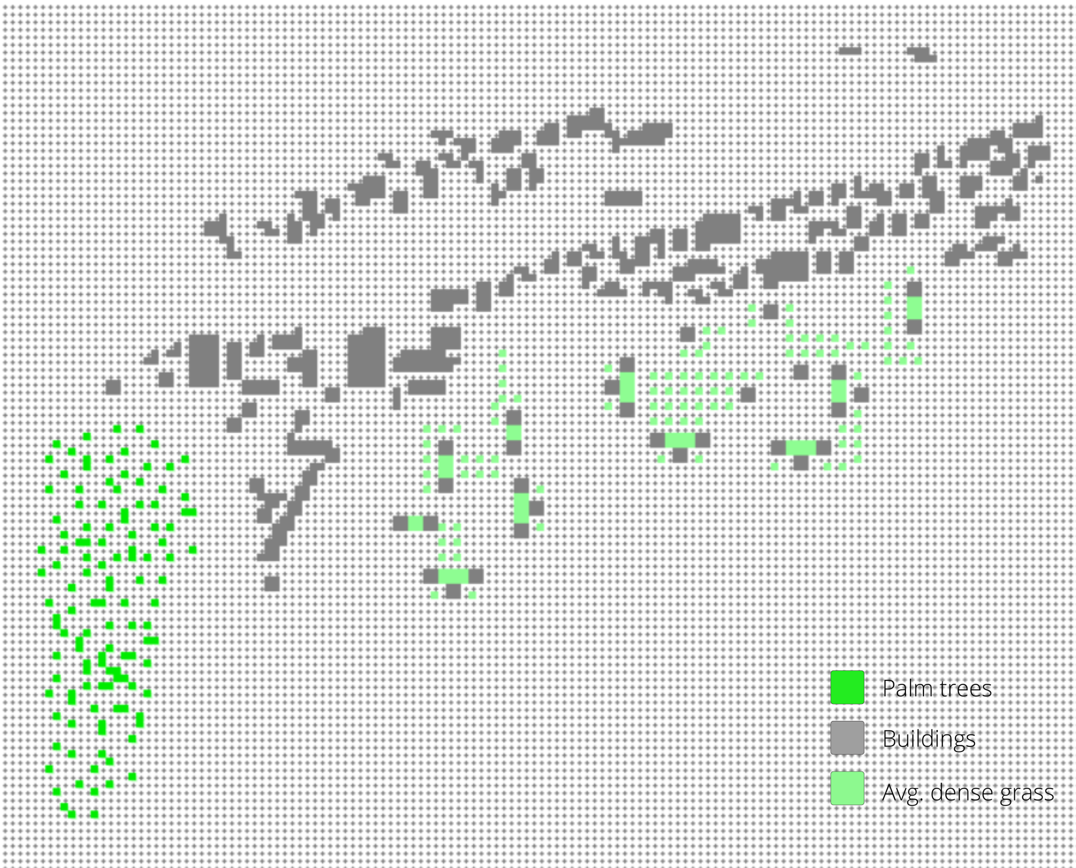

FIGURE 3.17: Building profile for Scenario O2

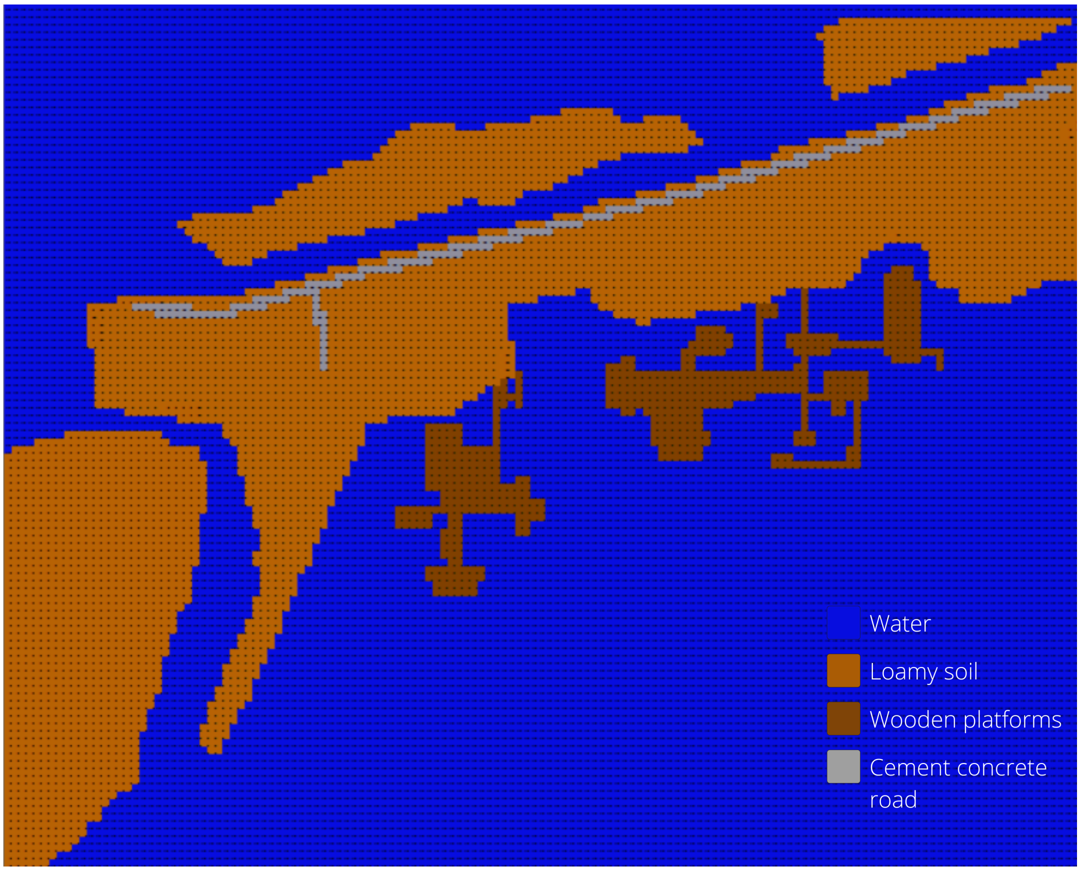

FIGURE 3.18: Soil profile for Scenario O2

3.3.3 Original Model with pavement replacement (O3):

In this model, the water body of the model area is entirely changed to gray concrete pavement. This drastically increases the heating properties of the surface. This scenario was analyzed to identify the water body's influence on the potential air temperature and wind speeds. Figure 3.19 shows the building and soil profiles with these modifications.

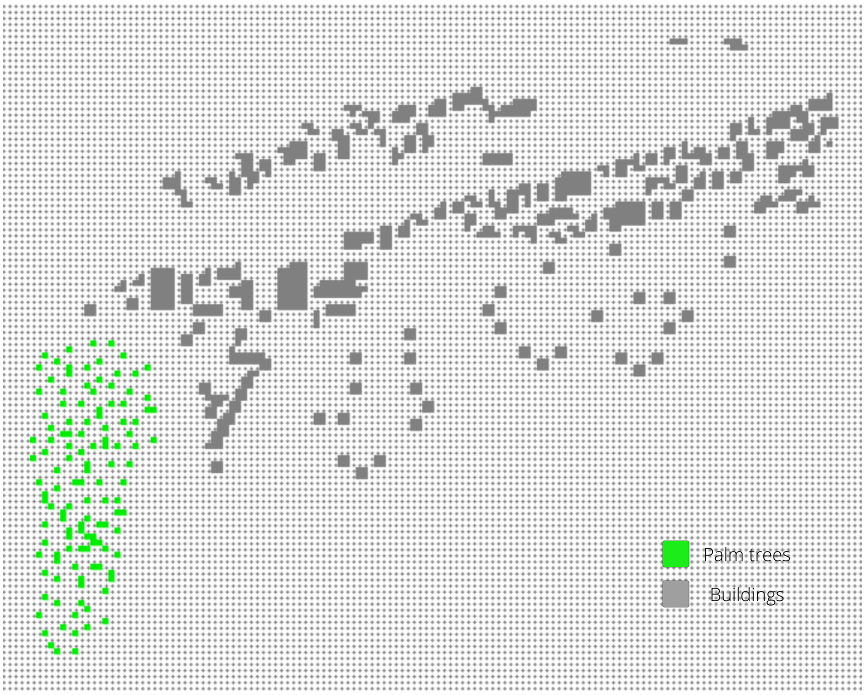

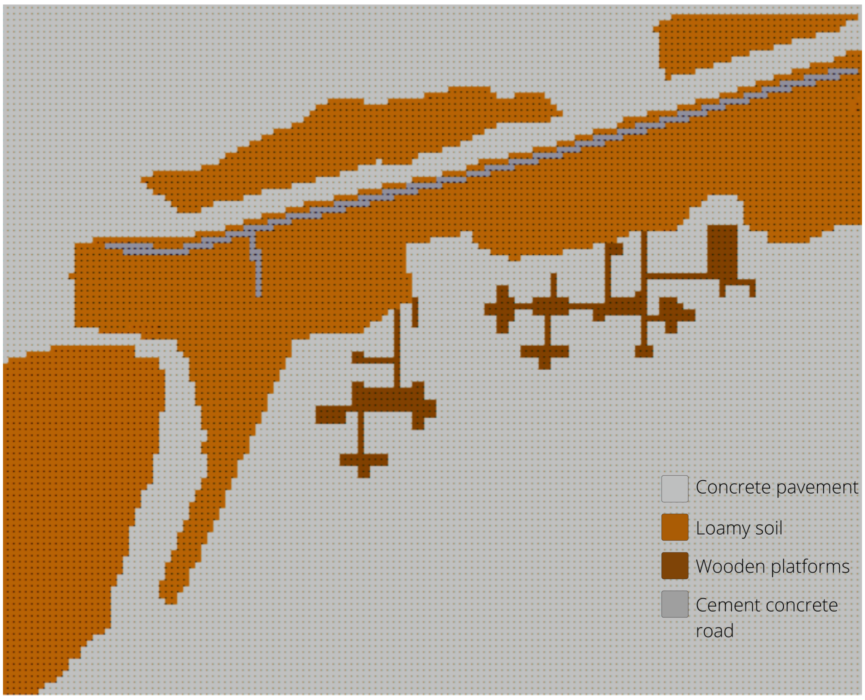

FIGURE 3.19: Building and soil profile for Scenario O3

3.3.4 Urban Form 1 (U1):

In this model, changes have been made to the urban layout to make it more symmetrical in appearance. This is to create an enclosure of buildings from the outside area to the inside area, to act as a wind block. However, it has a sufficient gap of at least 6 to 9 meters at the minimum between the clusters to avoid pressure-induced winds. It also provides increased outdoor areas for people to gather and plant more vegetation. In this scenario, approximately 10 percent of clustered and scattered vegetation is added to the typology. Apart from the vegetation already provided in Table 3.6, hedges are also provided with albedo and transmittance values of 0.2 and 0.3, respectively. They are 1-2 meters in height. This urban configuration also eliminates scattered houses and groups them together for better connectivity amongst residents. The typology is given in Figure 3.20.

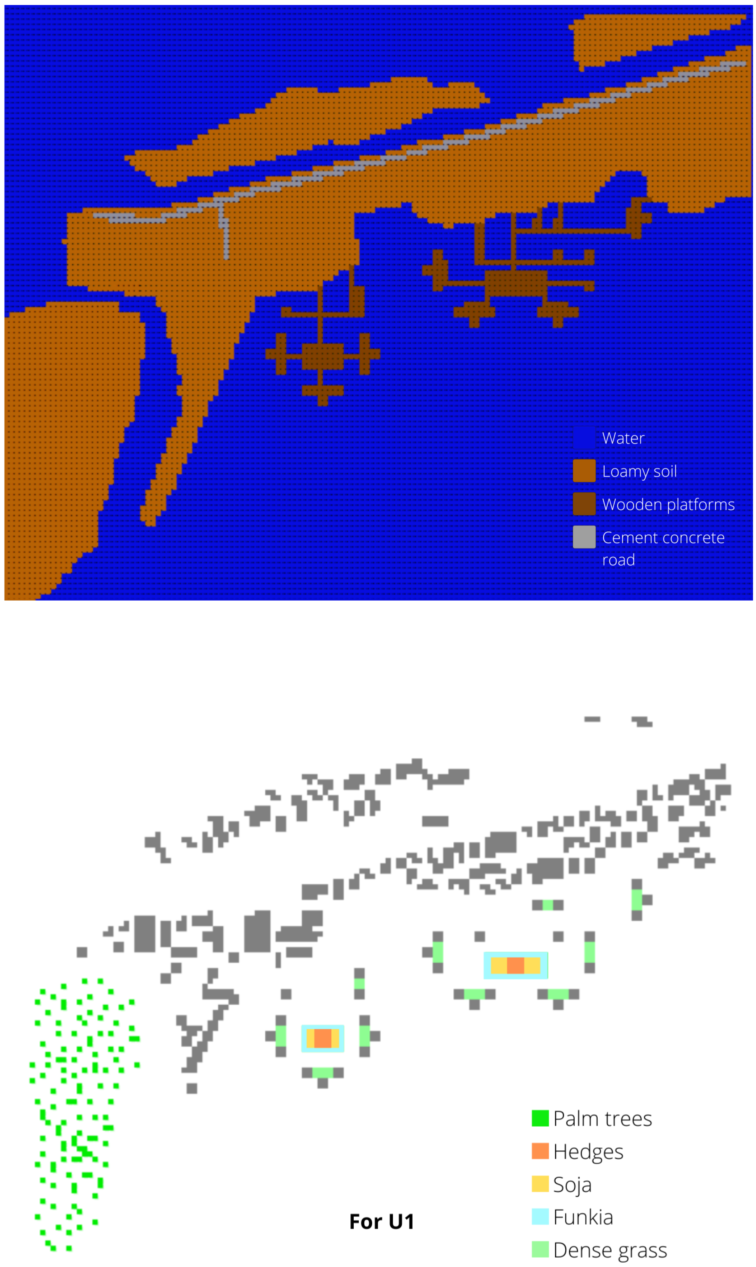

FIGURE 3.20: Soil, building, and vegetation, profile for Scenario U1

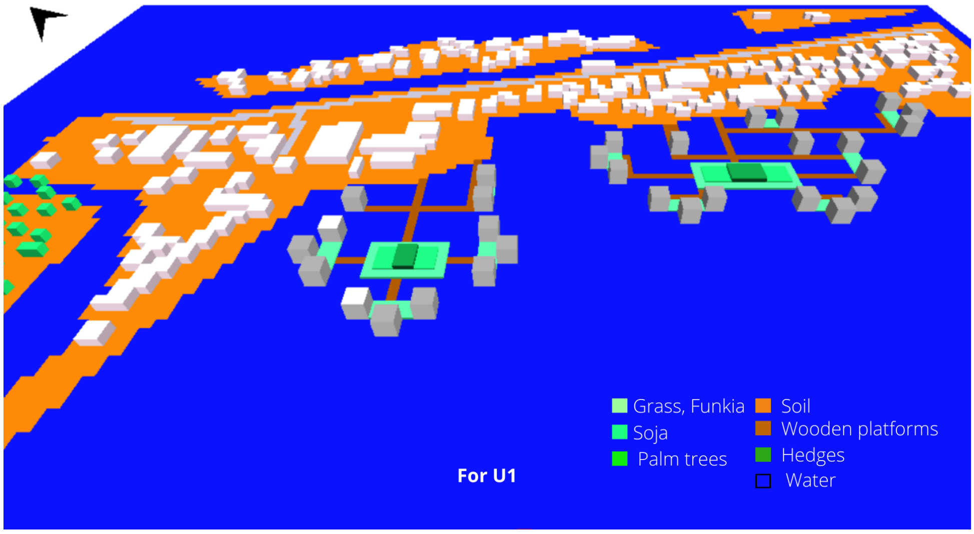

FIGURE 3.21: 3D view for Scenario U1

3.3.5 Urban Form 2 (U2V):

This configuration extends the U1, with further openness between the building clusters. This is primarily done to increase the percentage of vegetation in the open spaces to approximately 30 percent of the area of the floating home. The de-densification of the buildings, however, reduces the shading capacity of the adjacent buildings. The vegetation used here is the same as U1. Figure 3.23 gives the profile data.

3.3.6 Urban Form (U2):

U2 uses the same urban configuration without the vegetation, and is calculated from 1200 hrs to 1500 hrs (12pm - 3pm). The entire time span of 24 hours could not be calculated due to extensive computational load and limited time span (4-7 days for each simulation). This scenario is to determine the affect of urban form alone without the influence of vegetation.

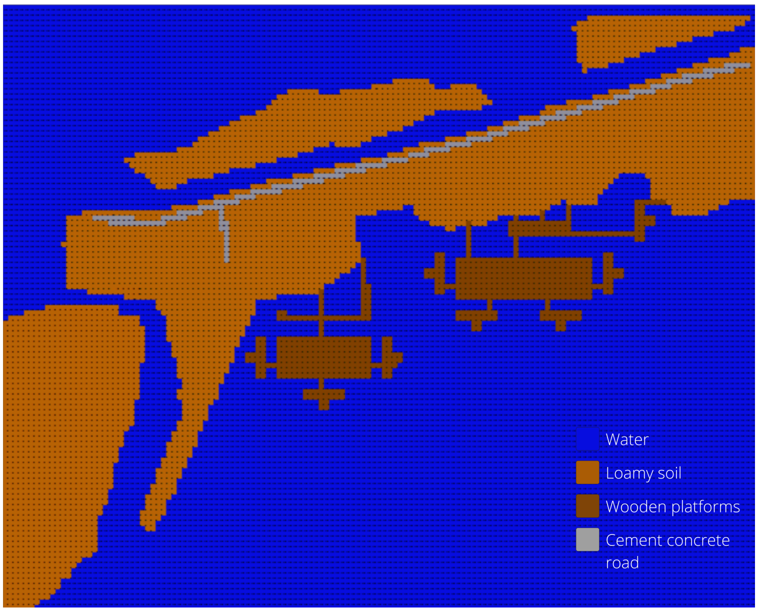

FIGURE 3.22: Soil profile for Scenario U2V

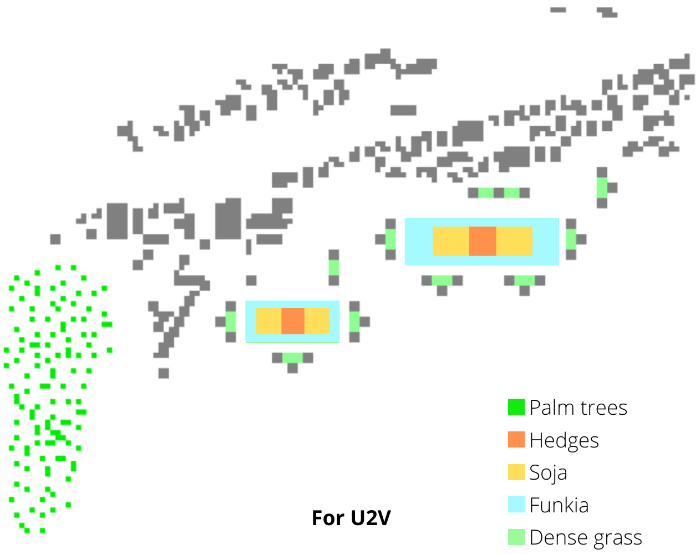

FIGURE 3.23: Building, and vegetation, profile for Scenario U2V

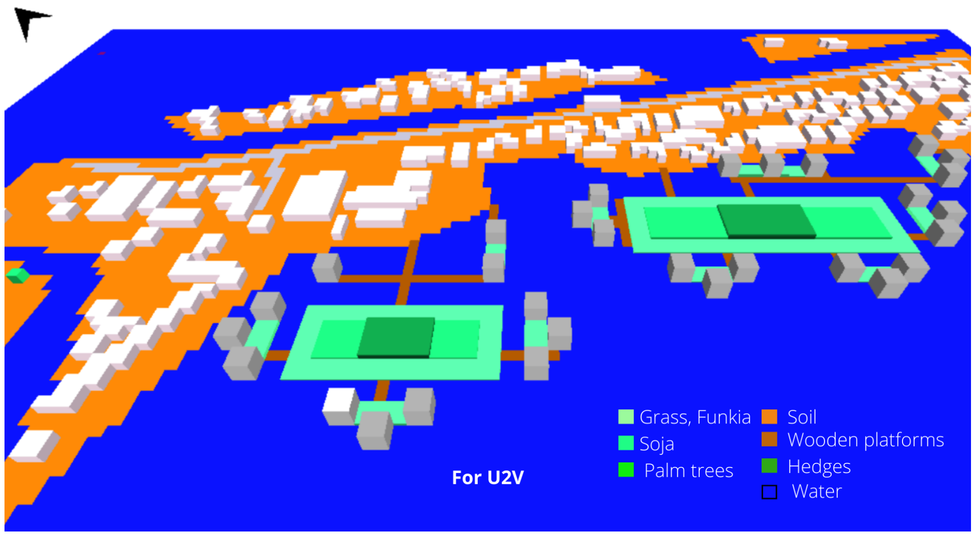

FIGURE 3.24: 3D view for Scenario U2V

3.3.7 Urban Form (U3V):

This configuration incorporates the pentagon courtyard-style clusters. It provides maximum shading area throughout the day amongst polygonal courtyards [79]. It also provides an increase in the number of open spaces. Additionally, the same vegetation as U2V is also present in this case. Figure 3.25 gives the building and soil profiles for U3V.

3.3.8 Urban Form (U3):

U3 uses the same urban configuration without the vegetation, and is calculated from 1200 hrs to 1500 hrs (12pm - 3pm). The entire time span of 24 hours could not be calculated due to extensive computational load and limited time span (4-7 days for each simulation). This scenario is to determine the affect of urban form alone without the influence of vegetation.

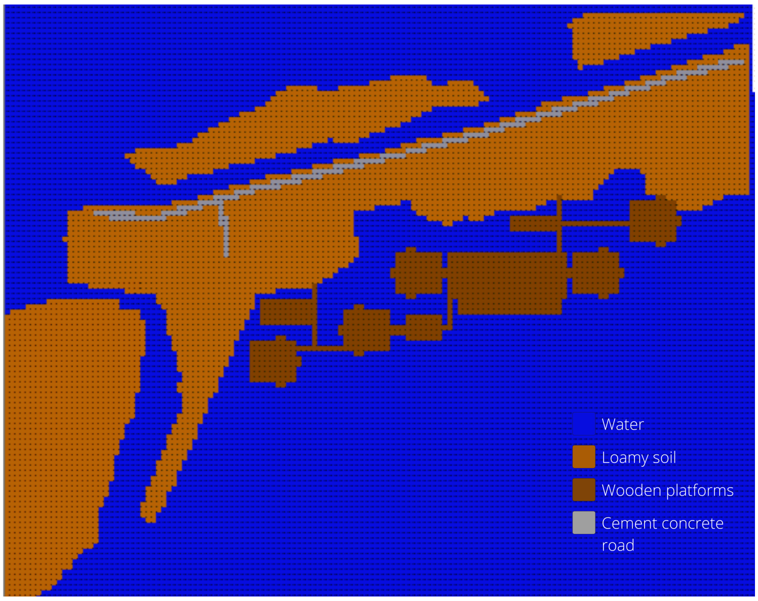

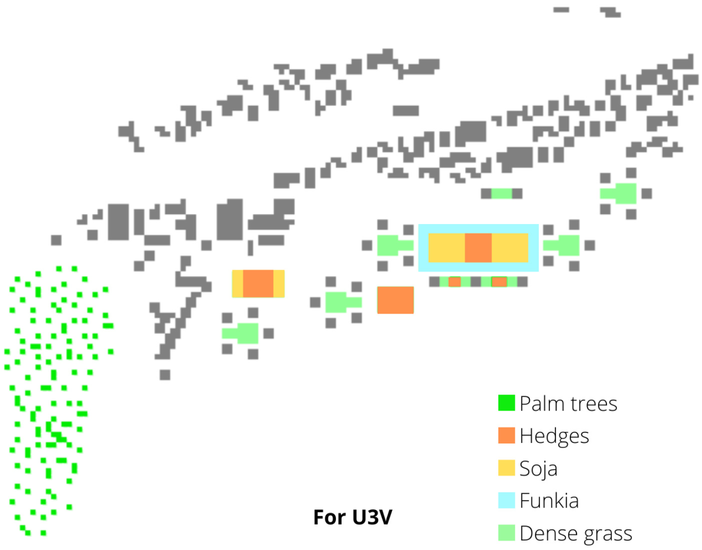

FIGURE 3.25: Soil, building, and vegetation, profile for Scenario U3V

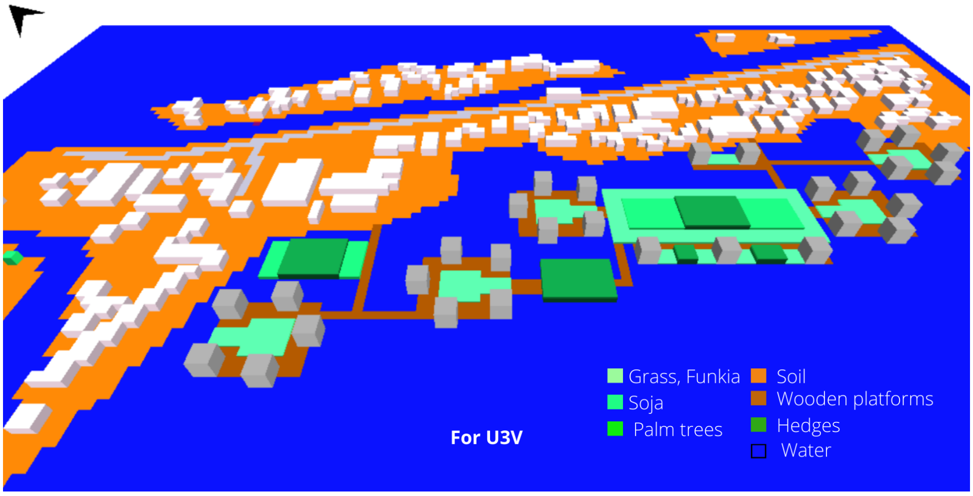

FIGURE 3.26: 3D view for Scenario U3V

Chapter 4

Results and Discussions

In this Chapter, the thermal comfort, wind comfort, and other parameters will be discussed from four points in the model area for all the urban configurations. These points are marked in Figure 4.1.

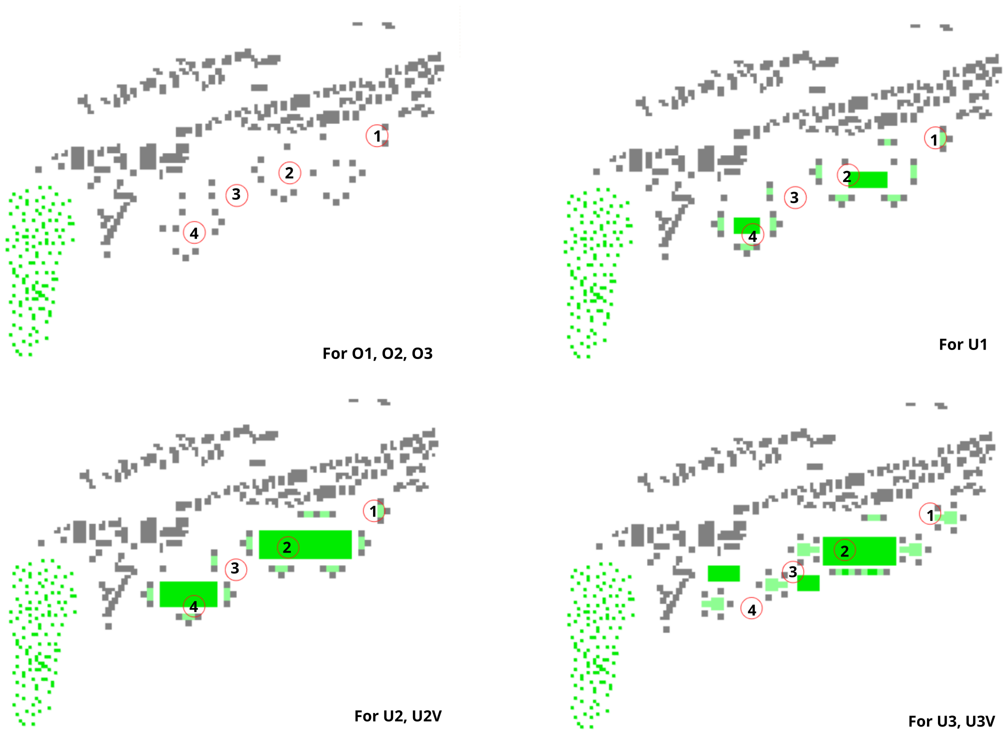

FIGURE 4.1: Four points of study in all the urban configurations

These 4 points provide information about a variety of locations in the floating homes model area.

- *Point 1:* This area constitutes the combination of floating homes and the open area in front of the housing.
- *Point 2*: This area constitutes the primary open space for gathering, with and without vegetation. This is of significant importance to the study.
- *Point 3:* This area constitutes the water body surface. However, in U3V and U3, this area falls under the area of the housing clusters.

- *Point 4:* This area constitutes another open space for gathering. However, this is smaller in size and is densely enclosed by housing from most sides.

Four time periods have been chosen for this study. They include:

- 0200 hrs, or 2 am: This time period was chosen to understand the influence on vegetation, waterbody, and urban form during the nighttime due to its significant changes
- 0800 hrs, or 8am: This time was chosen to understand the influence of micro-climate during early morning hours
- 1400 hrs, or 2 pm: This time period was chosen because highest temperatures were recorded during this hour
- 1900 hrs, or 7pm: This time period was chosen because highest wind speeds were recorded during this hour

In this section, only 0200 hrs and 1400 hrs is elaborated upon to understand the impact on microclimate during peak day and night hours, and for ease of understanding. The other time periods, 0800 hrs and 1900 hrs for the thermal comfort is tabulated in Appendix B.

4.1 Thermal comfort

PET is discussed in terms of thermal comfort. Firstly, the thermal comfort parameters: potential air temperature, wind speed, mean radiant temperature, and relative humidity are elaborated upon for all urban forms, along with its thermal comfort index. PET is chosen over UTCI because it is the most advanced thermal comfort index calculated by ENVI-met as it also takes into account the personal human parameters, clothing insulation and body metabolic rate. Peak temperatures are recorded at 1400 hrs, i.e., at 2pm on 8th May 2021 and are therefore considered as the maximum thermal index value that can be obtained. Thus, it is going to be the primary time stamp of this study. Along with this, to understand the night time effect of the configurations, 0200 hrs, i.e., at 2am on 8th May 2021 is also studied. All the thermal comfort parameters are tabulated and graphed for these 2 time stamps. Additional thermal comfort information about the time stamps 0800 hrs (8:00 am) and 1900 hrs (7:00 pm) is provided in Appendix B. In the tabulated results for the Points, the column *Change in PET from O1 (deg cel)*, a positive sign indicates that the PET value has reduced from the original scenario O1, leading to an improvement in performance. A negative sign in PET change indicates that the PET value has increased from the original scenario O1, leading to a decline in performance.

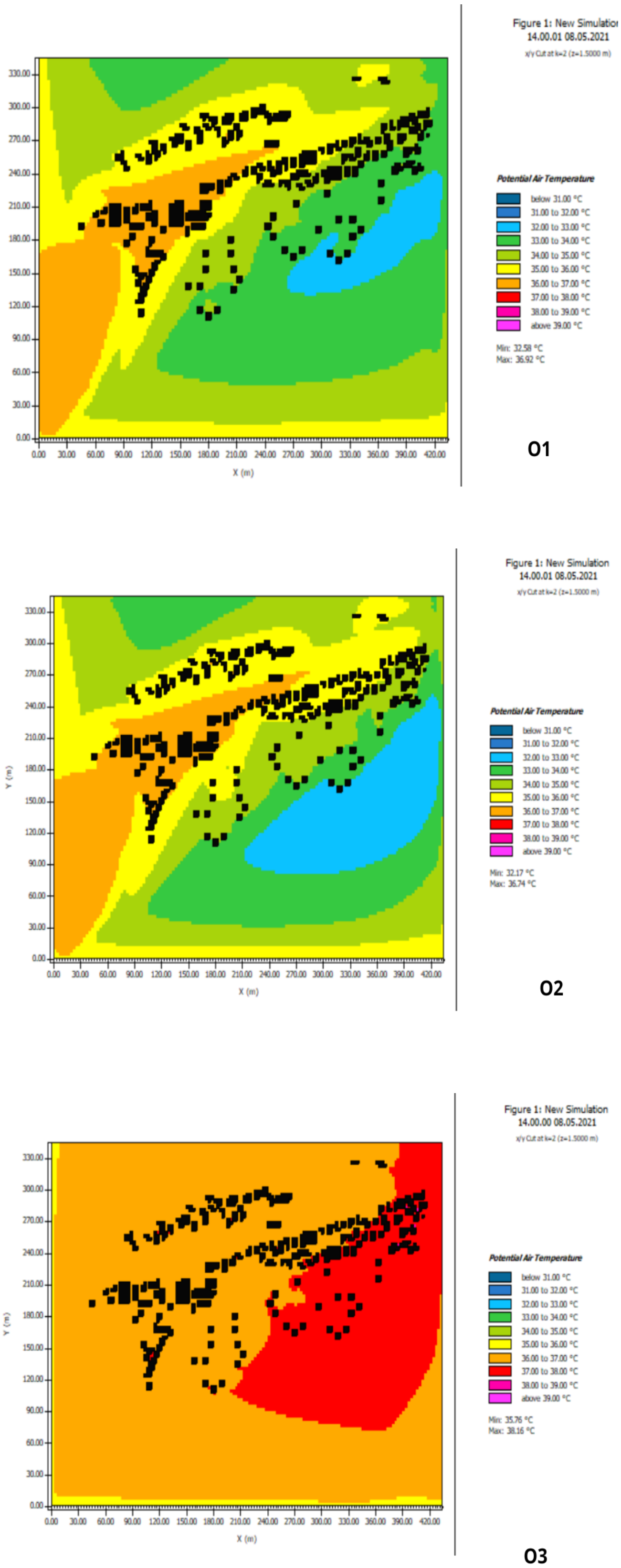

FIGURE 4.2: Potential air temperature at 1400 hrs for O1, O2, O3

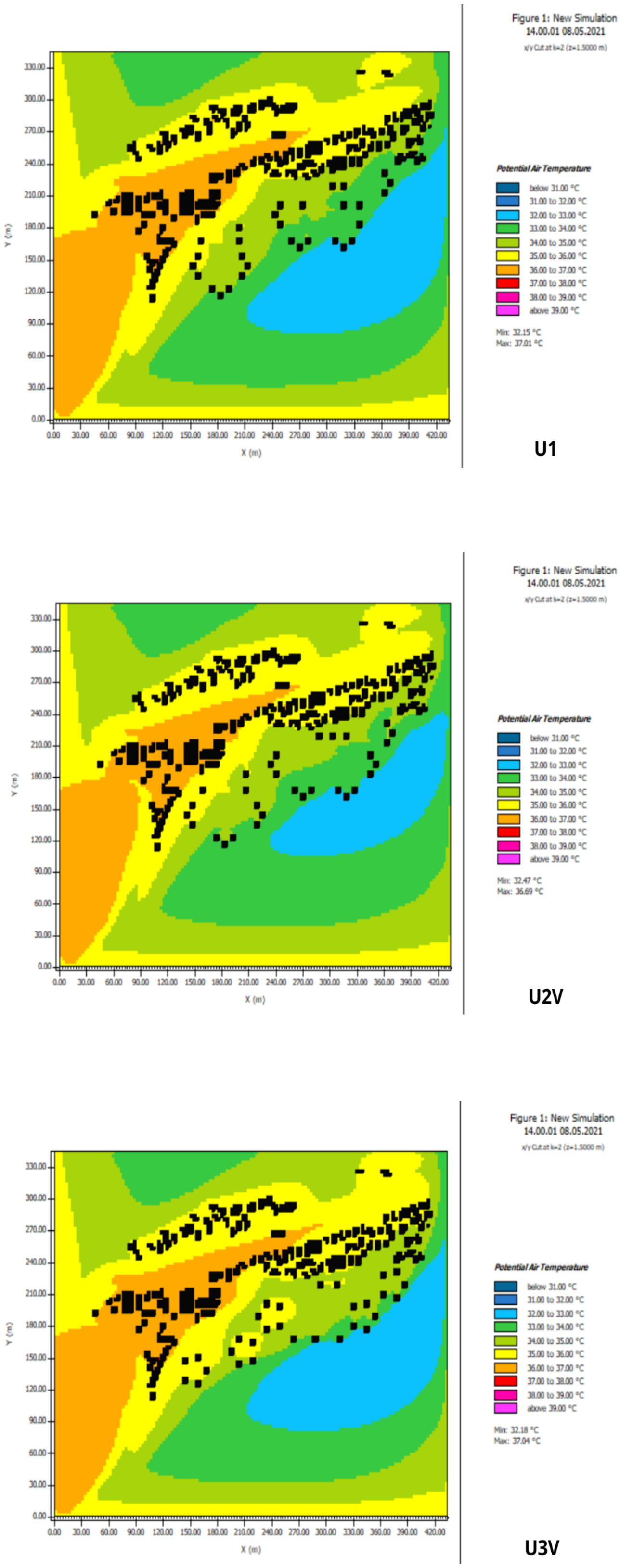

FIGURE 4.3: Potential air temperature at 1400 hrs for U1, U2V, U3V

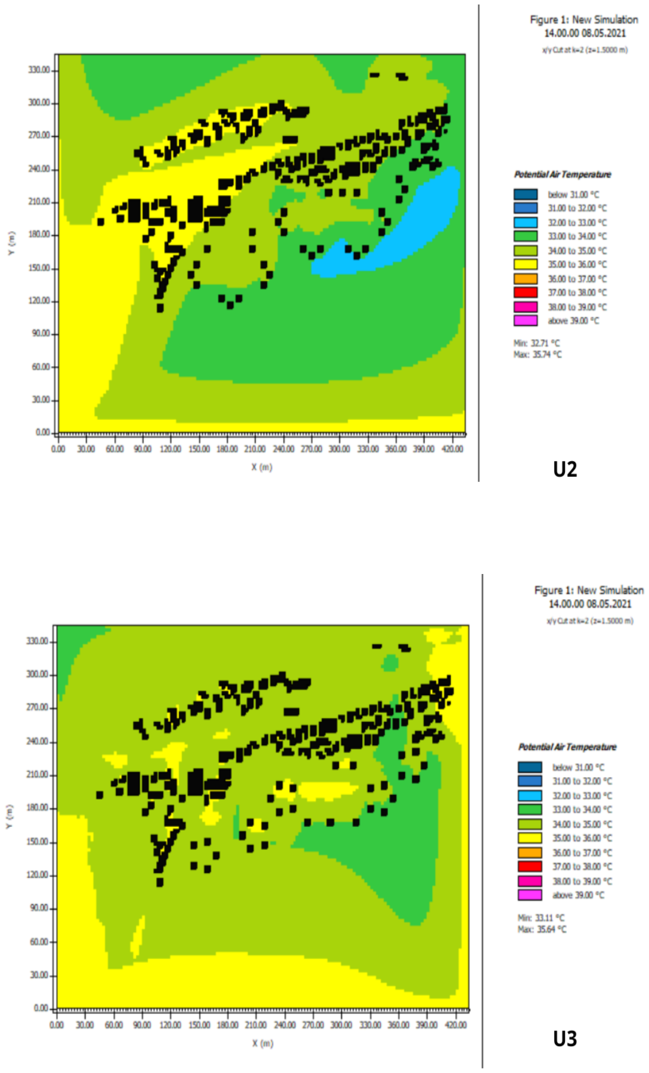

FIGURE 4.4: Potential air temperature at 1400 hrs for U2, U3

4.1.1 Point 1

Figure B.1 in Appendix B represents information for all the thermal comfort parameters and time periods across all the urban configurations. This section discusses only time stamps 0200 hrs and 1400 hrs.

This area is a combination of scattered vegetation in terms of dense grass, and housing. The tabulated results for 0200 hrs and 1400 hrs are provided in Table 4.1.

TABLE 4.1: Thermal comfort parameters for Point 1 across all urban configurations

Scenarios		**Potential air temperature (deg cel)**	**Wind speed (m/s)**	**Mean radiant temperature (deg cel)**	**Relative humidity (%)**	**PET (deg cel)**	**Change in PET from O1 (deg cel)**
0200 hrs	O1	25.2	1.4	14.7	88	18.5	
	O2	25.2	1.5	15	88	18.7	-0.2
	O3	25.4	1.5	16.1	87.8	19	-0.5
	U1	25.2	1.3	14.5	88	18.5	0
	U2V	25.2	1.2	14.3	87	18.8	-0.3
	U3V	25.2	1.2	14.3	87.6	18.8	-0.3
1400 hrs	O1	33.3	1.5	42	55.5	36	
	O2	33.8	1.6	43	52	33.6	2.4
	O3	37.2	1.3	60	44.3	43.6	-7.6
	U1	33.1	1.3	42.3	53.8	36	0
	U2V	33.7	1.3	42	54	37.2	-1.2
	U3V	34.1	1.2	41	51.3	37.6	-1.6
	U2	33.5	1.4	40.6	55	35.2	0.8
	U3	34.3	1.4	42	60	32.9	3.1

Potential air temperature: The graphical representation of potential air temperature for all the scenarios is provided in Figure 4.5. For 1400 hrs, the O1 registers a value of 33.3 °C. In O3, the value has increased to 37.2 °C. This is due to the higher thermal conductivity of the pavement. The temperature values are similar in all the configurations, with an approximate marginal difference of 0.5 °C between the cases. It has increased in all the cases, except for U1, which is likely a combined effect of shading from the adjacent buildings, vegetation, and openness. During 0200 hrs, the temperatures are same in all the scenarios except O3.

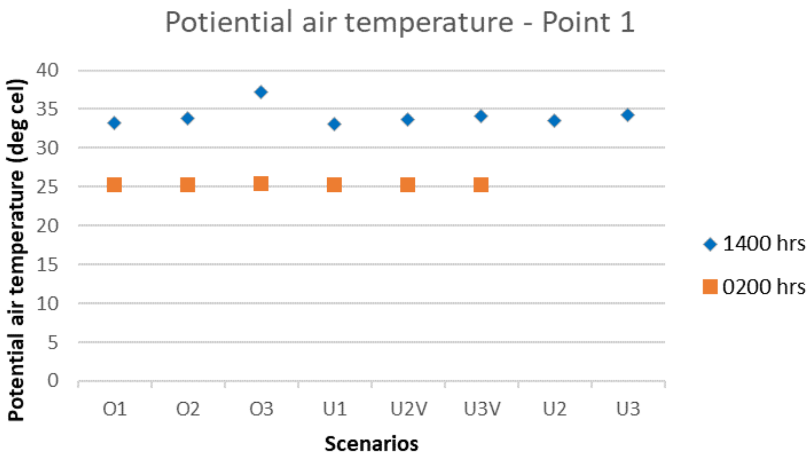

FIGURE 4.5: Potential air temperature for 0200 hrs and 1400 hrs for all scenarios - Point 1

Wind speed: The graphical representation of wind speed for all the scenarios is provided in Figure 4.6. Wind speeds have reduced in all the scenarios except O2. At 1400 hrs, the wind speed was recorded at 1.5 m/s. And the lowest recorded wind speed is in U3V with 1.2 m/s. Similar pattern follows during 0200 hrs. This is due to the enclosure of Point 1 from all sides, along with the effect of vegetation. It is interesting to note that this is also the point of maximum temperatures. This is due to the inverse relationship between temperature and wind speeds. Because of this relationship, it may not be comfortable for the residents with the reduced wind speeds because of this relationship.

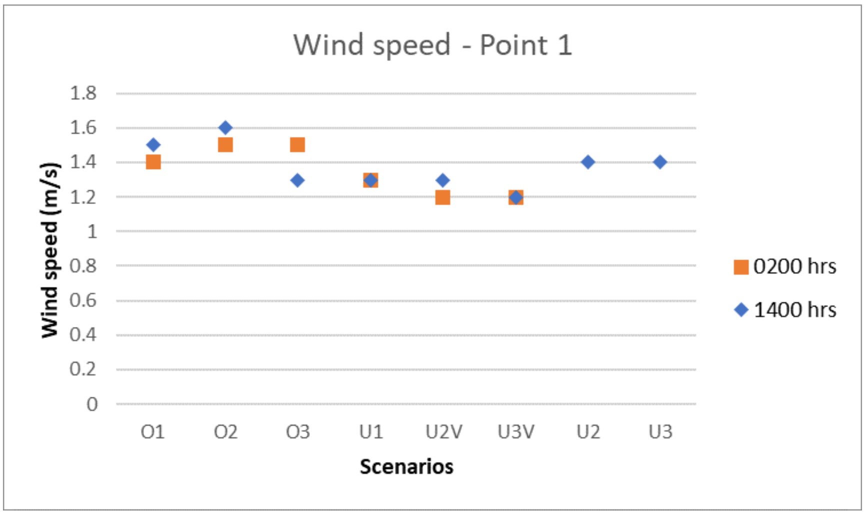

FIGURE 4.6: Wind speed for 0200 hrs and 1400 hrs for all scenarios - Point 1

Mean radiant temperature: The graphical representation of mean radiant temperature for all the scenarios is provided in Figure 4.7. At 1400 hrs, the mean radiant temperature for O1 is 42 °C. For O3, the MRT is exceedingly high at 60 °C. The lowest recorded value is 40.6 °C in U2, i.e., U2 without vegetation. During midnight, at 0200 hrs, the MRT reduces for all the scenarios except O2. The vegetation present at Point 1 is small plantations and grass, thereby not affecting the MRT much in any of the scenarios.

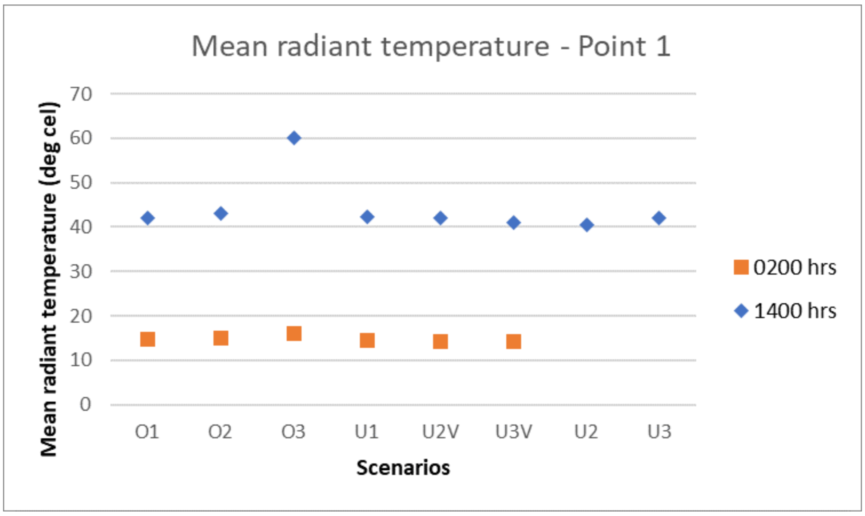

FIGURE 4.7: Mean radiant temperature for 0200 hrs and 1400 hrs for all scenarios - Point 1

Relative humidity: The graphical representation of Relative Humidity for all the scenarios is provided in Figure 4.8. Relative humidity shares an inverse relationship with air temperatures. This is because cooler air has a lower saturation point and cannot contain as much moisture as warm air. The highest recorded value is at 0200 hrs with 88 percent. It is similar in all scenarios with a marginal difference of 0.2 percent. At 1400 hrs, O1 records at 55.5 percent. O3 registers the lowest RH value at 44.3 percent. This is because of higher temperatures and lower evaporation rates. U2V has a slightly lower value of 54 percent.

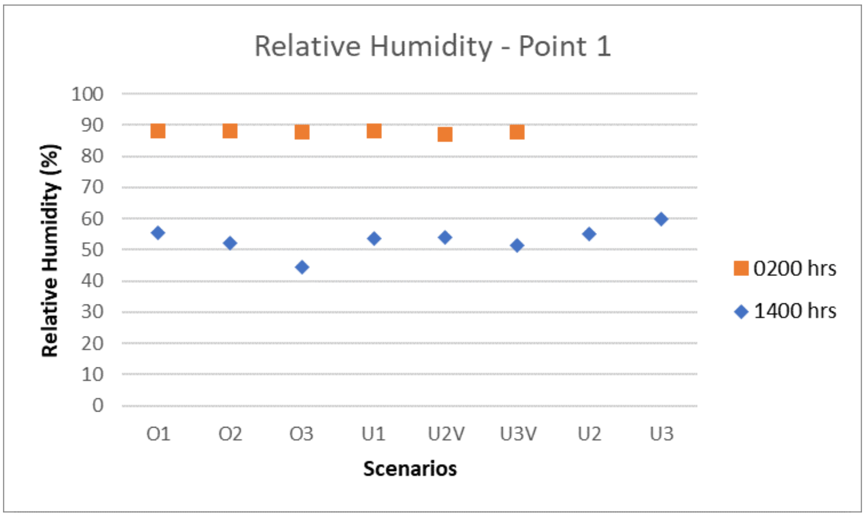

FIGURE 4.8: Relative Humidity for 0200 hrs and 1400 hrs for all scenarios - Point 1

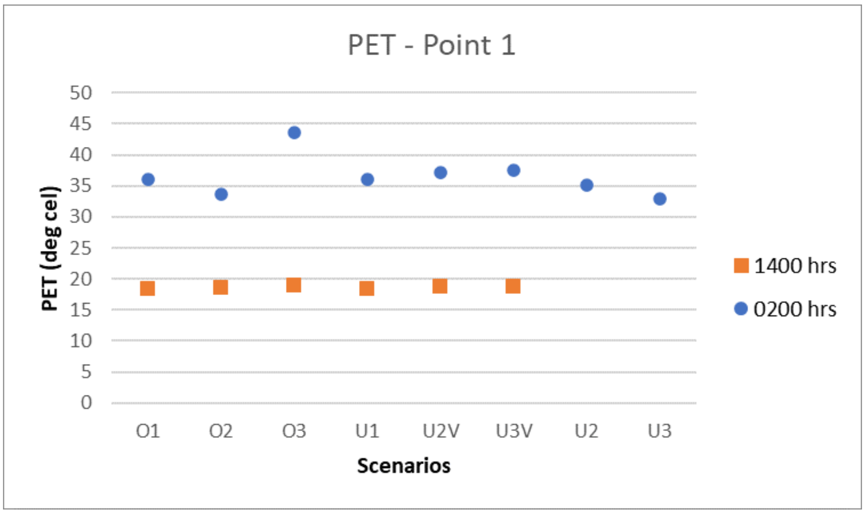

FIGURE 4.9: PET for 0200 hrs and 1400 hrs for all scenarios - Point 1

PET: The graphical representation of PET for all the scenarios is provided in Figure 4.9. The PET values are tabulated in Table 4.1. Since the vegetation present here is minimal, the changes in the index values are not very significant either. At 1400 hrs, O1 registers a value of 36 °C. The lowest PET value is in U3V with 32.9 °C. Understandably, the PET value only marginally increases during nighttime.

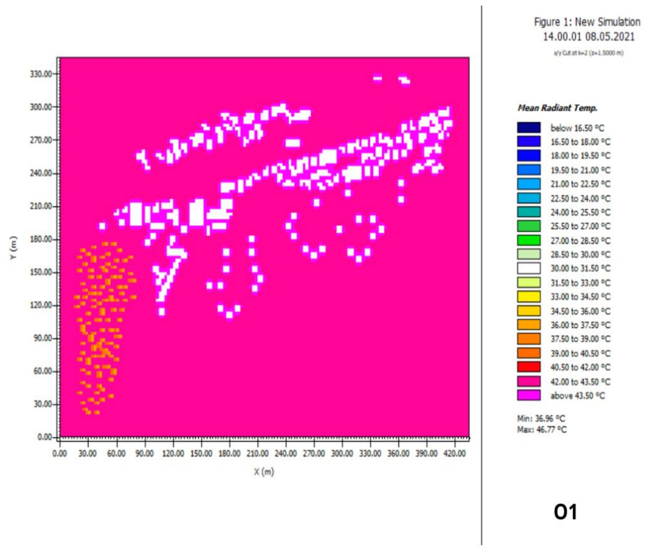

FIGURE 4.10: Mean radiant temperature at 1400 hrs for O1

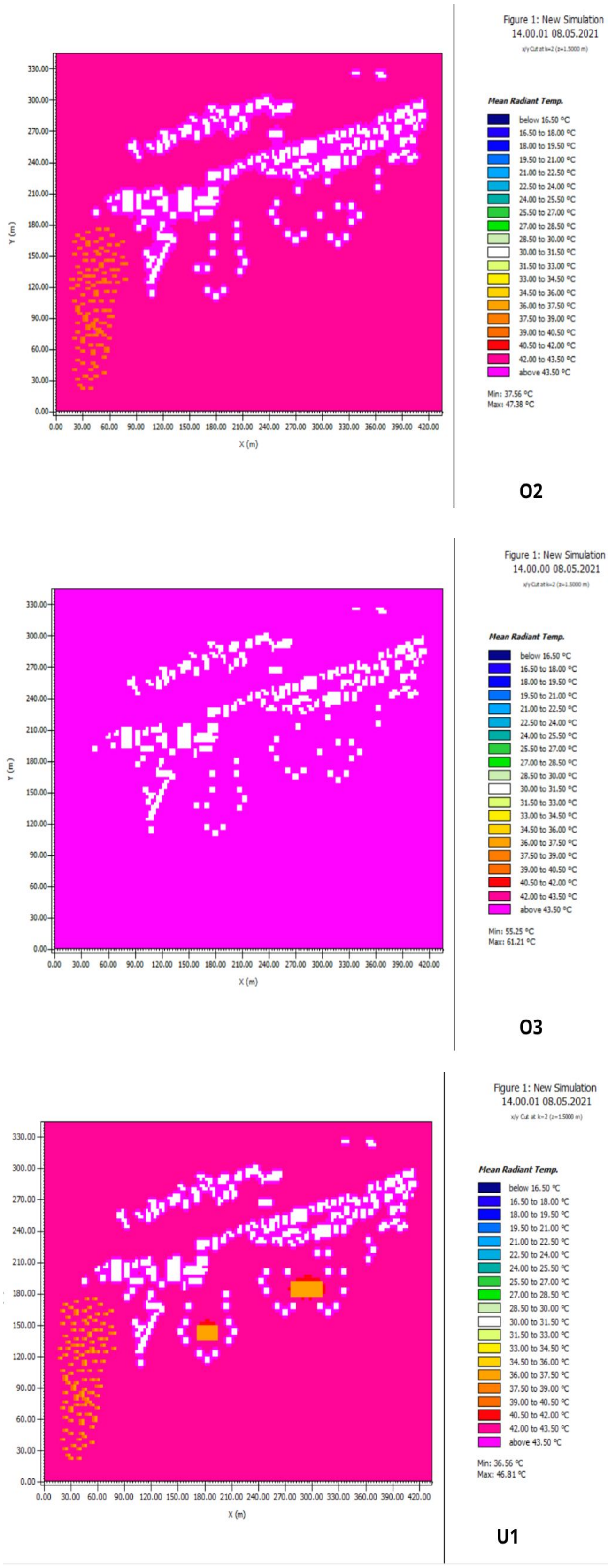

FIGURE 4.11: Mean radiant temperature at 1400 hrs for O2, O3, U1

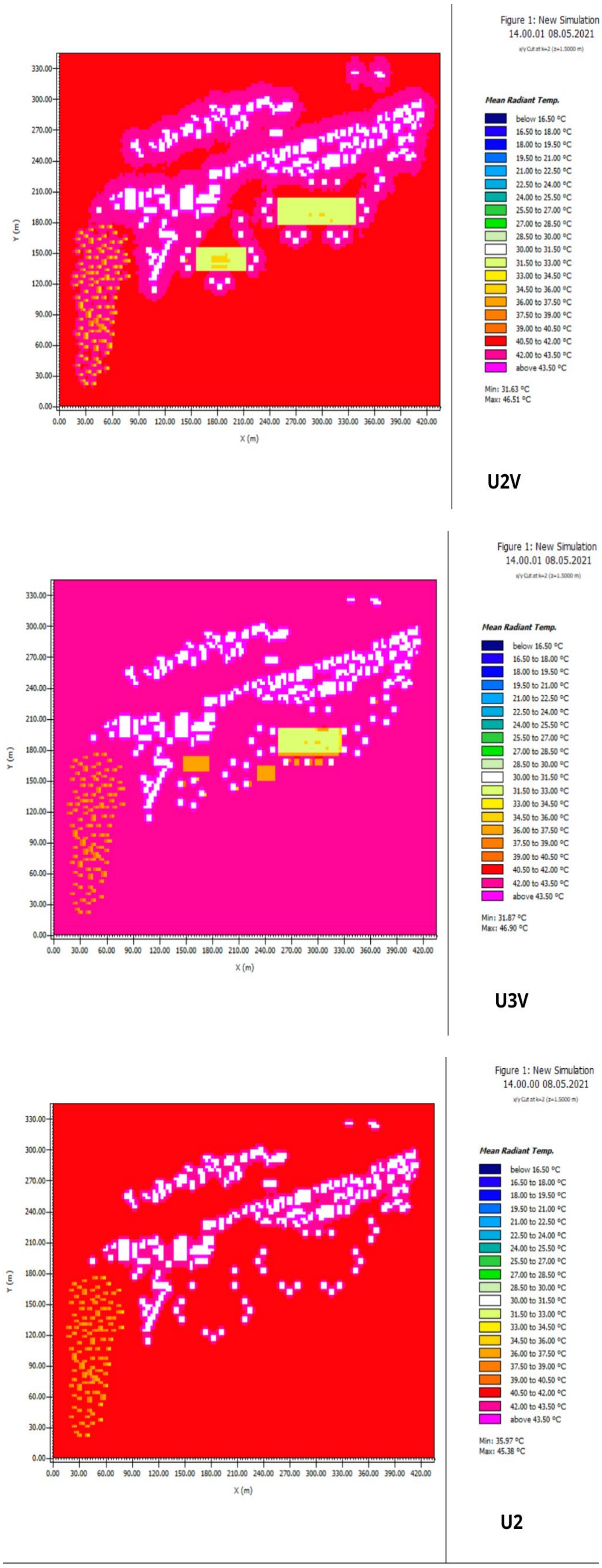

FIGURE 4.12: Mean radiant temperature at 1400 hrs for U2V, U3V, U2

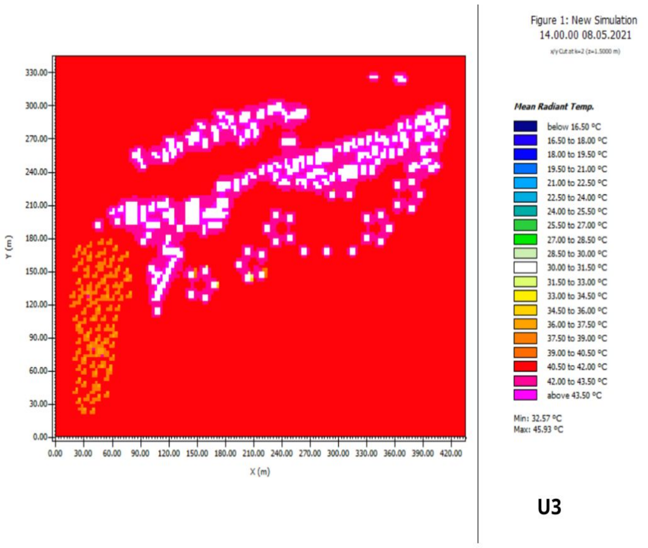

FIGURE 4.13: Mean radiant temperature at 1400 hrs for U3

4.1.2 Point 2

TABLE 4.2: Thermal comfort parameters for Point 2 across all urban configurations

Scenarios		Potential air temperature (deg cel)	Wind speed (m/s)	Mean radiant temperature (deg cel)	Relative humidity (%)	PET (deg cell)	Change in PET from O1 (deg cel)
0200 hrs	O1	25.1	1.4	14.7	86.6	18.5	
	O2	25.2	1.3	15.4	86.1	18.8	-0.3
	O3	25.3	1.4	16.4	86.3	19	-0.5
	U1	25.3	1.1	25	85.6	22.2	-3.7
	U2V	25.6	1	23.8	81.7	21.8	-3.3
	U3V	25.6	1	25.4	83.7	21.7	-3.2
1400 hrs	O1	33.4	1.9	42.3	55	36.4	
	O2	34.6	1.7	42	52	36.6	-0.2
	O3	37	1.8	60	45	47.5	-11.1
	U1	33.4	0.6	36.8	53.8	34.2	2.2
	U2V	33.7	0.4	31.6	55	32.1	4.3
	U3V	34.4	0.4	31.8	52	33	3.4
	U2	34	1.6	41	55	35.2	1.2
	U3	35	1.5	41	44.5	38	-1.6

The thermal comfort parameters for Point 2 for all the time stamps are given in Figure B.3 in Appendix B.

This area is of prime importance as this is the most significant open space present in the floating homes in any of the models, with varying percentages of vegetation. Therefore, significant changes occur in this area in most parameters. These values are tabulated in Table 4.2 for 0200 hrs and 1400 hrs.

Potential air temperature: The graphical representation of potential air temperature for all the scenarios is provided in Figure 4.14. The original model's potential air temperature is 33.4 degrees celsius at 1400 hrs. In O3, this value rises to 37°C. In other scenarios, there is a slight increase in potential temperatures because wooden planks and vegetation replace the water body (as in O1), which, as a combination, yields a higher result. In U2 and U3, the temperatures were higher by 0.7°C and 0.6°C when compared to their counterparts, U2V and U3V, indicating that this difference is solely because of the vegetation present and not the urban form itself. At 0200 hrs, temperature value has increased up to 0.5 °C in U2V and U3V. This is because vegetation has a lower Skyview factor, emitting lesser heat back into the atmosphere.

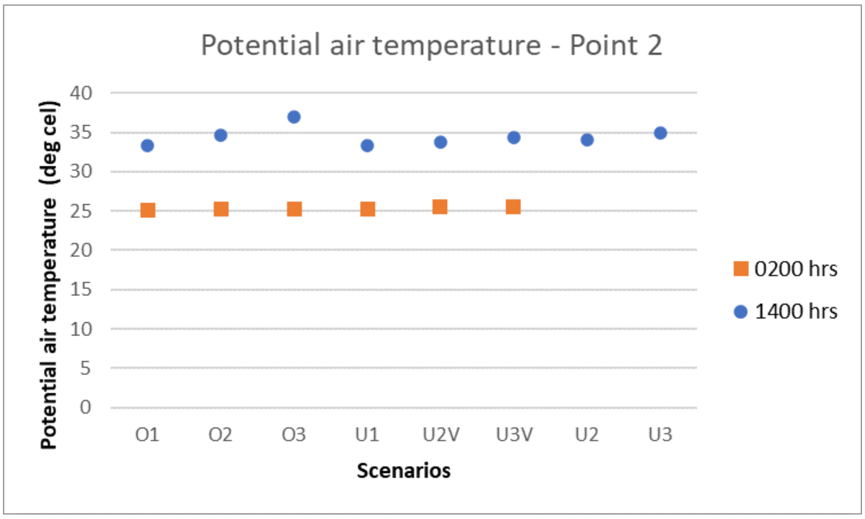

FIGURE 4.14: Potential air temperature for 0200 hrs and 1400 hrs for all scenarios - Point 2

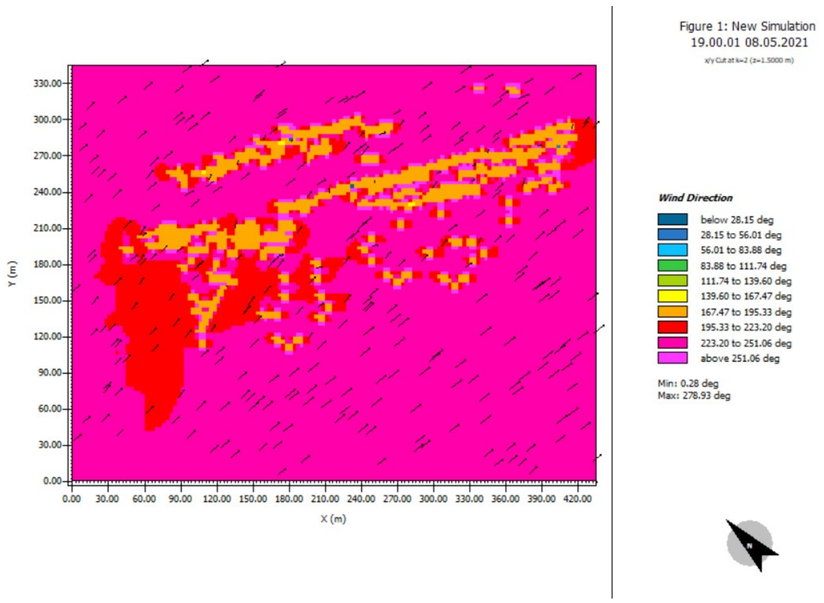

FIGURE 4.15: Wind direction at 1900 hrs for O1

Wind speed: The graphical representation of wind speed for all the scenarios is provided in Figure 4.16. At 1400 hrs, the wind speed in O1 is 1.9 m/s.

The lowest wind speeds were recorded in U2V and U3V at 0.4 m/s. This is coupled with an increase in potential air temperature in these two scenarios. This is due to the inverse relationship between these two parameters. The winds were blocked due to extensive vegetation. Since the wind flow is in the South direction as in Figure 4.15, it is advisable to not plant vegetation in this direction to let the wind flow.

However, during other periods, the wind speeds are below four m/s, meeting the Lawson comfort criteria, thereby creating a comfortable outdoor wind atmosphere.

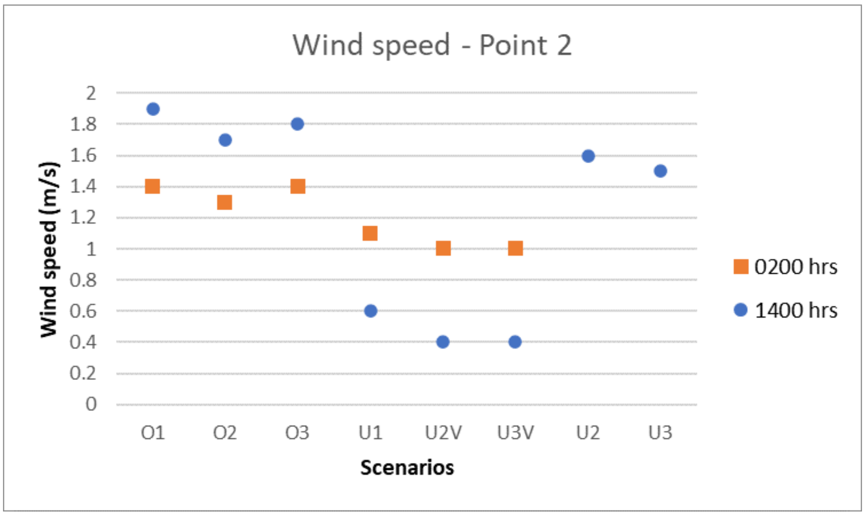

FIGURE 4.16: Wind speed for 0200 hrs and 1400 hrs for all scenarios - Point 2

Mean radiant temperature: The graphical representation of mean radiant temperature for all the scenarios is provided in Figure 4.17. For the original model, the recorded mean radiant temperature is 42.3°C at 1400 hrs. In O2, the temperature fell by 0.3 °C. In O3, and the mean radiant temperature reached an unacceptable limit of 60 °C. In U1, 10 percent vegetation is added to the floating model home area which resulted in an MRT reduction to 36.8 °C. In U2V, 30 percent vegetation is added to the area, leading to a value of only 31.6 °C. This is a 10.7 °C minimization. In U3V, the vegetation added is close to 20 percent, with an MRT value of 31.8 °C. Therefore, the MRT is proportional to the amount of vegetation added. However, this may stabilise after a percentage of vegetation. At 0200 hrs, the mean radiant temperature has increased in all the scenarios, by approximately 10 °C in the vegetation scenarios.

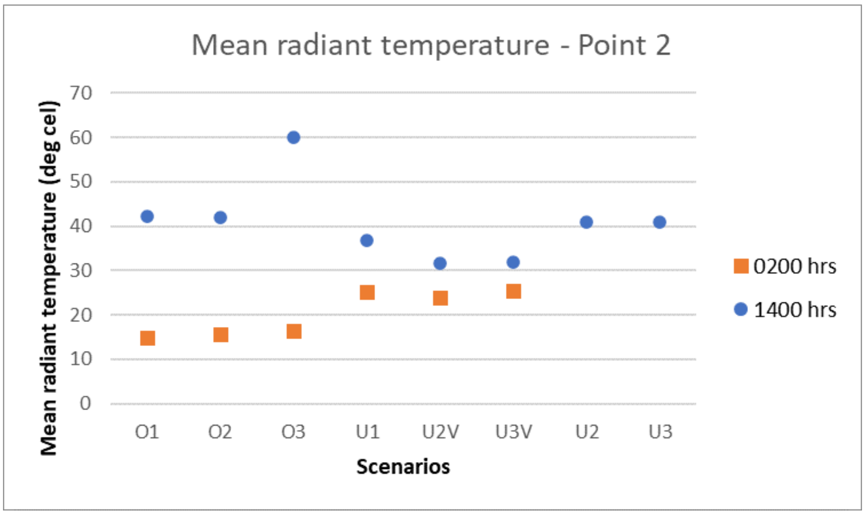

FIGURE 4.17: Mean radiant temperature for 0200 hrs and 1400 hrs for all scenarios - Point 2

Relative humidity: The graphical representation of mean radiant temperature for all the scenarios is provided in Figure 4.18. Relative Humidity is generally the highest during nighttime. In this case, it reaches up to 86.6 percent at 0200 hrs. The most significant difference can be seen in U3V at 83.7 percent. The temperatures are high during nighttime because of the added vegetation, resulting in the decrease in RH. During afternoon hours, at 1400 hrs, the RH value is 55 percent for O1. The lowest RH values are recorded in O3 and U3. This indicates the negative co-relation between PET/UTCI and RH.

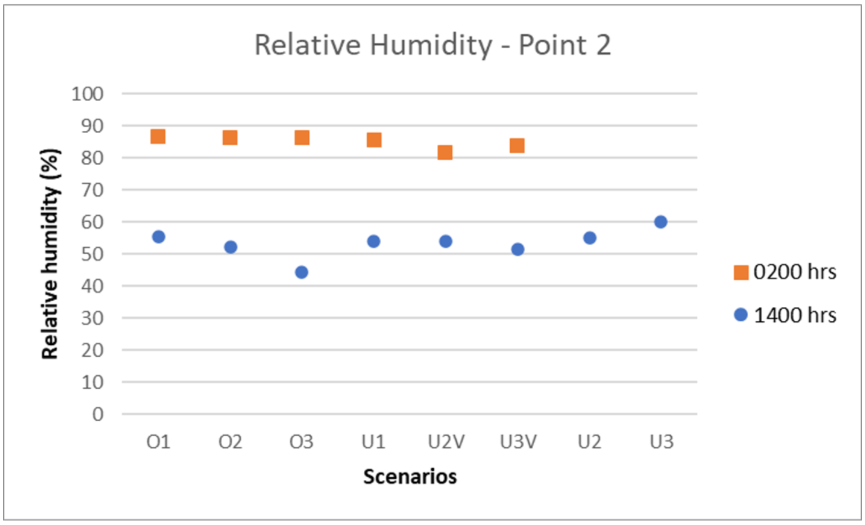

FIGURE 4.18: Relative humidity for 0200 hrs and 1400 hrs for all scenarios - Point 2

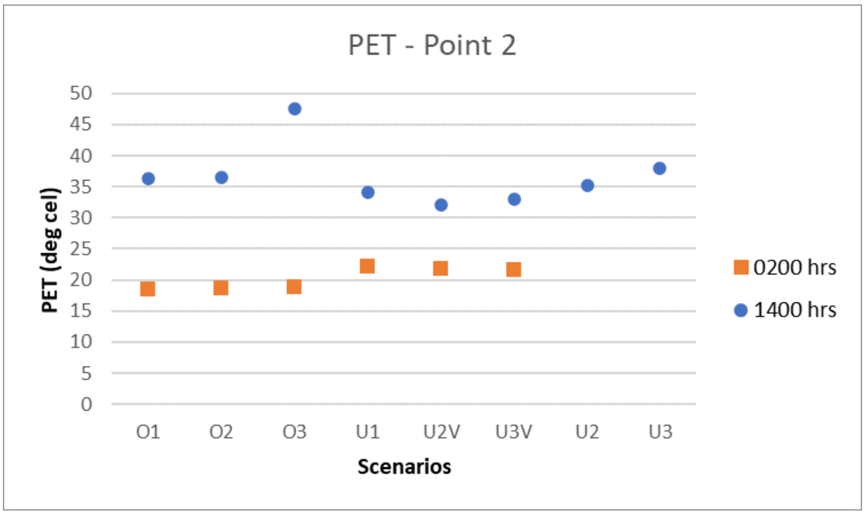

FIGURE 4.19: PET for 0200 hrs and 1400 hrs for all scenarios - Point 2

PET: The graphical representation of PET values for all urban configurations is given in Figure 4.19. The PET values are tabulated in Table 4.2. At 1400 hrs; the most positive PET effect is with the U2V form. The PET value reduced from 36.4 °C to 32.1°C. This reduces the thermal perception from heat stress to mild heat stress. U2 registers a value at 35.2 °C. Thus, 1 °C was reduced from O1 to U2, i.e., solely based on urban form. The additional 3 °C is due to the vegetation added.

At 0200 hrs, PET performance declines in all the scenarios. The vegetation scenarios are performing worse than pavement scenario O3. Therefore, the influence of vegetation is worse during nighttime over the concrete pavement material. This is because the latter dissipates heat quickly as well.

4.1.3 Point 3

The graphical representation of the thermal comfort parameters for all the time stamps is provided in Figure B.5 in the Appendix B.

Point 3 covers the area between the floating homes and is either waterbody itself (O1, O2, U3, U3V, U2, U2V), pavement (O3), or a partial wooden platform pathway (U1, U2, U2V) between the housing depending on the typology. The values for 0200 hrs and 1900 hrs are tabulated in Table 4.3.

TABLE 4.3: Thermal comfort parameters for Point 3 across all urban configurations

Scenarios		Potential air temperature (deg cel)	Wind speed (m/s)	Mean radiant temperature (deg cel)	Relative humidity (%)	PET (deg cel)	Change in PET from O1 (deg cel)
0200 hrs	O1	25	1.3	15.1	86.2	18.5	
	O2	25	1.3	15	86.1	18.5	0
	O3	25.3	1.4	16.4	85.8	19	-0.5
	U1	25.3	1.3	14.5	86	18.5	0
	U2V	25.2	1	14.3	83.8	18.8	-0.3
	U3V	25	1.3	14.3	83.2	18.8	-0.3
1400 hrs	O1	33.8	1.8	42	55	36.4	
	O2	34.1	1.9	43	52	33.6	2.8
	O3	36.9	1.8	59.4	45	47.5	-11.1
	U1	33.4	1.9	42.3	53.8	36.7	-0.3
	U2V	33.7	1.8	31.6	54.3	32.1	4.3
	U3V	35	1.4	41	48.6	38.3	-1.9
	U2	33.5	1.7	41	55	35.2	1.2
	U3	34.3	1.5	41.9	44.5	32.9	3.5

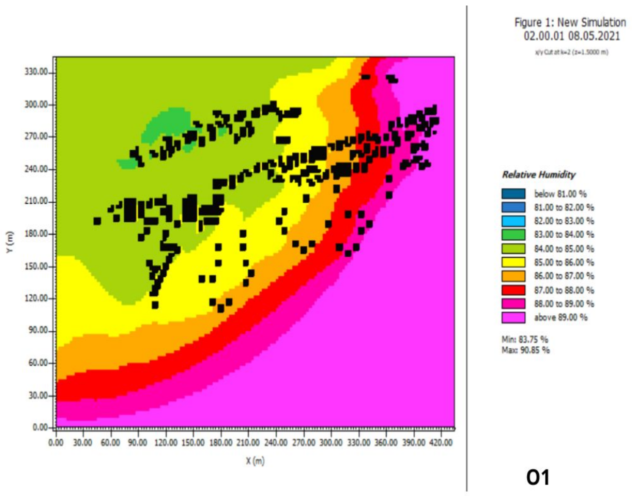

FIGURE 4.20: Relative Humidity at 0200 hrs for O1

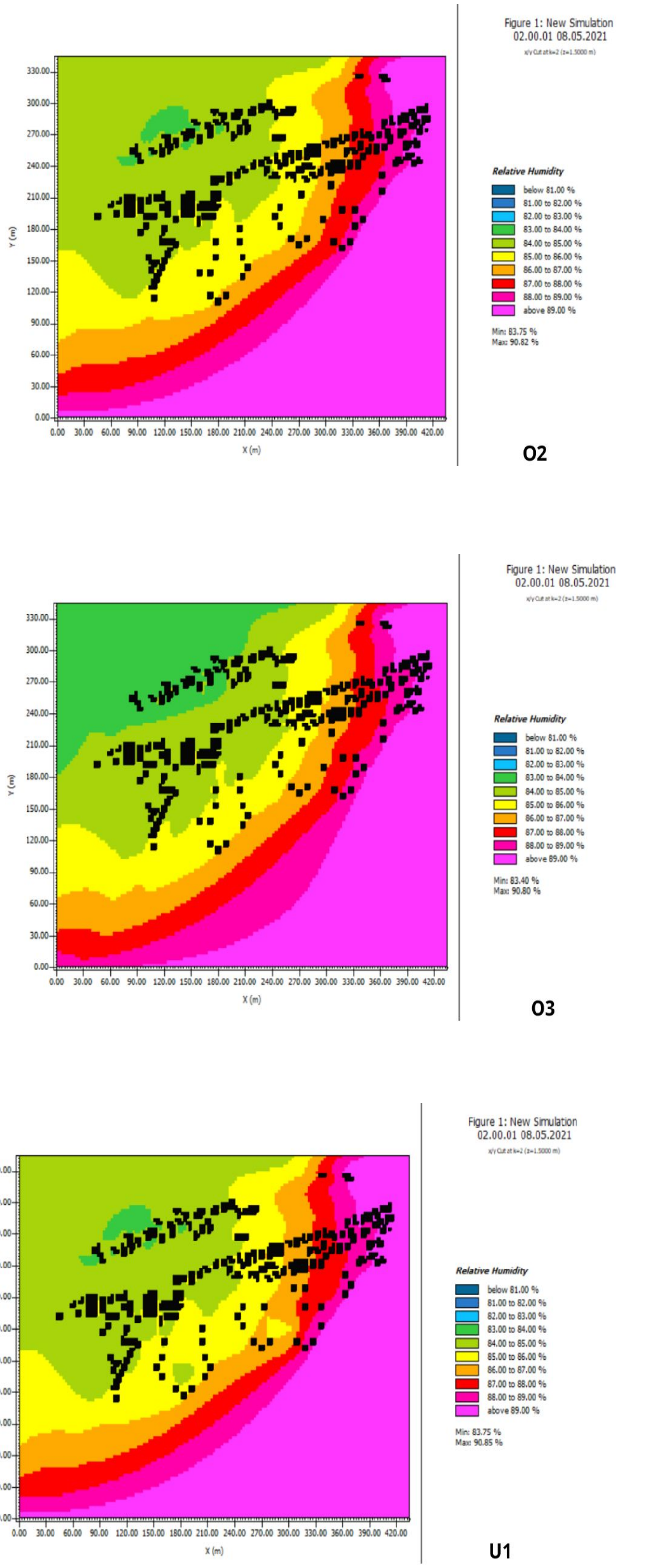

FIGURE 4.21: Relative Humidity at 0200 hrs for O2, O3, U1

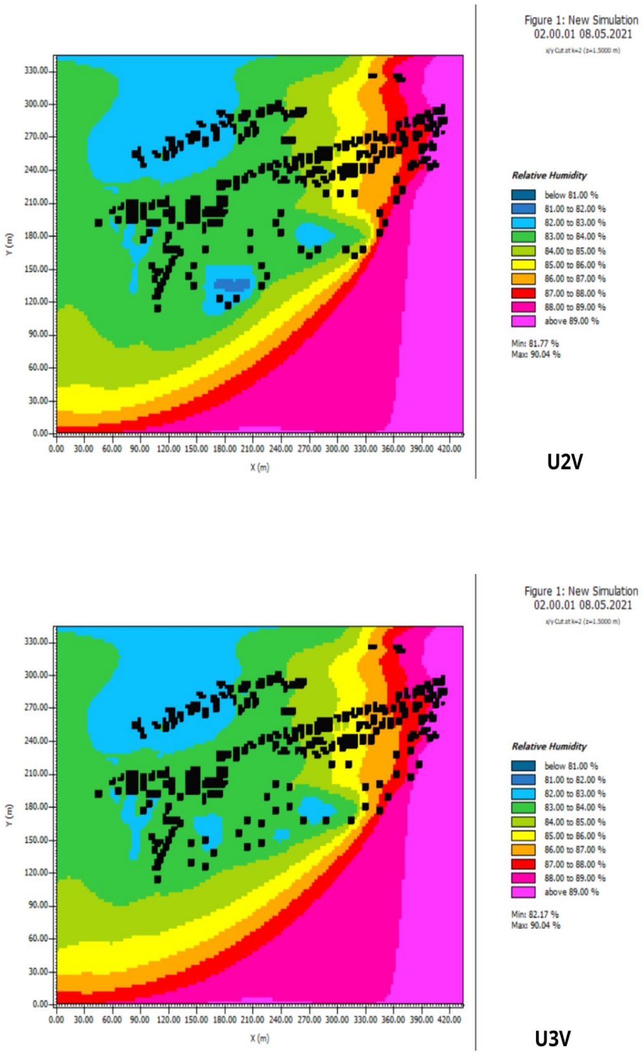

FIGURE 4.22: Relative Humidity at 0200 hrs for U2V, U3V

Potential air temperature: The graphical representation of potential air temperature values for all urban configurations is given in Figure 4.23. At 1400 hrs, the potential air temperature recorded is 33.8°C in O1.In O3, this value increases to 36.9°C. This is due to the high heat absorption of the pavement. In O2, U3V, and U3, there is a marginal increase in temperature values, whereas U1, U2v, and U2 record lower potential air temperature values. This may be due to the combination of wind speed and mean radiant temperatures U3, and U3V values are significantly higher because the wooden platform underneath Wood has a lower specific heat capacity than water, thereby absorbing more heat.

During the nighttime, the temperature slightly increases with the increase in vegetation. In the case of no vegetation, there is a decrease of 0.2 °C in this Point area.

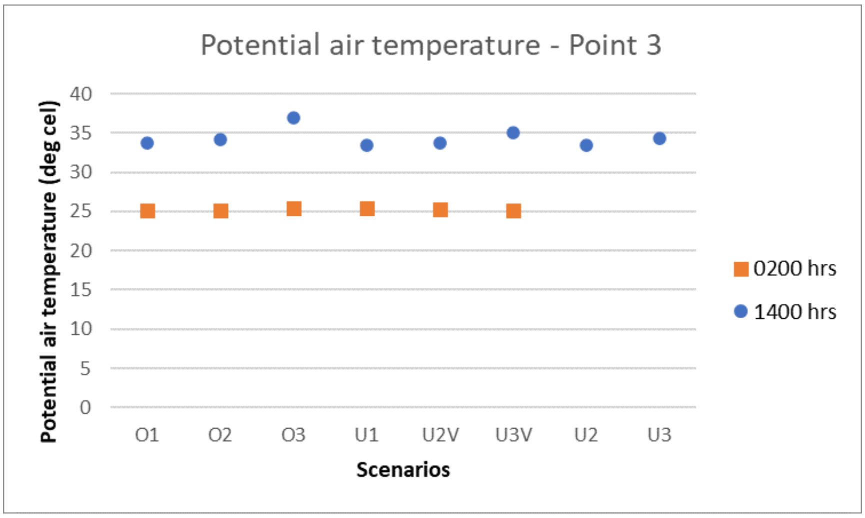

FIGURE 4.23: Potential air temperature for 0200 hrs and 1400 hrs for all scenarios - Point 3

Wind speed: The graphical representation of potential air temperature values for all urban configurations is given in Figure 4.24. At 1400 hrs, the wind speeds were registered at 1.8 m/s. Since it is an open area over the water body with no enclosure from any side, the wind speeds are similar in most configurations. In U3V and U3, the wind speeds are reduced to 1.4 and 1.5 m/s. This is due to the sufficient closeness between buildings to restrict the flow, but at the same time, not too narrow to create a passage problem in this area.

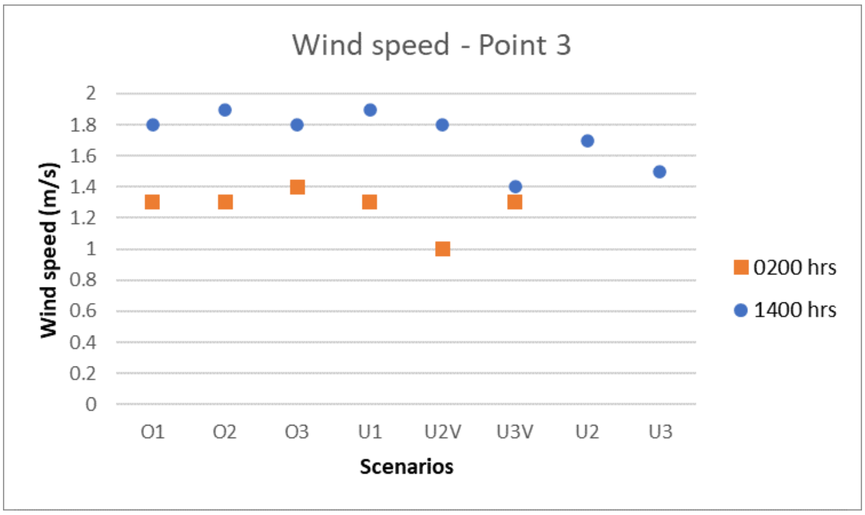

FIGURE 4.24: Wind speed for 0200 hrs and 1400 hrs for all scenarios - Point 3

Mean radiant temperature: The graphical representation of mean radiant temperature values for all urban configurations is given in Figure 4.25. Since there is no vegetation in this area, the MRT values are more or less the same in all the categories. In O1, the recorded value is 42°C.

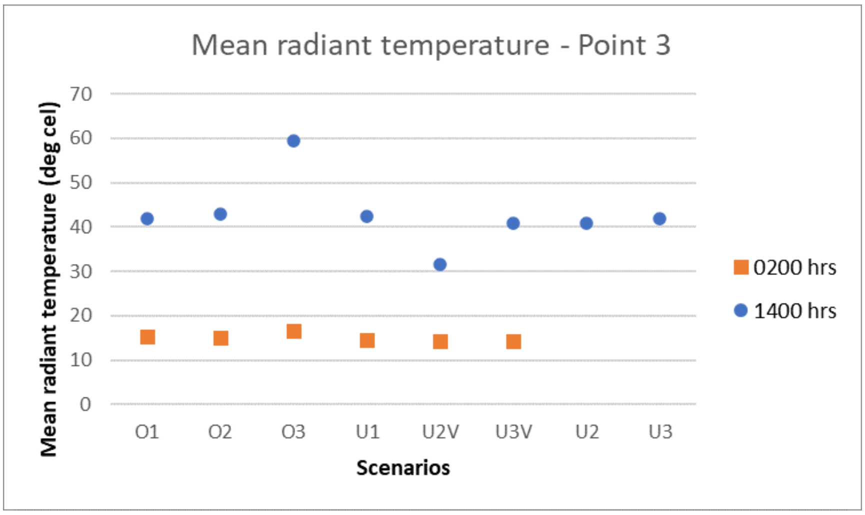

FIGURE 4.25: Mean radiant temperature for 0200 hrs and 1400 hrs for all scenarios - Point 3

Relative Humidity: The graphical representation of mean radiant temperature values for all urban configurations is given in Figure 4.26. In the original model O1, the highest recorded RH value is 86.2 percent at 0200 hrs. This value falls to 77.2 percent in U2V, i.e., more than 10 percent change. During afternoon hours, it stands at 55 percent, with a decrease of 10.5 percent in U3. As vegetation increases, RH keeps decreasing.

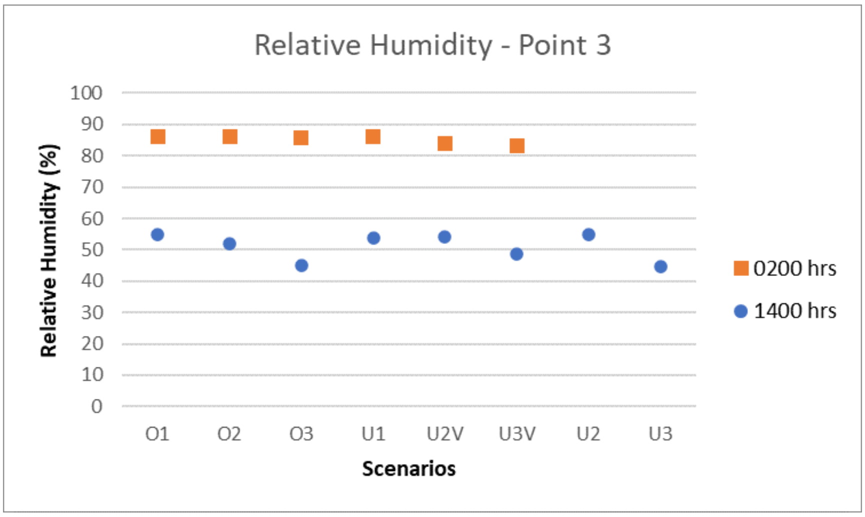

FIGURE 4.26: Relative humidity for 0200 hrs and 1400 hrs for all scenarios - Point 3

PET: The graphical representation of PET values for all scenarios is given in Figure 4.27. The tabulated results are provided in Table 4.3. There is a positive PET impact primarily in U1 configuration for 1400 hrs. At this point, vegetation plays a minimal role in heat stress reduction because there is no reduction in radiation. There is nothing new that is modified in this area. This indicates the difference in stress reduction on land and vegetation and waterbody.

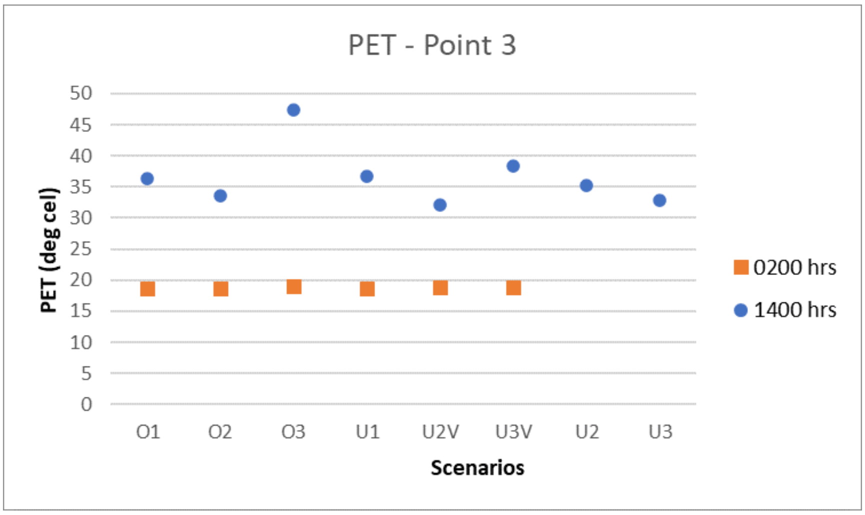

FIGURE 4.27: PET for 0200 hrs and 1400 hrs for all scenarios - Point 3

4.1.4 Point 4

TABLE 4.4: Thermal comfort parameters for Point 4 across all urban configurations

Scenarios		Potential air temperature (deg cel)	Wind speed (m/s)	Mean radiant temperature (deg cel)	Relative humidity (%)	PET (deg cel)	Change in PET from O1 (deg cel)
0200 hrs	O1	25	1.4	14.7	85.8	18.5	
	O2	25	1.4	15	85.6	18.5	0
	O3	25.2	1.4	16.1	85.5	19	-0.5
	U1	25.1	1.1	25	84.7	22.2	-3.7
	U2V	25.4	1	24.8	81.7	21.8	-3.3
	U3V	25.2	1.2	14.3	83.7	18.3	0.2
1400 hrs	O1	34.3	1.8	19.4	74	37.3	
	O2	34.3	1.9	19.5	73.6	36.6	0.7
	O3	36.8	1.8	60	47	47.5	-10.2
	U1	34.3	0.8	36.8	53	34.2	3.1
	U2V	34.1	0.6	31.6	55	32.1	5.2
	U3V	35.2	1.6	41	48.6	36	1.3
	U2	34.8	1.7	41	55	37	0.3
	U3	34.1	1.6	41	48	32.9	4.4

The graphical representation of thermal comfort parameters for Point 4 for all time stamps is given in Figure B.7 in Appendix B.

Point 4 is one of the highest heat stress points in the floating home's area, and also acts as one of the open spaces. The tabulated values for 0200 hrs and 1900 hrs are provided in Table 4.4.

Potential air temperature: The graphical representation of potential air temperature values for all scenarios is given in Figure 4.28. In the original model O1, the recorded potential air temperature at 1400 hrs is 34.3 degrees Celsius. This value is 2 degrees higher in the case of pavement O3. This value was reduced to only 34.1 degrees Celsius in U2V. In U3V, temperature increases because of the lower amount of vegetation and the housing clusters because of their higher density. In general, temperatures seem to be higher here because of the dense enclosure from all sides, which cuts down the wind speeds to the area. Similar pattern follows during the nighttime with marginal differences.

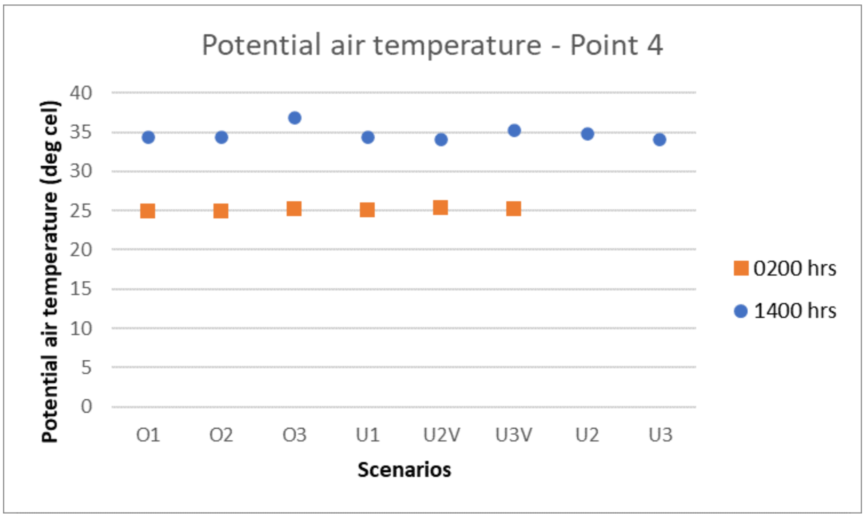

FIGURE 4.28: Potential air temperature for 0200 hrs and 1400 hrs for all scenarios - Point 4

Wind speed: The graphical representation of wind speed values for all scenarios is given in Figure 4.29. In O1, the wind speed at 1400 hrs is 1.8 m/s. This was reduced to 0.6 m/s in U2V which may create an uncomfortable atmosphere for the residents. In U2, the wind speed is reduced by 0.1 m/s. In U3V, this point does not come between the buildings but over the water body. Because of this, the wind speeds are similar to O1. Because of its inverse relationship with air temperature, this reduction in wind speeds increases the former value.

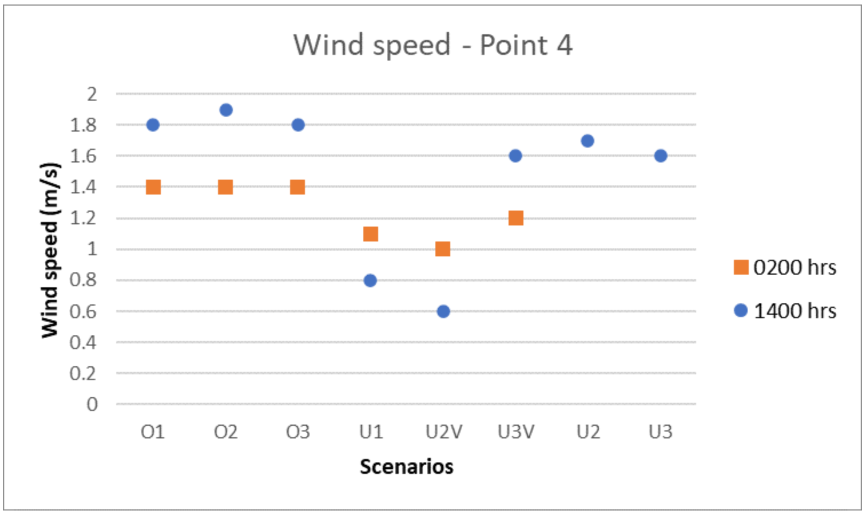

FIGURE 4.29: Wind speed for 0200 hrs and 1400 hrs for all scenarios - Point 4

Mean radiant temperature: The graphical representation of mean radiant temperature values for all scenarios is given in Figure 4.30. The MRT is 42.3°C for O1 at 1400 hrs. U2V fares the lowest recorded value of 31.6 °C, i.e., a difference of more than 10 degrees. Vegetation is the primary reason behind this reduction. As mentioned previously, the MRT in vegetative areas increases during the night. Since the U3 point lies over the waterbody, the values cannot be accurately compared to the land scenario in O1. At 0200 hrs, the scenarios with vegetation increases the MRT value.

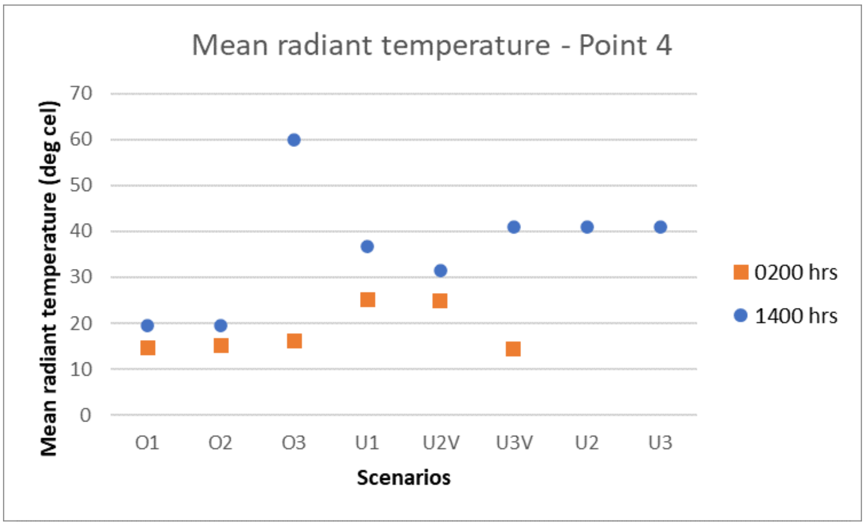

FIGURE 4.30: Mean radiant temperature for 0200 hrs and 1400 hrs for all scenarios - Point 4

Relative Humidity: The graphical representation of mean radiant temperature values for all scenarios is given in Figure 4.31. In O1, the RH value stands at 85.8 percent in the nighttime at 0200 hrs. It records the lowest in

U2V with a value of 81.7 percent. The relative humidity follows a similar trend as the points mentioned earlier.

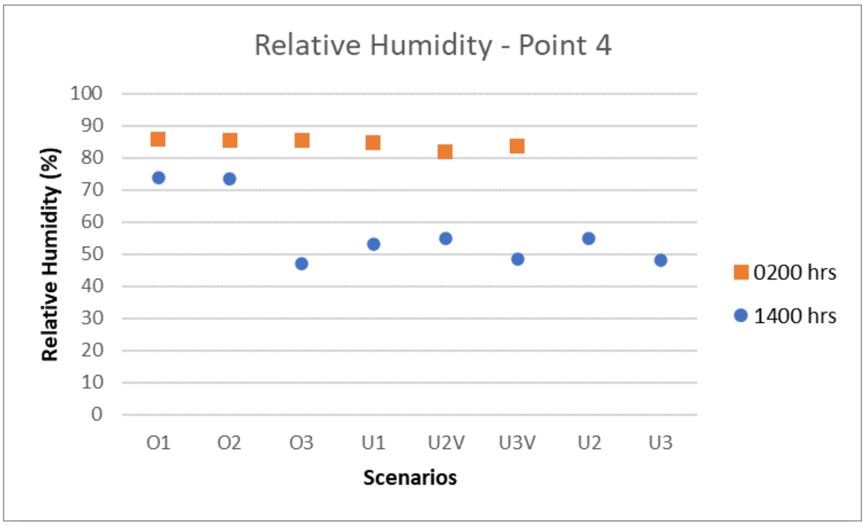

FIGURE 4.31: Relative humidity for 0200 hrs and 1400 hrs for all scenarios - Point 4

PET: The graphical representation of the thermal indices is provided in Figure 4.32. The tabulated values are provided in Table 4.4. The PET value at 1400 hrs in O1 is 37.3 degrees. This is the highest recorded stress value across all the Points. At 1400 hrs, U2V registers a 5 degree Celsius improvement. The urban form itself U2, is with a 0.3 °C improvement. This is solely due to urban form. U1 has a 3.1 °C improvement. At 0200 hrs, U1 fares the worst PET with 3.7 °C decline.

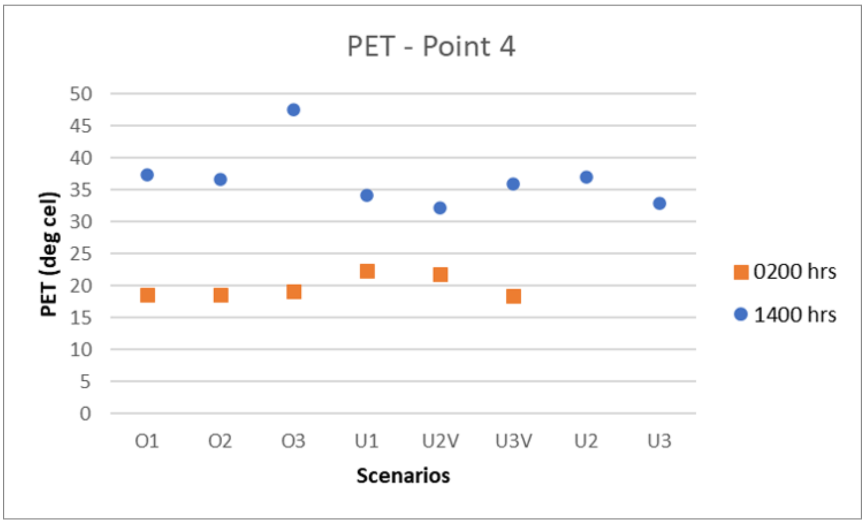

FIGURE 4.32: PET for 0200 hrs and 1400 hrs for all scenarios - Point 4

4.2 Wind comfort

The wind speeds for all the 4 Points across all urban configurations are discussed in Section 4.1 under thermal comfort parameters. Highest wind speeds were recorded at 1900 hours, shown in Figure 4.34. These graphs are charted as per the Lawson comfort criteria. As we can see from the charts, the modified scenarios bring the comfort levels to Class A category. It was initially in the Class B category.

As per the Lawson comfort criteria, the exceedance can be defined as the maximum allowable period per year. The wind speed can have a higher threshold value for pedestrian wind comfort. Since ENVI-met cannot calculate the wind speeds for the whole year, the wind speeds from the weather data file (EPW file) are assumed in this case. The wind speeds in the EPW files are calculated at a height of 10 m from the ground level. These values were scaled down to 1.5 m pedestrian height with a factor of 0.68 for the O1 scenario. These results are compared with U2V scenario as it provides the highest thermal comfort index. For the U2V scenario, the scale factor is 0.35 of the original values. These values are tabulated for Point 2 in the model area.

The average hourly wind speeds are considered to calculate the exceedance for all the Classes. These results are tabulated in Table 4.5.

TABLE 4.5: Lawson comfort criteria calculations

Class	Velocity (m/s)	Exceedance (percent) criteria	Scenario	No. of hours wind speed>threshold	Exceedance (percent)
Class A: Sitting/Standing - Long	>4	<5	O	2400	27.4
			U2V	380	4.3
Class B: Sitting/Standing - Short	>6	<5	O	965	11
			U2V	53	0.6
Class C: Leisurely walking	>8	<5	O	379	4.3
			U2V	5	0.05
Class D: Fast walking	>10	<5	O	135	1.5
			U2V	0	0
Class Safety: Distress	>15	>0.002	O	7	0.8
			U2V	0	0

According to this Table, the exceedance is greater than the acceptable limits for Class A and Class B for the O1 scenario. However, the average wind speed for the year was recorded at 2.9 m/s, which suits all the classes. In the U2V scenario, the wind speeds are drastically reduced across all the Classes. This is because of its dense configuration and enclosure from all sides, and the added vegetation. This pattern is already discussed in Section 4.1 for Point 1 and Point 2. However, the wind speeds are reduced to a level which may be uncomfortable for the people living there. It is also important to note that in the original scenario O1, the exceedance is very high for Class Safety, which causes drastic situations in case of high-winds. This is brought down to 0 percent in U2V. Therefore, a balance must be maintained with a middle ground between O1 and U2V. This is also coupled with the surveys conducted by Alazne Eduardo, as the residents do not prefer wind blockage indicating their perceived wind comfort.

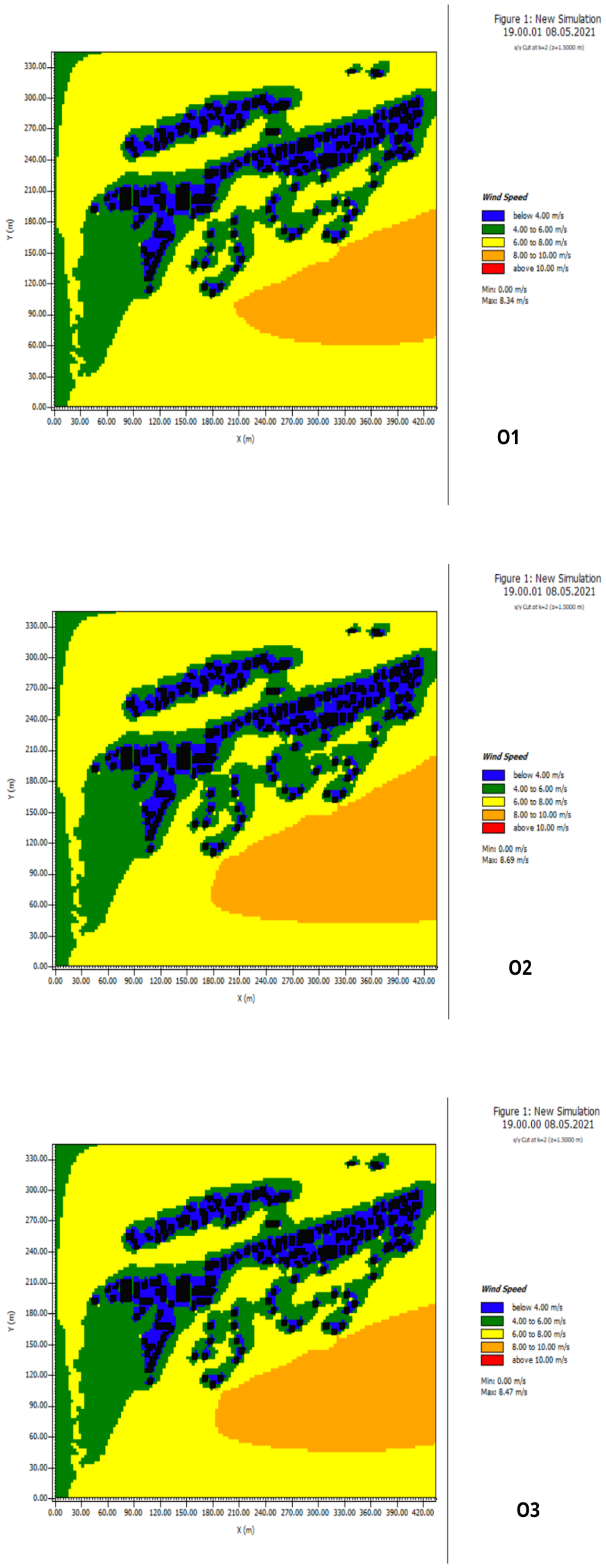

FIGURE 4.33: Wind speed at 1900 hrs for O1, O2, O3 as per Lawson comfort criteria

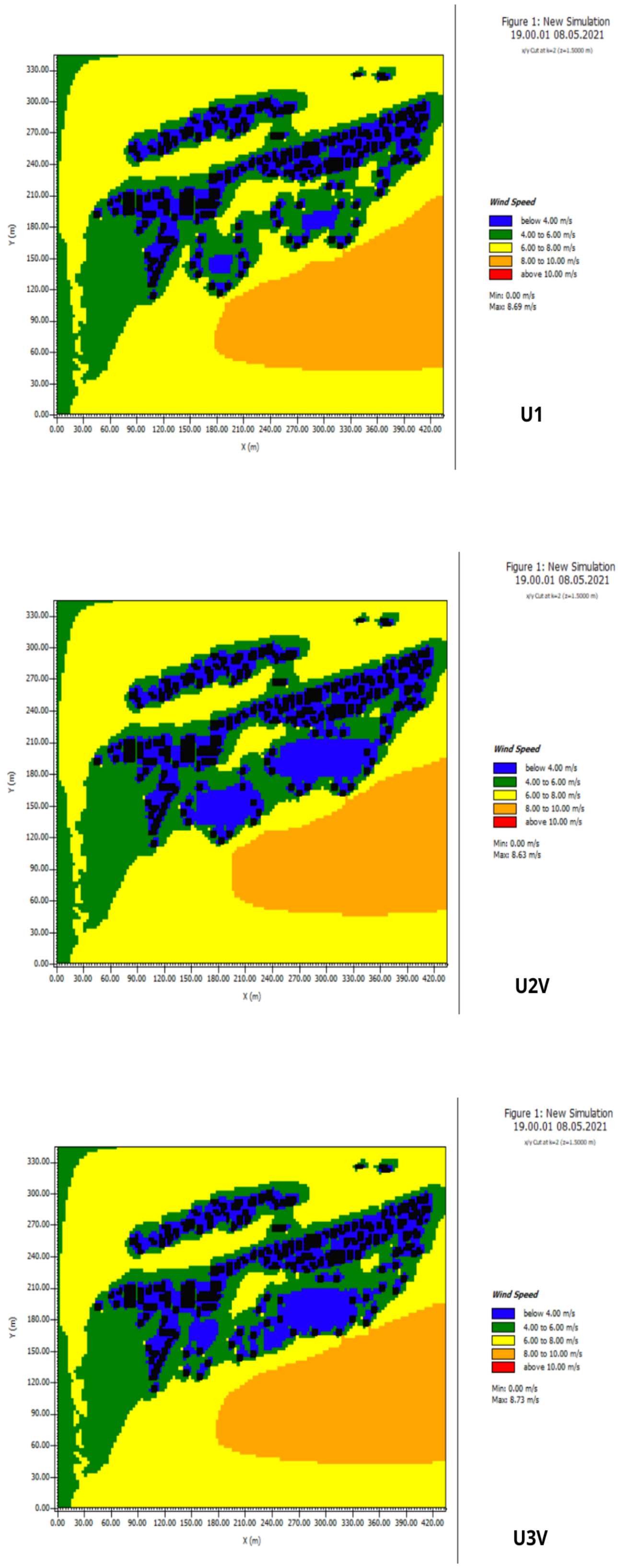

FIGURE 4.34: Wind speed at 1900 hrs for U1, U2V, U3V as per Lawson comfort criteria

4.3 Influencing Parameters

4.3.1 Effect of water-body

A waterbody's presence is influential in determining the heat stress of the surrounding areas. In one of the scenarios, the water surface was replaced by used grey pavement material properties. At 1400 hrs, the peak afternoon hours, the PET value is 47.5 °C in O3 scenario. The MRT value in O3 is 60 °C. According to the PET comfort criteria, this indicates an extreme heat stress situation.

The existing situation with a waterbody results in a 36.4 degree Celsius PET value. This is a 11 °C improvement in PET performance. With this value, the heat stress is intense in this area. It also reduces the mean radiant temperature by 17.7°C to 42.3°C, showcasing a higher thermal absorption capacity.

The difference between the minimum and maximum potential air temperature is slight throughout the day. During the nighttime, the radiation is slightly lower in O1 than O3 by 2-3°C. The relative humidity is increased by 10 percent in O1, owing to the significant drop in potential air temperatures. However, these effects are not adverse compared to the benefits of a surrounding water body. Therefore, it is the most significant positive performance indicator.

4.3.2 Effect of vegetation

In the original model, the potential air temperature of O1 is 33.4 °C. In the other scenarios with vegetation, this value either remains the same or marginally increases by up to 1 °C. However, at the same time, the vegetation acts as natural wind blocks reducing the wind speeds by up to 70 percent (comparing U2 and U2V). However, as mentioned earlier, it is not comfortable for people to live in such low wind velocity atmosphere. Therefore, it is not advisable to block wind to such a capacity, and to mediate the balance between temperatures and winds. High wind speeds were recorded in the South direction, therefore this direction should not be blocked.

TABLE 4.6: Percentage of vegetation added in different scenarios

Model	Amount of vegetation added (percentage)
O2	12.5
U1V	10
U2V	30
U3V	20

The mean radiant temperatures are reduced from 42.3 °C to 31.6 °C (O1 and U2V). In this scenario, 30 percent of the floating homes model area is replaced by vegetation. The more the area of vegetation, the more the area with reduced radiation, resulting in lower heat stress over larger areas. The relative humidity reduces by 5-10 percent in the presence of vegetation (U2V and U3V, respectively). Even though U1 also has vegetation, its effects are insignificant as it includes only a tiny percentage of the area.

The improved performance is up to 4.3 °C in the vegetative areas in the U2V scenario. It is also important to acknowledge that the data provided in this Chapter only tabulate the results at specific points. Therefore, the results yielded are much better when the whole area is considered. The more vegetative area, the more the area with a lower PET value. This shares a direct relationship. Considering the vegetative scenarios, PET is calculated for specific singular points. However, this improvement is spread over more than 30 percent of the area compared to its original counterpart.

However, it is impossible to reach the no thermal heat stress situation even with an increase in vegetation in the area of the floating home. This is because the increase in vegetation does not lead to a continuing improvement in PET performance. The temperatures stablises after a specific percentage, without further reduction. Additionally, 30-50 percent of the floating homes area for vegetation is s relatively high area, leaving little scope for other amenities. Therefore, alternative options must also be considered to expand the area of scope. Water plantations such as mangroves (already prevalent in the area), willow trees, water tupelo, river birch, etc. The vegetative density should be high enough to benefit the floating homes' open spaces.

During the nighttime, the PET value worsened by 3.7°C in the U2V scenario. To ensure that the heat stress is acceptable throughout the day, there needs to be a balance in the amount of vegetation added to the area.

On an additional note, the simulations are for a 24-hour cycle when peak temperatures were obtained in the whole year, indicating that this is the maximum heat stress that can be reached. Since other days record lesser temperature values, the heat stresses are also lower. It can also reach no heat stress situation with a lower vegetative area.

4.3.3 Effect of urban morphology

U2 and U3 have been simulated at 1400 hrs (peak afternoon hours). The housing mapping is the same in U2V and U3V, respectively, but without vegetation. This is to determine the improvement/decline in performance solely based on urban morphology from the original model without the influence of vegetation.

The potential air temperatures are higher in U2 and U3 for 1400 hrs compared to the original model O1, U2V, and U3V. The wind speeds are, however, reduced by 15 percent and 21 percent in U2 and U3 concerning O1. The wind flow is relatively better in U2 and U3 compared to the U2V and U3V. This is due to no vegetation in the former scenarios. The MRT is reduced by 1.3 degrees Celsius. The PET performance improved by 1.2 °C and declined by 1.6 °C in U3.

The pentagonal clusters in U3 resulted in increased PET values in its central areas. This is not a suitable solution to reduce heat stress unless dense vegetation is provided in these areas. The wind speeds are high at the housing borders because of the low area and high pressure. However, they act as good wind blocks to the interiors, with up to 20-25 percent reduction with a 3-6 meters gap between the buildings. Such a design is helpful in situations where wind blockage is necessary.

In U2, the enclosure of the open spaces by buildings on all sides (such as Point 2) improved the PET performance by 1.2°C. U2V stands at 4.3°C difference, indicating a 3°C improvement solely due to vegetation present. They also act as wind barriers in case of high wind velocity regions. Therefore, such an enclosed 3-housing cluster configuration improves thermal comfort. Wind comfort is subjective depending on the area of study. Since the residents are interested in organic farming, U2 provides larger spaces for vegetative growth. They also act as coherent designated places for people to gather, such as Point 2 and Point 4, depending on the attendance of people.

4.4 Optimal layout

Keeping into consideration all the Points, the following scenarios fared best results for each of them.

- Point 1: U3 performed the best for Point 1 across all the scenarios.
- Point 2: U2V performed the best for Point 2. This is due to decreased MRT and improved PET performance. However, wind flows were reduced. This can be compensated with different varities of vegetation to be included in the area.
- Point 3: U2V fared the best results in terms of PET and wind comfort. However, since this is an open waterbody area, it does not play a significant role in outdoor comfort. However, all the buildings can be interconnected with each other with a wooden platform between the areas.
- Point 4: U2V fared the best results in terms of comfortability levels. This is due to similar reasions pointed out for Point 2.

Therefore, combining the best results for all the Points, the following layout has been drafted. Figure 4.36 represents the building layout for the modified scenario. Figure 4.35 represents the soil layout of this scenario.

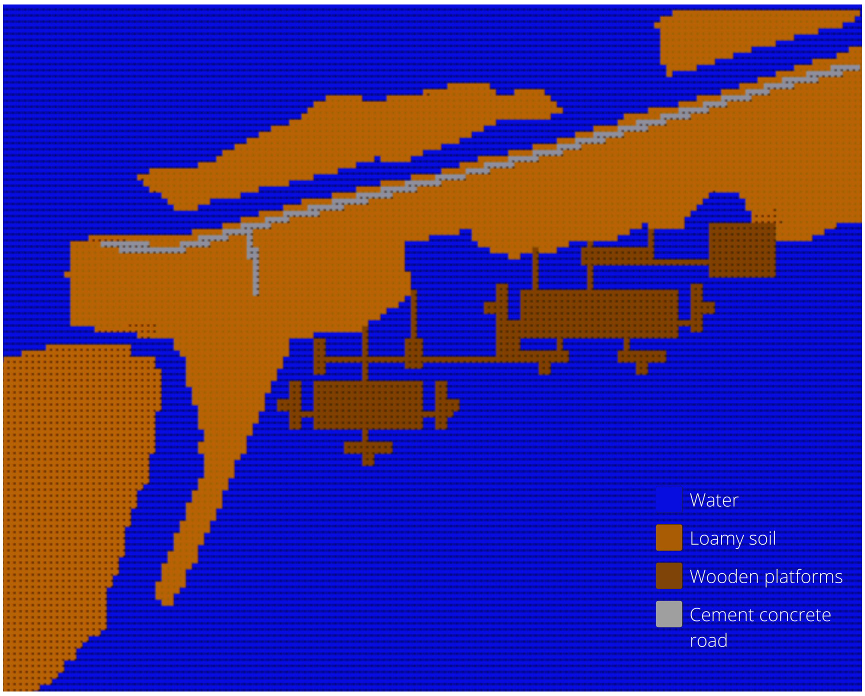

FIGURE 4.35: Optimised floating homes soil profile

FIGURE 4.36: Optimised floating homes building profile

Chapter 5

Conclusions and Recommendations

5.1 Conclusions

Scenarios:

From the results and discussions, it can be concluded that the presence of waterbodies has the highest positive impact on PET performance. O1 and O3 scenarios are compared to understand this relationship. It has improved the PET value by over 11 °C during the daytime and 0.5 °C improvements during night hours.

In all the scenarios, U2V fared the best results with a 4.3 °C improvement over O1. In this scenario, 30 percent of the area of the floating home was added with vegetation. However, more percentage of vegetation does not equate to a further decline in PET, as the curve flattens at a specific percentage of area. Vegetation has the subsequent best influence on PET during peak afternoon hours. However, during night hours, at 0200 hrs, the PET performance declined in U2V by 3.7°C. This is due to the low Skyview factor of vegetation, which dissipates less heat into the atmosphere. Due to the thermal conductivity of materials, vegetation fares worse performance during night hours compared to pavement material (comparison of U2V and O3).

It is important to note that U2V is a combination of vegetation and urban configuration changes. Solely, based on urban configurations, U2 (without vegetation) registered the best results with a 1.2°C improvement. This is due to more openness and spacing between buildings compared to the original scenario O1.

Thermal comfort parameters:

Firstly, mean radiant temperature (MRT) has the most significant influence on PET thermal comfort index. Therefore, material properties with lesser radiation emittance improve PET performance. This needs to be given careful consideration when during the selection of materials in outdoor spaces.

Secondly, this is followed by wind speed. These parameters also largely influence the PET index. In the simulations conducted, wind speeds were drastically reduced because of added vegetation. Since wind speeds share an inverse relation with PET, this hampered the performance of PET to a limited extent. Therefore, it is necessary to look out for allowing wind flow in hot-tropical regions to ease their comfort levels. However, if the situation calls for wind blockage, it is essential to find out the direction of high-wind speeds and provide natural blocking elements such as vegetation. Since it is difficult to improve both wind speeds and temperatures together, it is crucial to find a balance between both variables without one inhibiting the other.

Thirdly, potential air temperature plays the following influence on PET. They share a direct relationship with each other. An increase in potential air temperatures causes an increase in PET value. However, as discussed above, the presence of water bodies decreases the empirical potential air temperature value without affecting the wind speeds. Vegetation also improves the potential air temperature values, but at the cost of declining wind speeds. The latter would mean decreased wind comfortability for the residents in the area.

Finally, relative humidity has a negligible impact on the overall performance value of PET. Relative humidity shares an inverse relationship with the PET value. Higher RH indicates a lower PET value and vice versa. This is due to a lower saturation point in cold air compared to hot air. As this shares a strong relationship with potential air temperatures, these changes directly affect the relative humidity. Unless relative humidity is a drastic issue in the area, it can be neglected while conducting different performance improvement scenarios.

Wind comfort criteria:

Coming to the wind comfort based on Lawson comfort criteria, the original scenario exceeds the acceptability limits in Class A and B categories. The U2V scenario reduced the exceedance limits to acceptable values for both classes. However, it is not necessary to block the winds to such a degree in the Mercado region. Therefore, different varieties of vegetation need to be further looked into to understand the wind blocking mechanism in further detail. Bushes, shrubs, and small vegetative plantations may help in allowing wind flow, however, with decreased thermal comfort compared to larger plantations. The direction of high wind speeds is also important to determine in such scenarios.

It is also worthwhile to note that in the O1 scenario, Class Safety greatly exceeds its acceptance limit, causing an unsafe atmosphere for the residents living there. U2V reduces its probability to 0. While this does not indicate a safe environment for the people, it does indicate lower wind speeds.

5.2 Recommendations

Future designers must first study the site area and its brief weather history to determine their main problem areas in the meteorological values. It is also valuable to conduct surveys to understand better the comfortability of people living in the area and their future expectations. Each region will differ in its problem areas and also in its approach. Therefore, it is necessary to know what the problem definition is for the area.

In the hot-tropical regions, the primary parameters to focus on would be to improve the PET performance by decreasing temperatures and allowing wind flow to an acceptable degree. In such scenarios, it is determined that the presence of water bodies has the highest positive impact on PET. This may also be compensated with artificial waterbody reservoirs, leading to similar results. While doing so, materials with lower radiation emittance must be selected in the outdoor spaces as MRT has the highest impact on PET. For the region of Hagonoy, it is better to allow wind flow by decreasing the height of vegetation. It should be in the South direction if it needs to be blocked. Also, since it is not possible to cover the land area with vegetation to such a capacity, it is important to look further into floating vegetation such as mangroves and willow trees. This may give scope for organic farming for the residents due to the limited population of the community.

The enclosure of gathering spots, vegetation, openness between buildings, and building height primarily affects thermal comfort and wind comfort. Enclosure causes a reduction in wind speeds. Openness improves the PET performance by reducing temperatures, and also does not cause the venturi effect in the wind. Whereas, vegetation may act as a natural barrier and reduces temperatures and PET during day-time and vice versa. Building height is more subject to wind draft and increases the wind speeds around the corners. Therefore, depending on the requirement of the designer, pertaining strategies must be adopted.

Even though the focus area in this project is a hot-tropical region, certain assumptions can be made about cold climates, such that air temperatures need to be increased. Therefore, higher radiance emittance materials must be selected. In case these areas are coupled with high wind velocities, vegetation with increased height must be provided in its respective direction.

Lower density with more open areas improved the PET and wind comfort levels. And vice versa also holds true. Due to limited land availability, a medium densely built environment with low building height is preferable for floating homes on wooden platforms. Even though not all the points were included in the study, it can be extrapolated that this is a better layout due to social housing standards, structural capacity, and thermal and wind comfort level index. More openness also leads to more possibilities for vegetation.

5.3 Outlook

- For future urban projects, it is preferable to use predictive weather forecast data for the expected year of construction. For example, the Horizon 1 of this project is expected to complete in the year 2023. However, the time frame for Horizon 3 is 2030. For this Horizon, the meteorological data should be extrapolated with predictive analysis tools for 2030, which will be further used in simulations. This is especially important because of the rising global warming situation.

- The outdoor microclimate affects the building energy demand at the micro-scale. This determines the cooling demand of the urban spaces. The lighting demand can be evaluated at the micro and macro scale. This data can be coupled with each other to create an empirical urban energy demand for the community, which can be used as an estimation to create self-sufficient energy grids. Renewable sources such as PV panels on floating platforms can be used for this purpose.

- Additional methods to reduce urban heat stress are: insulated metal sheets (used in this case), green roofs, green facades, sun-shading devices, high-reflective or light-colored pavements and platforms, and artificial or artificial water bodies.

5.4 Limitations

- ENVI-met cannot take non-planar surfaces as inputs. Therefore the sloping roofs were converted to box surfaces based on radiation analysis. Additionally, sun-shading surfaces had to be eliminated. Rhino3D software must be used to study the behavior of the sun-shading device on thermal comfort.

- The simulations are calculated for a 24-hour cycle period for 8th May 2020. In wind comfort criteria, exceedance is calculated based on 365 days. Therefore, a general assumption has been made, and raw wind speed data for 365 days from the EPW file was used. This is not an accurate representation of the ground reality.

- ENVI-met software cannot be used as an optimization tool to run different scenarios such as Octopus in Rhinoceros3D. Therefore, only limited options are available for trial, which can be used to analyze and extrapolate data. This is primarily because of heavy simulation time. To run multiple optimization tools simultaneously, it is preferable to use Rhino3D and Grasshopper software with their built-in plugins.

Bibliography

1 https:www.urban-hub.comauthordiana-kaehlerauthor. (2021, 19 maart). *Urban microclimates inspire change.* URBAN HUB. Geraadpleegd op 9 januari 2022, van https://www.urban-hub.com/energy_efficiency/rethinking-the-use-of-urban-microclimates/

[0] [1] Palme, M., and Salvati, A. (2021). *Urban Microclimate Modelling for Comfort and Energy Studies.* Springer Publishing.

[2] Santamouris, M. (2020). Recent progress on urban overheating and heat island research. Integrated assessment of the energy, environmental, vulnerability and health impact. Synergies with the global climate change. Energy and Buildings, 207, https://doi.org/10.1016/j.enbuild.2019.109482

[3] Ritchie, H. (2018, 13 juni). Urbanization. Our World in Data. Geraadpleegd op 9 januari 2022, van https://ourworldindata.org/urbanization

[4] World Energy Council (2016). World Energy Scenarios 2016 – The Grand Transition. London: World Energy Council.

[5] Giridharan, R. (2016). Urban climate modelling - challenges in tropics. In R. Emmanuel (Ed.), Urban climate challenges in the tropics: Rethinking the design basis and opportunities (pp. 255–299). London: Imperial College Press.

[6] Moonen, P., Defraeye, T., Dorer, V., Blocken, B., Carmeliet, J. (2012). Urban Physics: Effect of the micro-climate on comfort, health and energy demand. Frontiers of Architectural Research, 1(3), 197–228. https://doi.org/10.1016/j.foar.2012.05.002

[7] United Nations, 2010. Department of Economic and Social Affairs. Population Division. World Urbanisation Prospects. The 2009 Revision. CD-ROM.

[8] Bherwani, H., Singh, A., Kumar, R. (2020). Assessment methods of urban microclimate and its parameters: A critical review to take the research from lab to land. *Urban Climate,* 34, 100690. https://doi.org/10.1016/j.uclim.2020.100690

[9] "How is climate change affecting the Philippines?," Climate Reality, Jan. 19, 2016. https://www.climaterealityproject.org/blog/how-climate-change-affecting-philippines.

[10] World Economic Forum. (2020). The Global Risks. Report 2020

[11] "No easy solutions to growing PH housing backlog problem," The Manila Times, Sep. 13, 2020. https://www.manilatimes.net/2020/09/13/opinion/editorial/no-easy-solutions-to-growing-ph-housing-backlog-problem/767620/.

[12] Wingard, J., Brandlin, A. S. (2015, may). Philippines: A country prone to natural disasters. Retrieved from www.dw.de/philippines-a-country-prone-to-natrual-disasters/a-17217404

[13] Ham, P. H. (2016). The design of a modular, amphibious structure for a flood and typhoon- prone municipality: Haganoy, the Philippines. TU Delft Repository. Published. http://resolver.tudelft.nl/uuid:cd8fce02-5a6c-4d87-b52f-c820438b9684

[14] Santos, L. A. (2013, November). How to build disaster-resilient homes in the Philippines. Retrieved from deveex: www.devex.com/news/how-to-build-reselient-homes-in-the-philippines-82408

[15] Kendall, S. H. (1976). The barangay as community in the Philippines (Vol. 41, Issue 242). https://www.jstor.org/stable/43618621

[16] Jurado, A. E. (2021). Designing resilient coastal neighbourhoods. *TU Delft Repository.*

Published. http://resolver.tudelft.nl/uuid:33da889f-11f5-48bc-a494-0ecfa663bc4b

[17] De Waard, N. (2021). Development of a parametric PET assessment model for the early design stage and evaluation of building-related heat mitigation measures for extreme heat events in the Netherlands. *TU Delft Repository.* Published. http://resolver.tudelft.nl/uuid:6c5cdb1c-29cf-4ecc-a3a7-b11f595179bb

[18] Givoni, B. (1992). Climatic aspects of urban design in tropical regions. Atmospheric Environment. Part B. Urban Atmosphere, 26(3), 397–406. https://doi.org/10.1016/0957-1272(92)90015-k

[19] Moonen, P., Defraeye, T., Dorer, V., Blocken, B., and Carmeliet, J. (2012). Urban Physics: Effect of the micro-climate on comfort, health and energy demand. *Frontiers of Architectural Research*, 1(3), 197–228. https://doi.org/10.1016/j.foar.2012.05.002

[20] ISO. International Standard 7730. ISO Geneva, revised 1990; 1984.

[21] Ashare Standard 55-2017. Thermal Enviromentla Conditions for Human Occupancy; American Society of Heating, Refrigerating and Air-Conditioning Engineers: Atlanta, GA, USA, 2017

[22] Yoram Epstein and Daniel S. Moran. Thermal comfort and the heat stress indices. Industrial Health, 44(3):388–398, 2006

[23] *Heat production and Heat loss in Human Body.* BrainKart. https://www.brainkart.com/article/Heat-production-and-Heat-loss-in-Human-Body_2283/

[24] George Havenith. Heat balance when wearing protective clothing. Annals of Occupational Hygiene, 43(5):289–296, 1999.

[25] Spittka, R. (2019). *Passive design guidelines for Philippine housing based on the bahay kubo.* TU Delft Repository.

[26] Max Planck and Morton Masius. The theory of heat radiation. P. Blakiston's Son Co, 1914.

[27] Igor Luginbuehl, Bruno Bissonette, and Peter J. David. Thermoregulation: Physiology and Perioperative Disturbances. pages 157 – 178. 2011.

[28] Benoy, R. (2020). *Recommendations for Improvement of the Building Design by Evaluating the Indoor Environmental Quality of the Pilot Floating House Project in Macabebe, the Philippines.* TU Delft Repository.

[29] No¨el Djongyang, Ren´e Tchinda, and Donatien Njomo. Thermal comfort: A review paper. Renewable and Sustainable Energy Reviews, 14(9):2626–2640, 2010

[30] Auliciems, A., Szokolay, S. V. (1997). Thermal comfort. PLEA

[31] *Thermal Comfort Indices - Universal Thermal Climate Index, 1979–2020.* Climate-ADAPT. Geraadpleegd op 10 januari 2022

[32] Bröde, P., Fiala, D., Błażejczyk, K., Holmér, I., Jendritzky, G., Kampmann, B., Tinz, B., and Havenith, G. (2011). Deriving the operational procedure for the Universal Thermal Climate Index (UTCI). *International Journal of Biometeorology*, 56(3), 481–494. https://doi.org/10.1007/s00484-011-0454-1

[33] *What is UTCI?* The UTCI Story Hub. Geraadpleegd op 10 januari 2022, van https://utci.lobelia.earth/what-is-utci

[34] Andreas Matzarakis, Stefan Muthers, and Frank Rutz. Application and comparison of UTCI and pet in temperate climate conditions. Finisterra, 49(98):21–31, 2014

[35] Andreas Matzarakis, Helmut Mayer, and Moses G Iziomon. Applications of a universal thermal index: physiological equivalent temperature. International Journal of Biometeorology, 43:76–84, 1999.

[36] ANSI/ASHRAE Standard 55-2010

[37] Nisa'ul Khoir, A., Kurdiyan, Utaminingtyas, B., Safril, A. (2018). ANALYSIS OF CLIMATE THERMAL COMFORT USING PHYSIOLOGICALLY EQUIVALENT TEMPERATURE (PET) IN JAKARTA. *International Proceeding ASEAN YOUTH CONFERENCE 2018.* https://doi.org/10.5281/zenodo.2582313

[38] Bernard, T. E., Ramsey, J. D. (2020). Ergonomics Guidelines and Problem Solving. *Elsevier Ergonomics Book Series.*

[39] Silvia Coccolo, J´er^ome K¨ampf, Jean Louis Scartezzini, and David Pearlmut ter. Outdoor human comfort and thermal stress: A comprehensive review on models and standards. Urban Climate, 18:33–57, 2016

[40] Oke, T. (1976). The distinction between canopy and boundary-layer urban heat islands. *Atmosphere,* 14(4), 268–277. https://doi.org/10.1080/00046973.1976.9648422

[41] The British Geographer, 2015. Urban Climates. [Online] Available at: http://thebritishgeographer.weebly.com/urban-climates.html

[42] Natalie E. Theeuwes, Gert Jan Steeneveld, Reinder J. Ronda, and Albert A.M. Holtslag. A diagnostic equation for the daily maximum urban heat island effect for cities in northwestern Europe. *International Journal of Climatology,* 37(1):443–454, 2017.

[43] Edward Arens, Tyler Hoyt, Xin Zhou, Li Huang, Hui Zhang, and Stefano Schiavon. Modeling the comfort effects of short-wave solar radiation indoors. *Building and Environment,* 88:3–9, 2015.

[44] A.C. van der Linden, P. Erdtsieck, L. Kuijpers-van Gaalen, and A. Zeegers. *Building Physics.* Textbook. ThiemeMeulenhoff. 2013

[45] Broede, P.; Blazejczyk, K.; Fiala, D.; Havenith, G.; Holmer, I.; Jendritzky, G.; Kuklane, K.; Kampmann, B.The Universal Thermal Climate Index UTCI Compared to Ergonomics Standards for Assessing the Thermal Environment.Ind. Health2013,51, 16–24

[46] Mouffouk, A. (2020, 12 oktober). *Assessing Wind Comfort In Urban Areas With CFD.* SimScale. Geraadpleegd op 12 januari 2022, van https://www.simscale.com/blog/2017/11/wind-comfort-urban-areas-cfd/

[47] Reiter, S. (2010). Assessing Wind Comfort in Urban Planning. *Environment and Planning B: Planning and Design,* 37(5), 857–873. https://doi.org/10.1068/b35154

[48] Stathopoulos T, 2006, "Pedestrian level winds and outdoor human comfort" *Journal of wind engineering and industrial aerodynamics* 94 769-780.

[49] Fernando, H. J. S. (2010). Fluid dynamics of urban atmospheres in complex terrain. *Annual Review of Fluid Mechanics,* 42, 365–389

[50] Britter, R. E., Hanna, S. (2003). Flow and dispersion in urban areas. *Annual Review of Fluid Mechanics*, 35, 469–496.

[51] W.J. Beranek, H. Van Koten Beperken van windhinder om gebouwen, deel 1, Stichting Bouwresearch no. 65 Kluwer Technische Boeken BV, Deventer (1979) (in Dutch)

[52] Jenkins, M. (2021, 14 april). *Wind Comfort Criteria: Lawson, Davenport, and NEN 8100*. SimScale. Geraadpleegd op 12 januari 2022, van https://www.simscale.com/blog/2019/12/wind-comfort-criteria/

[53] Santamouris M, 1998 Natural Ventilation in Buildings: A design Handbook *(F.Allard Editor, London, UK)*

[54] Shetty, S. (2020, 9 juni). *Evaluate pedestrian wind comfort using globally recognized comfort criteria.* SimulationHub. Geraadpleegd op 12 januari 2022, van https://www.simulationhub.com/blog/evaluate-pedestrian-wind-comfort-using-global-comfort-criteria

[55] United Nations 2015 Sustainable Development Goals (SDG), Goal 11: Make cities inclusive, safe, resilient and sustainable.

[56] United Nations, Framework Convention on Climate Change, Initiatives in the Area of Human Settlements and Adaptation, https://unfccc.int/news/rapidurbanization-increases-climate-risk-for-billions-of-people, (2017).

[57] Natanian, J., Maiullari, D., Yezioro, A., Auer, T. (2019). Synergetic urban microclimate and energy simulation parametric workflow. *Journal of Physics: Conference Series, 1343*(1), 012006. https://doi.org/10.1088/1742-6596/1343/1/012006

[58] L.G. Swan, V.I. Ugursal, Modeling of end-use energy consumption in the residential sector: a review of modeling techniques, *Renew. Sustain. Energy Rev. 13 (2009) 1819–1835,* https://doi.org/10.1016/j.rser.2008.09.033.

[59] Santamouris, M., Papanikolaou, N., Livada, I., Koronakis, I., Georgakis, C., Argiriou, A. and Assimakopoulos, D.N. (2001) On the Impact of Urban Climate to the Energy Consumption of Buildings. *Solar Energy*, 70, 201-216. http://dx.doi.org/10.1016/S0038-092X(00)00095-5

[60] Mosteiro-Romero, M. (2020). *An Integrated Microclimate-Energy Demand Simulation Method for the Assessment of Urban Districts.* Frontiers. Geraadpleegd op 15 januari 2022, van https://www.frontiersin.org/articles/10.3389/fbuil.2020.553946/full

[61] Stewart, I. D., Oke, T. R. (2012). *Local climate zones for urban temperature studies.* Bulletin of the American Meteorological Society, 93(12), 1879–1900.

[62] *Ladybug Tools | Dragonfly*. Ladybug Tools. Geraadpleegd op 15 januari 2022, van https://www.ladybug.tools/dragonfly.html

[63] *Philippines Deforestation Rates Statistics* | GFW. Global Forest Watch. Geraadpleegd op 15 januari 2022, van https://www.globalforestwatch.org/

[64] Ahmed, A., Ossen, D., Jamei, E., Manaf, N., Said, I., and Ahmed, M. (2015). *Urban surface temperature behaviour and heat island effects in a tropical planned city.* Theoretical and Applied Climatology, 119, 493–514.

[65] Barisky T., Carter C., Crego-Liz, E. (2014). *Towards a Local Climate Change Action Plan in Hagonoy Bulacan Philippines. Policy briefing to Municipality of Hagonoy and Department of Local Governments Philippines*

[66] Liu, Y., and Harris, D. J. (2008). Effects of shelterbelt trees on reducing heating-energy consumption of office buildings in Scotland

[67] Martinelli, A., Kolokotsa, D., and Fiorito, F. (2020). *Urban heat island in mediterranean coastal cities: The case of Bari (Italy).* Climate (Basel), 8(6), 79. doi:10.3390/cli8060079

[68] Habib, C. (2021). *ASSESSING OUTDOOR THERMAL COMFORT IN A WATERFRONT DEVELOPMENT: THE CASE OF WATERFRONT CITY, DBAYEH*

[69] Manteghi, G., Limit, H. B., Remaz, D. (2015). Water Bodies an Urban Microclimate: A Review. *Modern Applied Science, 9(6).* https://doi.org/10.5539/mas.v9n6p1

[70] Chen, Z., Zhao, L., Meng, Q., Wang, C., Zhai, Y., Wang, F. (2009). Field measurements on microclimate in residential community in Guangzhou, China. Frontiers of Architecture and Civil Engineering in China, 3(4), 462-468.

[71] Murakawa, S., Sekine, T., Narita, K. i., Nishina, D. (1991). Study of the effects of a river on the thermal environment in an urban area. Energy and buildings, 16(3), 993-1001.

[72] Coutts, A. M., Tapper, N. J., Beringer, J., Loughnan, M., Demuzere, M. (2013). Watering our cities The capacity for Water Sensitive Urban Design to support urban cooling and improve human thermal comfort in the Australian context. Progress in Physical Geography, 37(1), 2-28.

[73] Nishimura, N., Nomura, T., Iyota, H., and Kimoto, S. (1998). Novel water facilities for creation of comfortable urban micrometeorology. Solar Energy, 64(4), 197-207.

[74] Robitu, M., Musy, M., Inard, C., and Groleau, D. (2006). Modeling the influence of vegetation and water pond on urban microclimate. Solar Energy, 80(4), 435-447

[75] Mostofa, T., Manteghi, (2020). G. INFLUENTIAL FACTORS OF WATER BODY TO ENHANCE THE URBAN COOLING ISLANDS (UCIs): A REVIEW. International Transaction Journal of Engineering, Management, Applied Sciences Technologies.

[76] *Thermodynamics: Albedo | National Snow and Ice Data Center.* National Snow and Ice Data Centre. Geraadpleegd op 16 januari 2022

[77] *The Energy Impact of Urban Form: An Approach to Morphologically Evaluating the Energy Performance of Neighborhood.* (2012). University of California, Berkely. https://escholarship.org/content/qt6zd36454/qt6zd36454_noSplash_15f9d4c4e6169f412f39c7ed7d8df6a8.pdf

[78] Bahgat, R., Reffat, R. M., Elkady, S. L. (2020). Analyzing the impact of design configurations of urban features on reducing solar radiation. *Journal of Building Engineering, 32*, 101664. https://doi.org/10.1016/j.jobe.2020.101664

[79] McGrath, B. M. (2021, 9 augustus). Climate change: IPCC report is *"code red for humanity".* BBC News. https://www.bbc.com/news/science-environment-58130705

[80] Palme M., Privitera R., La Rosa D. The shading effects of Green Infrastructure in private residential areas: Building Performance Simulation to support urban planning. Energy Build. 2020;229:110531. doi: 10.1016/j.enbuild.2020.110531.

[81] Li, J., Mao, Y., Ouyang, J., Zheng, S. (2022). A Review of Urban Microclimate Research Based on CiteSpace and VOSviewer Analysis. International Journal of Environmental Research and Public Health, 19(8), 4741. https://doi.org/10.3390/ijerph19084741

[82] Department of Earth Climate Sciences. Geraadpleegd op 31 augustus 2022, van https://tornado.sfsu.edu/geosciences/classes/m201/buoyancy/SkewTMastery/mesoprim/s

[83] Gagge, A., Stolwijk, J., and Nishi, Y. (1971): An effective temperature scale based on a simple model of human physiological regulatory response. ASHRAE Trans., 77(1):247–262.

[84] Höppe, P. (1984). Die Energiebilanz des Menschen: In: Münchener Universitätsschriften- Fachbereich Physik, Wissenschaftliche Mitteilungen Nr. 49. Meteorologisches Institut, Universität München, München.

[85] Höppe, P. (1999): The physiological equivalent temperature – a universal index for the biometeorological assessment of the thermal environment. - International Journal of Biometeorology 43, 71-75.

[86] Fröhlich, D., Matzarakis, A. (2020). Calculating human thermal comfort and thermal stress in the PALM model system 6.0. Geoscientific Model Development, 13(7), 3055–3065. https://doi.org/10.5194/gmd-13-3055-2020

[87] Zhang, X., Weerasuriya, A. U., Zhang, X., Tse, K. T., Lu, B., Li, C. Y., Liu, C. H. (2020). Pedestrian wind comfort near a super-tall building with various configurations in an urban-like setting. Building Simulation, 13(6), 1385–1408. https://doi.org/10.1007/s12273-020-0658-6

Appendix A

Appendix A

A.1 Philippines Climate Data

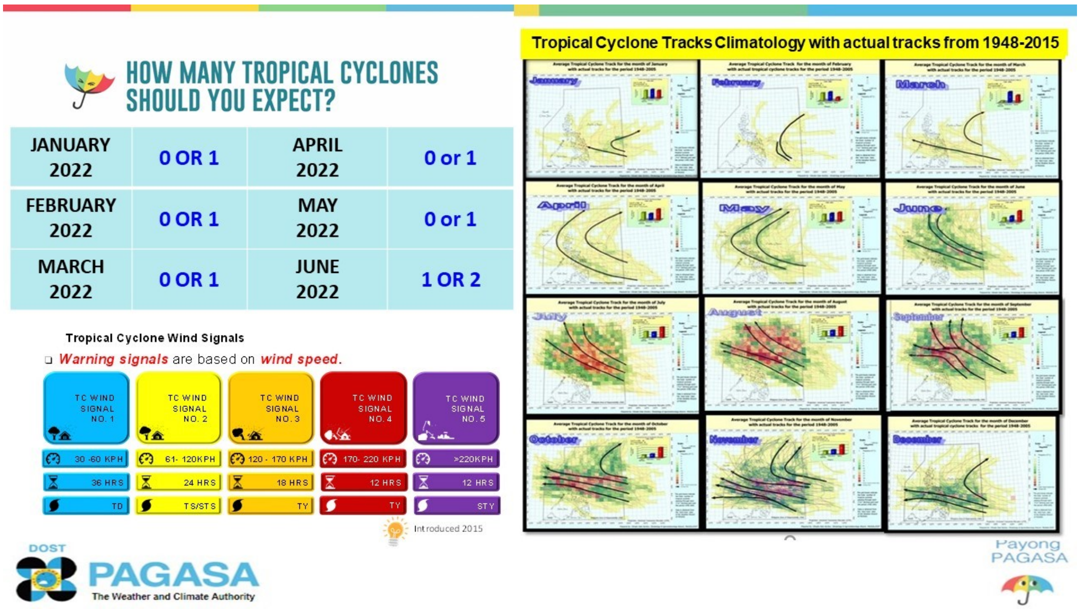

FIGURE A.1: Tropical cyclone tracks from 1948-2015 Philippines (Source:PAGASA)

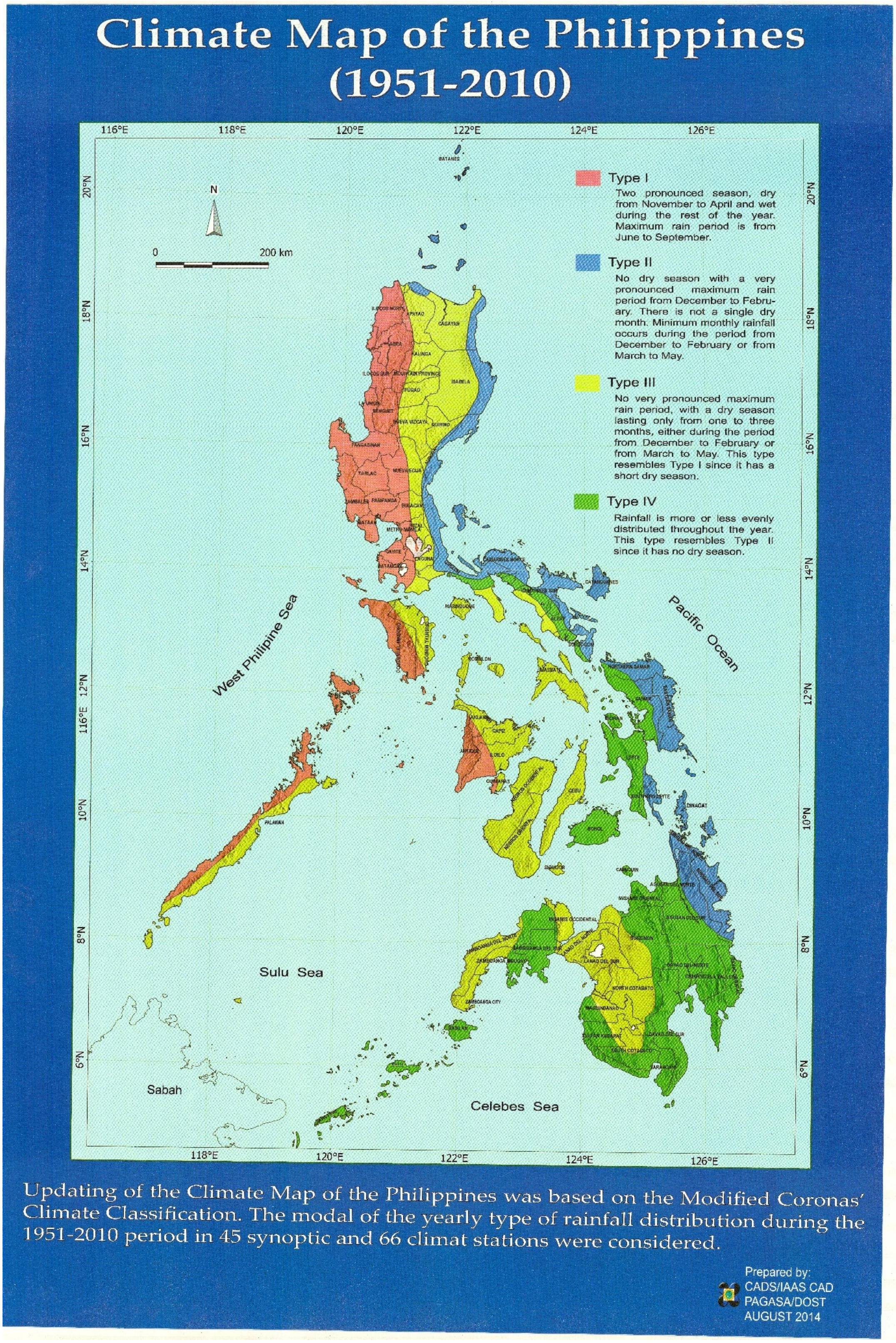

FIGURE A.2: Climate Map of the Philippines (Source: PAGASA

WEATHER DATA SUMMARY

LOCATION: MANILA, -, PHL
Latitude/Longitude: 14.52° North, 121.0° East, **Time Zone from Greenwich** 8
Data Source: IWEC Data 984290 WMO Station Number, **Elevation** 21 m

MONTHLY MEANS	JAN	FEB	MAR	APR	MAY	JUN	JUL	AUG	SEP	OCT	NOV	DEC	
Global Horiz Radiation (Avg Hourly)	310	364	433	446	420	359	342	354	324	326	314	283	Wh/sq.m
Direct Normal Radiation (Avg Hourly)	110	152	218	238	191	97	98	108	58	67	97	68	Wh/sq.m
Diffuse Radiation (Avg Hourly)	235	253	266	258	264	282	265	271	278	277	248	240	Wh/sq.m
Global Horiz Radiation (Max Hourly)	773	837	941	974	967	846	889	778	796	759	804	601	Wh/sq.m
Direct Normal Radiation (Max Hourly)	637	637	741	796	695	565	578	523	483	442	597	389	Wh/sq.m
Diffuse Radiation (Max Hourly)	473	546	576	584	578	576	569	579	580	535	481	451	Wh/sq.m
Global Horiz Radiation (Avg Daily Total)	3486	4188	5174	5508	5325	4611	4377	4411	3926	3800	3562	3161	Wh/sq.m
Direct Normal Radiation (Avg Daily Total)	1238	1752	2602	2947	2417	1251	1255	1350	708	790	1106	767	Wh/sq.m
Diffuse Radiation (Avg Daily Total)	2646	2923	3175	3191	3350	3626	3383	3383	3366	3238	2811	2688	Wh/sq.m
Global Horiz Illumination (Avg Hourly)	34759	40736	48511	50423	47439	40813	38892	40018	36887	36923	35536	31933	lux
Direct Normal Illumination (Avg Hourly)	9322	12980	18932	19845	16086	7796	7964	8543	4797	5500	7648	5704	lux
Dry Bulb Temperature (Avg Monthly)	25	26	27	29	29	28	27	27	27	27	27	26	degrees C
Dew Point Temperature (Avg Monthly)	21	20	21	23	23	24	23	23	23	23	24	21	degrees C
Relative Humidity (Avg Monthly)	75	72	69	73	71	79	80	81	79	80	84	77	percent
Wind Direction (Monthly Mode)	90	110	80	90	90	270	250	260	100	270	90	90	degrees
Wind Speed (Avg Monthly)	4	3	5	4	5	3	2	2	2	3	3	3	m/s
Ground Temperature (Avg Monthly of 3 Depths)	26	25	26	26	27	27	27	28	28	28	27	26	degrees C

FIGURE A.3: Weather Data Summary of Manila region

ASHRAE Standard 55, current Handbook of Fundamentals Comfort Model (select Help for definitions)

1. COMFORT: (using ASHRAE Standard 55)

1.0	Winter Clothing Indoors (1.0 Clo=long pants,sweater)
0.5	Summer Clothing Indoors (.5 Clo=shorts,light top)
1.1	Activity Level Daytime (1.1 Met=sitting,reading)
90.0	Predicted Percent of People Satisfied (100 - PPD)
20.3	Comfort Lowest Winter Temp calculated by PMV model(ET* C)
24.3	Comfort Highest Winter Temp calculated by PMV model(ET* C)
26.7	Comfort Highest Summer Temp calculated by PMV model(ET* C)
84.6	Maximum Humidity calculated by PMV model (%)

2. SUN SHADING ZONE: (Defaults to Comfort Low)

23.8	Min. Dry Bulb Temperature when Need for Shading Begins (°C)
315.5	Min. Global Horiz. Radiation when Need for Shading Begins (Wh/sq.m)

3. HIGH THERMAL MASS ZONE:

8.3	Max. Outdoor Temperature Difference above Comfort High (°C)
1.7	Min. Nighttime Temperature Difference below Comfort High (°C)

4. HIGH THERMAL MASS WITH NIGHT FLUSHING ZONE:

16.7	Max. Outdoor Temperature Difference above Comfort High (°C)
1.7	Min. Nighttime Temperature Difference below Comfort High (°C)

5. DIRECT EVAPORATIVE COOLING ZONE: (Defined by Comfort Zone)

20.0	Max. Wet Bulb set by Max. Comfort Zone Wet Bulb (°C)
6.6	Min. Wet Bulb set by Min. Comfort Zone Wet Bulb (°C)

6. TWO-STAGE EVAPORATIVE COOLING ZONE:

50.0	% Efficiency of Indirect Stage

7. NATURAL VENTILATION COOLING ZONE:

2.0	Terrain Category to modify Wind Speed (2=suburban)
0.2	Min. Indoor Velocity to Effect Indoor Comfort (m/s)
1.5	Max. Comfortable Velocity (per ASHRAE Std. 55) (m/s)

8. FAN-FORCED VENTILATION COOLING ZONE:

0.8	Max. Mechanical Ventilation Velocity (m/s)
3.0	Max. Perceived Temperature Reduction (°C)
	(Min Vel, Max RH, Max WB match Natural Ventilation)

9. INTERNAL HEAT GAIN ZONE (lights, people, equipment):

12.8	Balance Point Temperature below which Heating is Needed (°C)

10. PASSIVE SOLAR DIRECT GAIN LOW MASS ZONE:

157.7	Min. South Window Radiation for 5.56°C Temperature Rise (Wh/sq.m)
3.0	Thermal Time Lag for Low Mass Buildings (hours)

11. PASSIVE SOLAR DIRECT GAIN HIGH MASS ZONE:

157.7	Min. South Window Radiation for 5.56°C Temperature Rise (Wh/sq.m)
12.0	Thermal Time Lag for High Mass Buildings (hours)

12. WIND PROTECTION OF OUTDOOR SPACES:

8.5	Velocity above which Wind Protection is Desirable (m/s)
11.1	Dry Bulb Temperature Above or Below Comfort Zone (°C)

13. HUMIDIFICATION ZONE: (defined by and below Comfort Zone)

14. DEHUMIDIFICATION ZONE: (defined by and above Comfort Zone)

FIGURE A.4: ASHRAE Standard 55, current Handbook of Fundamentals Comfort Model

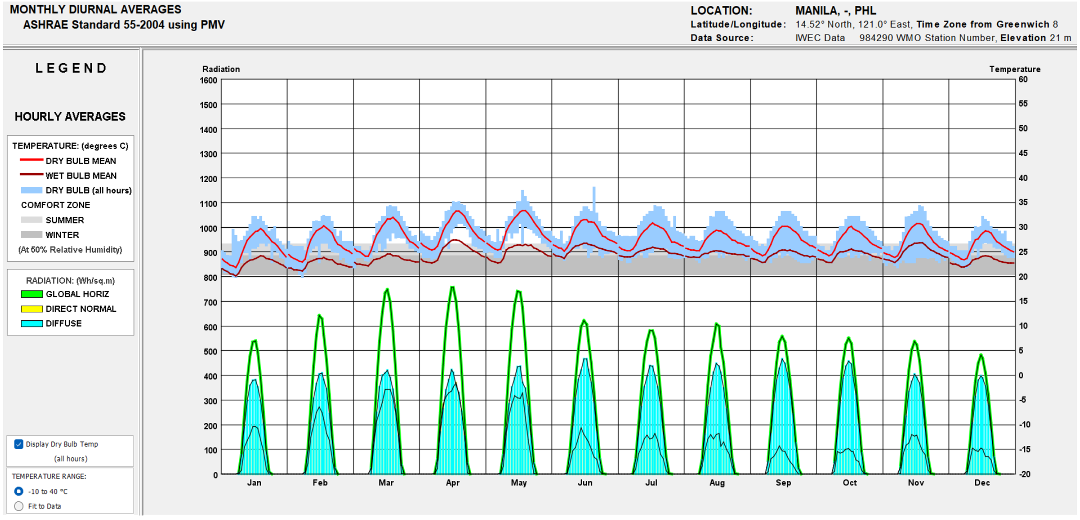

FIGURE A.5: Monthly Diurnal Averages of Manila region

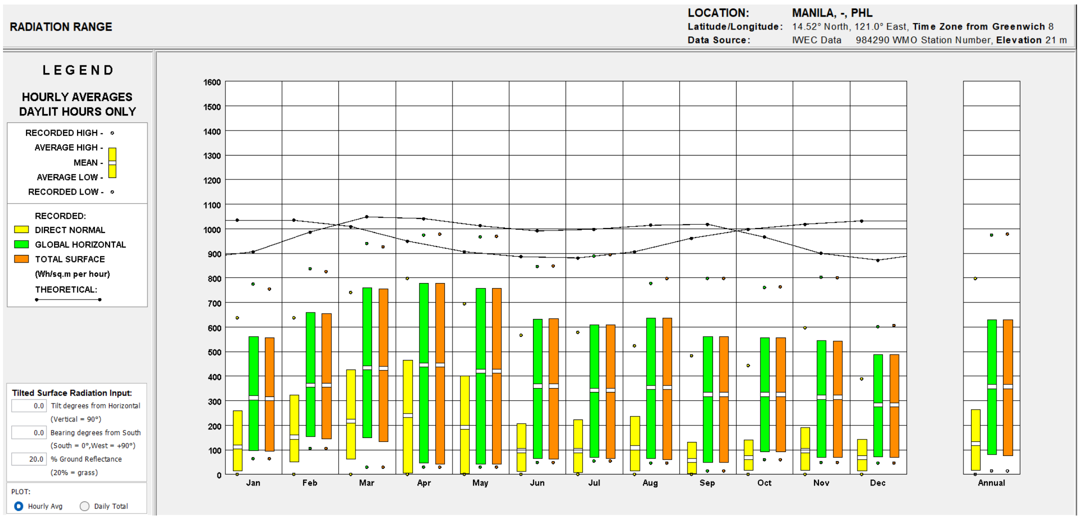

FIGURE A.6: Radiation Range of Manila region

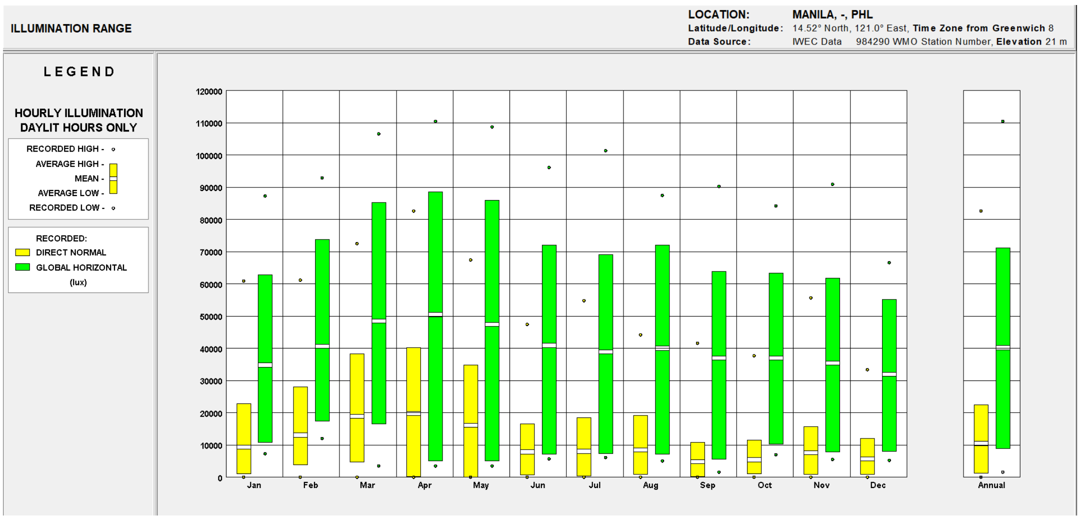

FIGURE A.7: Illumination Range of Manila region

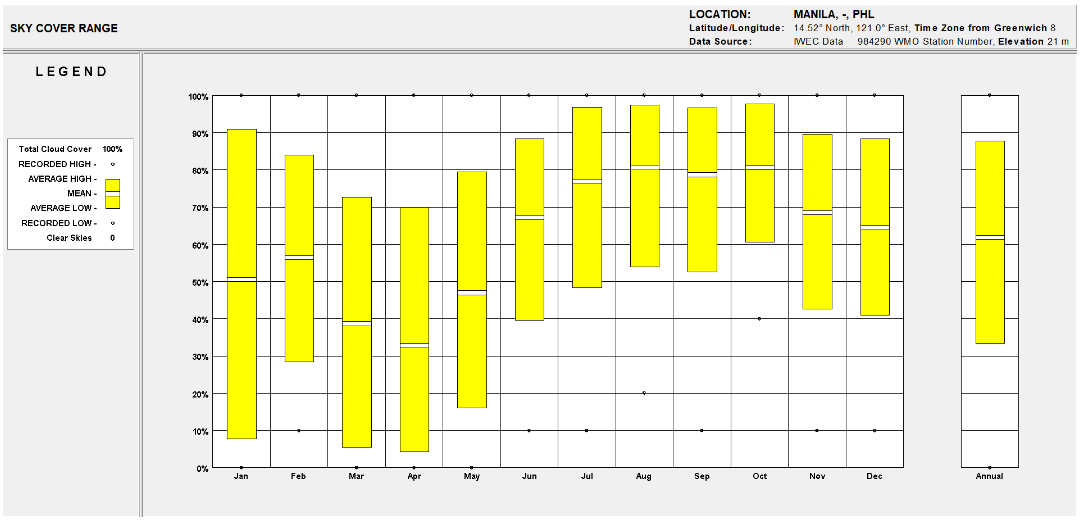

FIGURE A.8: Sky Cover Range of Manila region

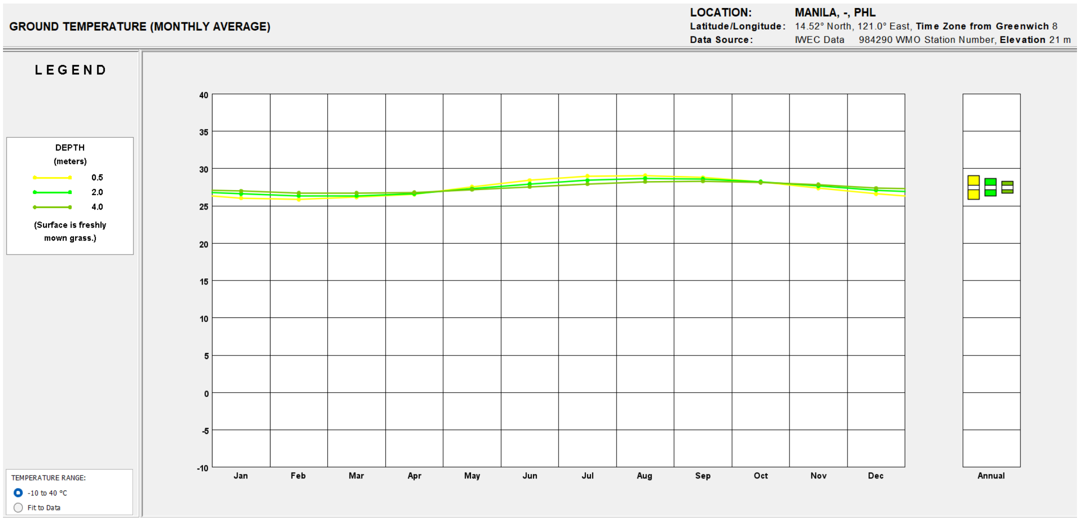

FIGURE A.9: Ground temperature (Monthly Average) of Manila region

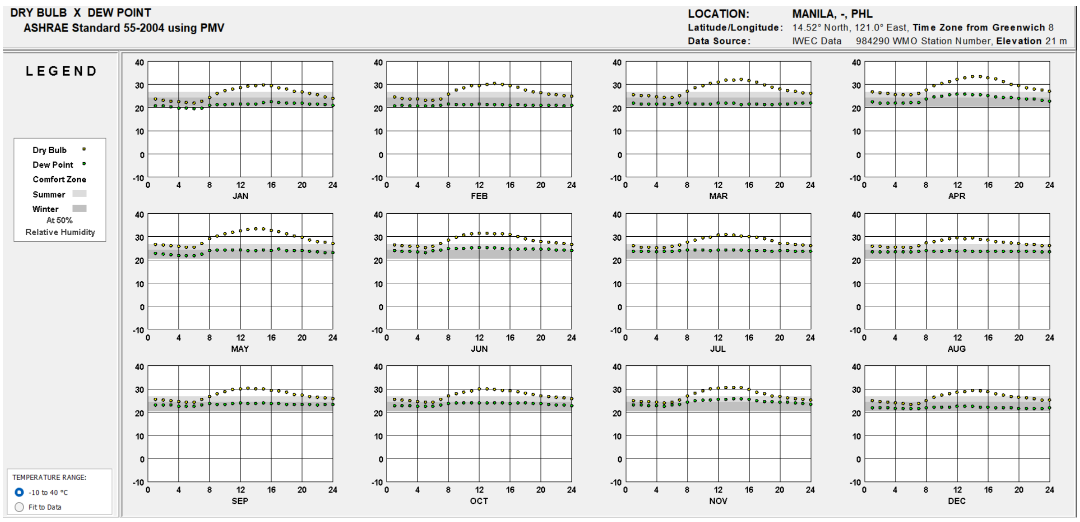

FIGURE A.10: Dry Bulb x Dew Point of Manila region

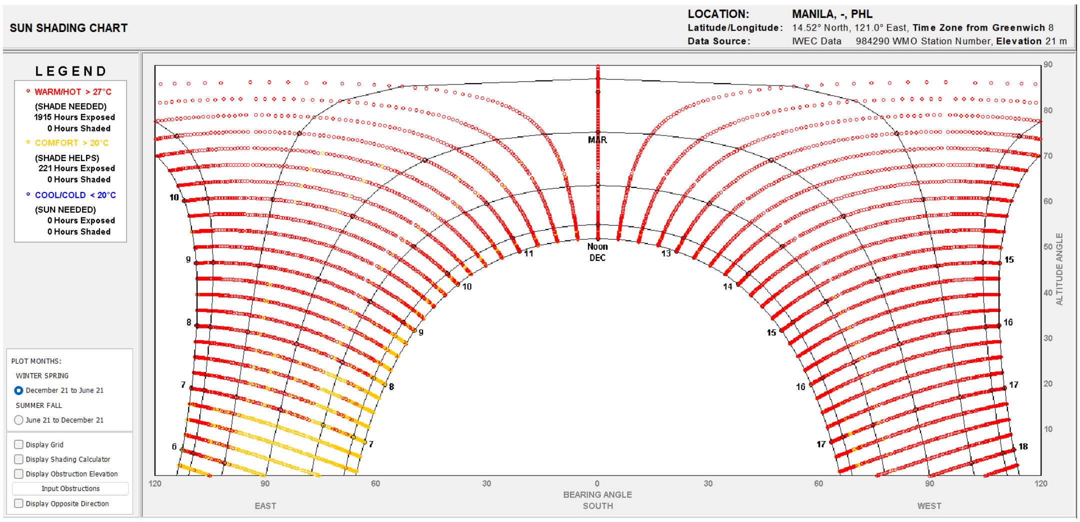

FIGURE A.11: Sun shading chart of Manila region

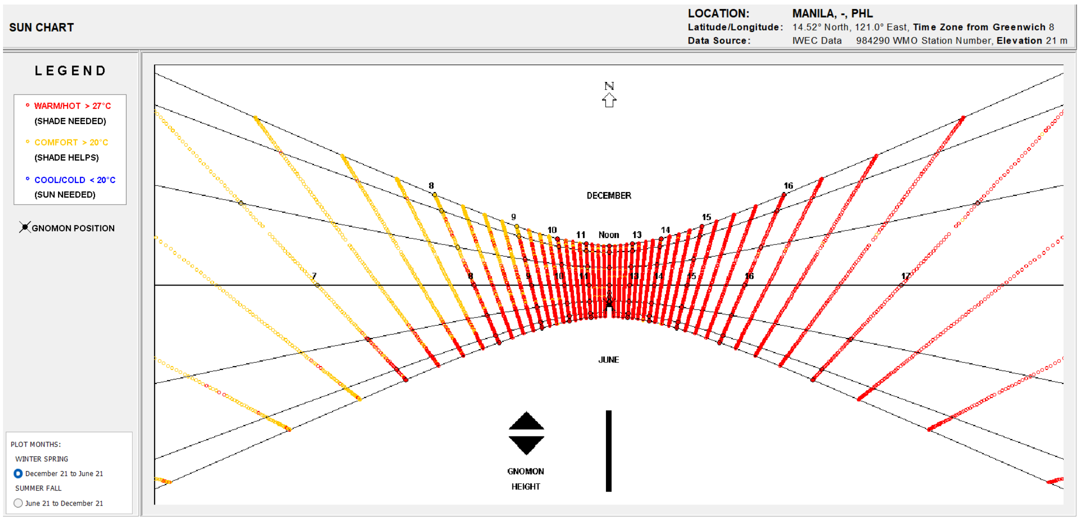

FIGURE A.12: Sun chart of Manila region

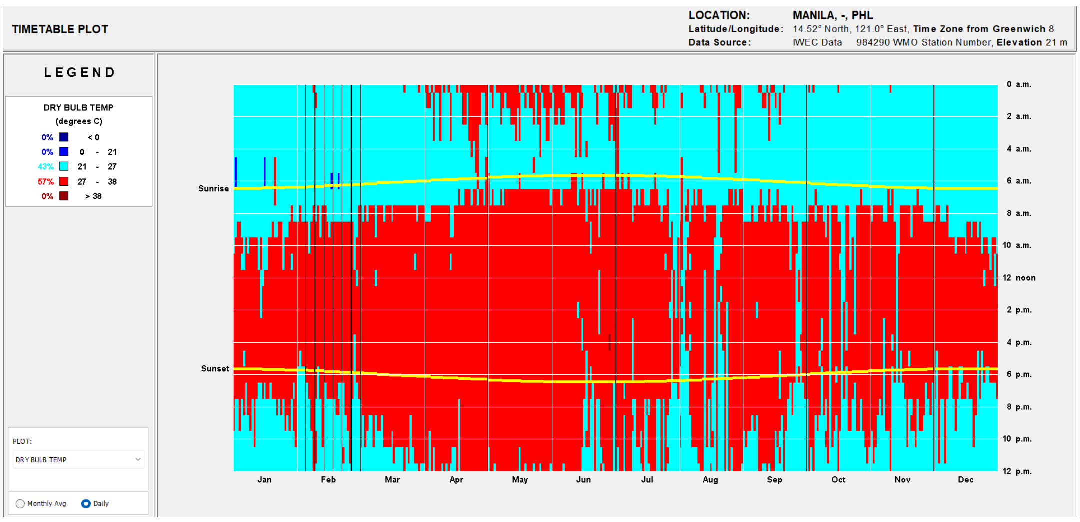

FIGURE A.13: Timetable plot of Manila region

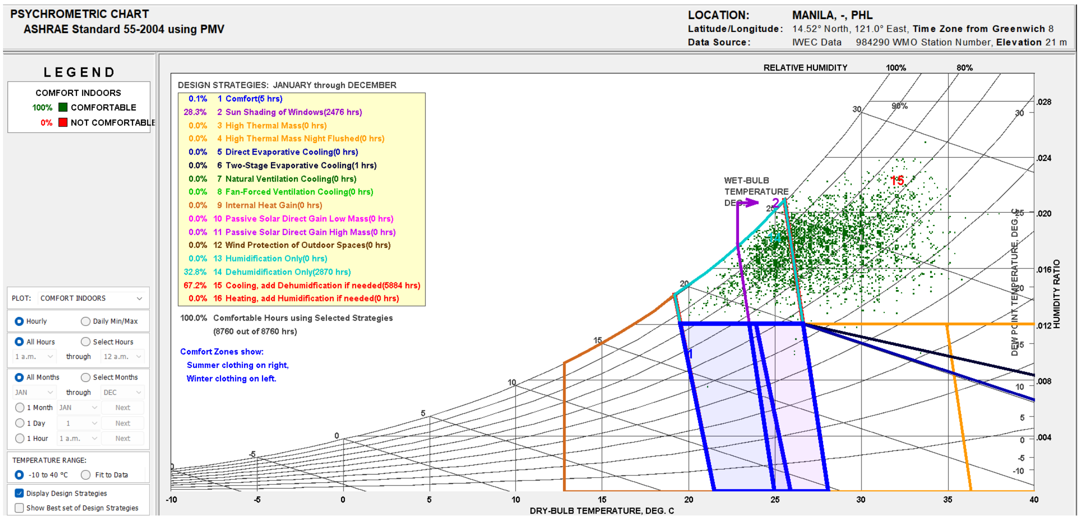

FIGURE A.14: Psychometric chart of Manila region

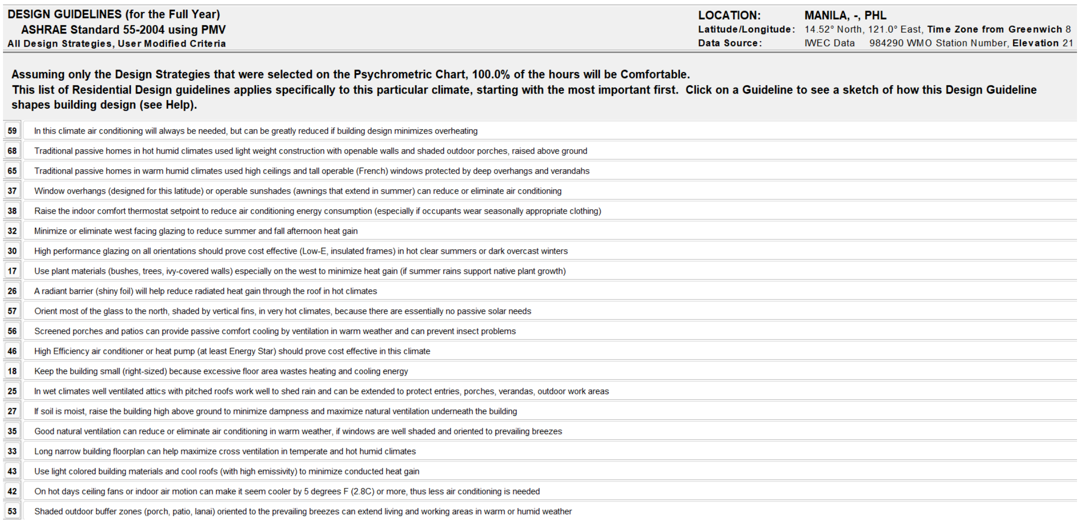

FIGURE A.15: Design guidelines as per ASHRAE guidelines for Manila region

Appendix B

Appendix B

B.1 Thermal comfort

B.1.1 Point 1

TABLE B.1: Thermal comfort parameters for Point 1 for all time stamps

POINT 1		Potential air temperature (deg cel)	Wind speed (m/s)	MRT (deg cel)	RH (percent)
0200 hrs	O1	25.2	1.4	14.7	88
	O2	25.2	1.5	15	88
	O3	25.4	1.5	16.1	87.8
	U1	25.2	1.3	14.5	88
	U2V	25.2	1.2	14.3	87
	U3V	25.2	1.2	14.3	87.6
0800 hrs	O1	28.5	0.2	37	78.5
	O2	27.8	1	37	79
	O3	28.6	0.8	43	77.3
	U1	27.8	0.9	36.6	79
	U2V	28	0.8	35.4	77.2
	U3V	28.1	0.8	37	76.6
1400 hrs	O1	33.3	1.5	42	55.5
	O2	33.8	1.6	43	52
	O3	37.2	1.3	60	44.3
	U1	33.1	1.3	42.3	53.8
	U2V	33.7	1.3	42	54
	U3V	34.1	1.2	41	51.3
	U2	33.5	1.4	40.6	55
	U3	34.3	1.4	42	60
1900 hrs	O1	28.4	6.2	19.4	73
	O2	28.7	5.8	19.5	73
	O3	29.7	6.2	22.3	70
	U1	28.5	5.8	19.5	73.1
	U2V	28.6	5.1	19.5	70.7
	U3V	28.7	4.3	19.5	70.6

TABLE B.2: PET thermal comfort index for Point 1 for all time stamps

POINT 1		**PET (deg cel)**	**PET (change from O1)) (deg cel)**
0200 hrs	O1	18.5	
	O2	18.7	-0.2
	O3	19	-0.5
	U1	18.5	0
	U2V	18.8	-0.3
	U3V	18.8	-0.3
0800 hrs	O1	32.2	
	O2	29.4	2.8
	O3	33.9	-1.7
	U1	29.7	2.5
	U2V	29.5	2.7
	U3V	29.2	3
1400 hrs	O1	36	
	O2	33.6	2.4
	O3	48.6	-12.6
	U1	36	0
	U2V	37.2	-1.2
	U3V	37.6	-1.6
	U2	35.2	0.8
	U3	32.9	3.1
1900 hrs	O1	21.2	
	O2	21	0.2
	O3	22.7	-1.5
	U1	21	0.2
	U2V	21.8	-0.6
	U3V	21.6	-0.4

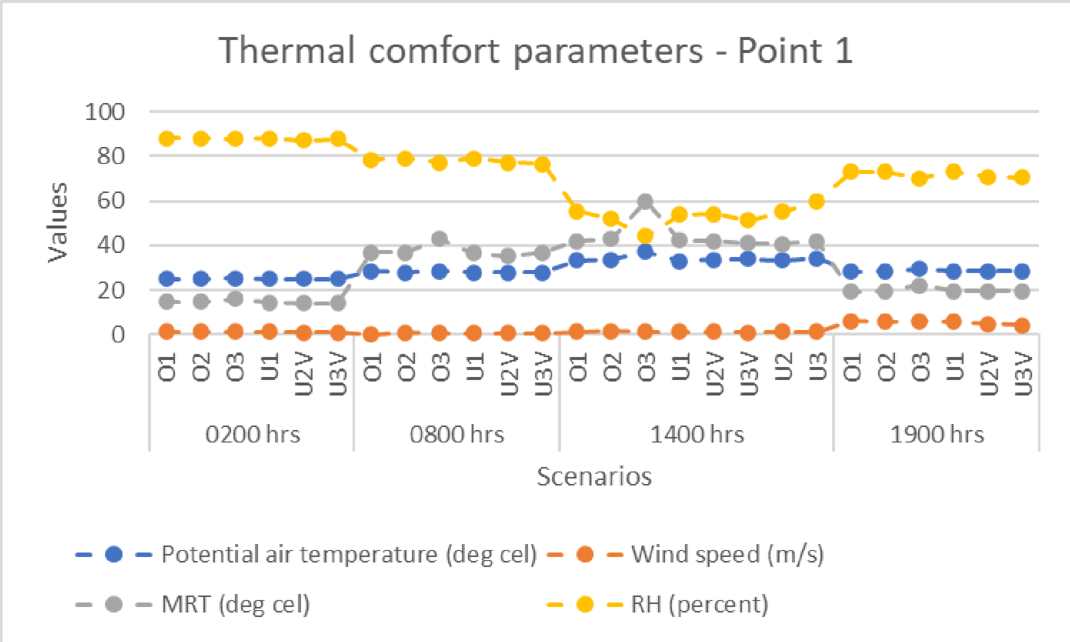

FIGURE B.1: Thermal comfort parameters for Point 1 for all time stamps

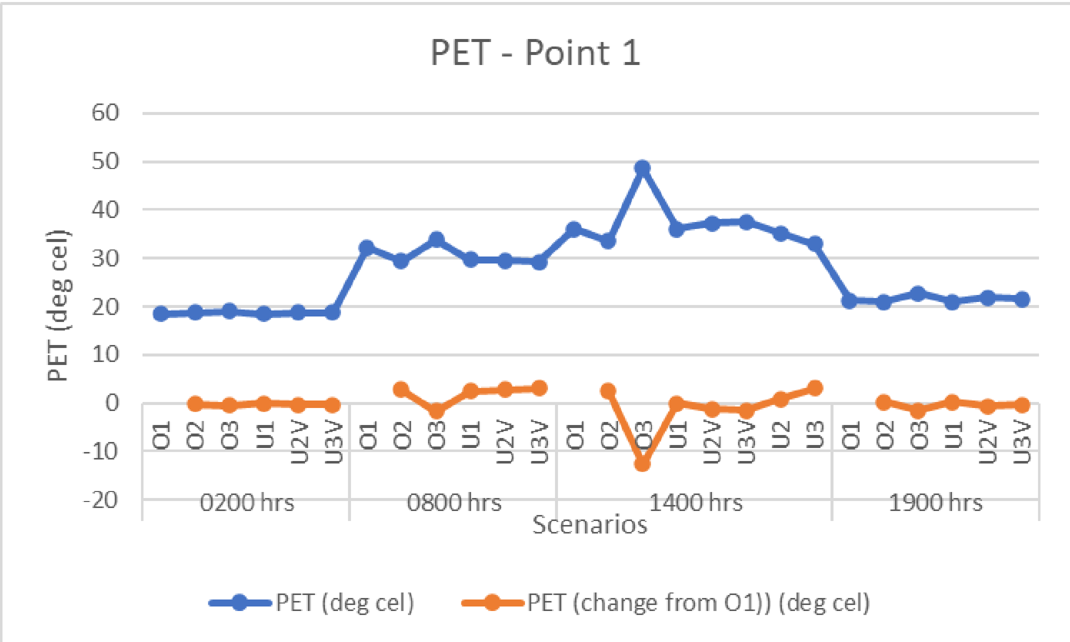

FIGURE B.2: PET for Point 1 for all time stamps

B.1.2 Point 2

TABLE B.3: Thermal comfort parameters for Point 2 for all time stamps

POINT 2		Potential air temperature (deg cel)	Wind speed (m/s)	MRT (deg cel)	RH (percent)
0200 hrs	O1	25.1	1.4	14.7	86.6
	O2	25.2	1.3	15.4	86.1
	O3	25.3	1.4	16.4	86.3
	U1	25.3	1.1	25	85.6
	U2V	25.6	1	23.8	81.7
	U3V	25.6	1	25.4	83.7
0800 hrs	O1	28.6	0.2	36.3	77.4
	O2	27.9	0.8	36	78.1
	O3	28.6	1.1	43	77
	U1	28.2	0.3	27.8	78.7
	U2V	28.4	0.1	23.8	77.8
	U3V	28.5	0.3	26	77.8
1400 hrs	O1	33.4	1.9	42.3	55
	O2	34.6	1.7	42	52
	O3	37	1.8	60	45
	U1	33.4	0.6	36.8	53.8
	U2V	33.7	0.4	31.6	55
	U3V	34.4	0.4	31.8	52
	U2	34	1.6	41	55
	U3	35	1.5	41	44.5
1900 hrs	O1	28.8	6.2	19.4	74
	O2	28.8	4.6	21	73
	O3	29.7	6	22.3	70.5
	U1	28.8	2.9	29.4	72.8
	U2V	29	2	26.9	70.7
	U3V	29	1.6	26	70.6

TABLE B.4: PET thermal comfort index for Point 2 for all time stamps

POINT 2		PET (deg cel)	PET (change from O1)) (deg cel)
0200 hrs	O1	18.5	
	O2	18.8	-0.3
	O3	19	-0.5
	U1	22.2	-3.7
	U2V	21.8	-3.3
	U3V	21.7	-3.2
0800 hrs	O1	32.4	
	O2	29.6	2.8
	O3	33.9	-1.5
	U1	27.6	4.8
	U2V	28.5	3.9
	U3V	28.2	4.2
1400 hrs	O1	36.4	
	O2	36.6	-0.2
	O3	47.5	-11.1
	U1	34.2	2.2
	U2V	32.1	4.3
	U3V	33	3.4
	U2	35.2	1.2
	U3	38	-1.6
1900 hrs	O1	21.1	
	O2	21.7	-0.6
	O3	22.7	-1.6
	U1	24.5	-3.4
	U2V	25.8	-4.7
	U3V	26.6	-5.5

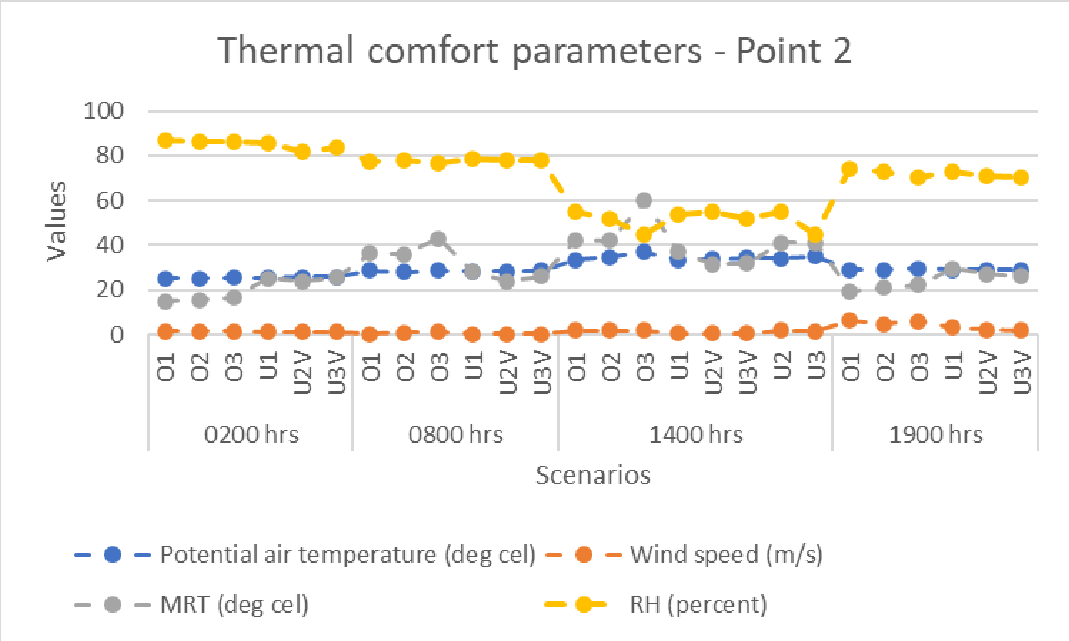

FIGURE B.3: Thermal comfort parameters for Point 2 for all time stamps

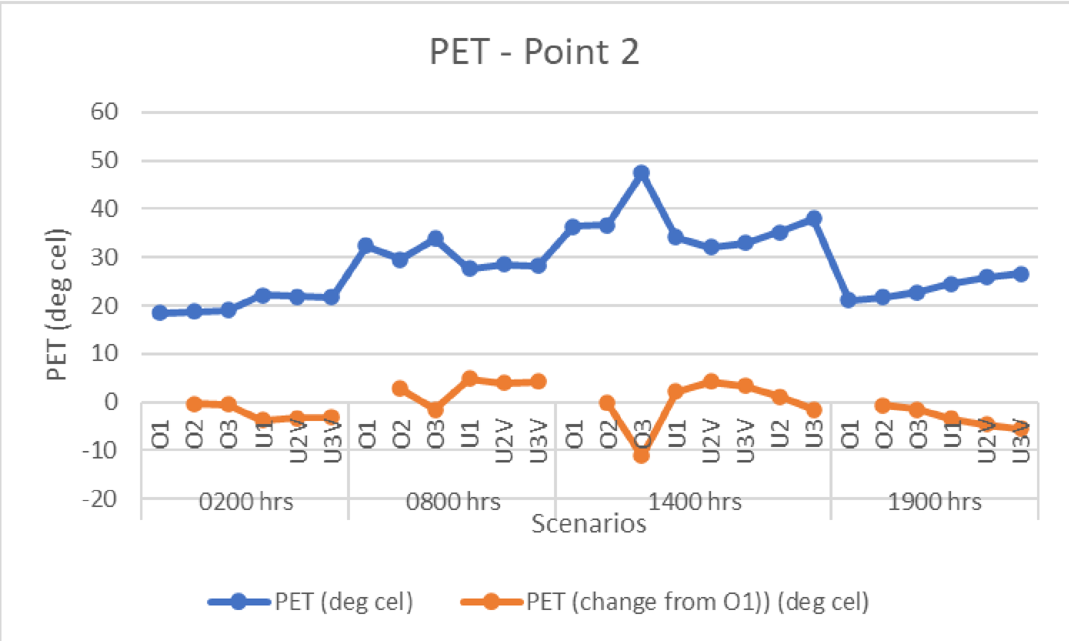

FIGURE B.4: PET for Point 2 for all time stamps

B.1.3 Point 3

TABLE B.5: Thermal comfort parameters for Point 3 for all time stamps

POINT 3		Potential air temperature (deg cel)	Wind speed (m/s)	MRT (deg cel)	RH (percent)
0200 hrs	O1	25	1.3	15.1	86.2
	O2	25	1.5	15	86.1
	O3	25.3	1.4	16.4	85.8
	U1	25.3	1.3	14.5	86
	U2V	25.2	1	14.3	83.8
	U3V	25	1.3	14.3	83.2
0800 hrs	O1	28.6	0.6	36	77.4
	O2	27.8	1.2	36	78.4
	O3	28.7	1.1	43	76.6
	U1	27.8	1.2	34.8	78.7
	U2V	28	0.8	35.4	77.2
	U3V	28.1	1.4	41	48.6
1400 hrs	O1	33.8	1.8	42	55
	O2	34.1	1.9	43	52
	O3	36.9	1.8	59.4	45
	U1	33.4	1.9	42.3	53.8
	U2V	33.7	1.8	31.6	54.3
	U3V	35	1.4	41	48.6
	U2	33.5	1.7	41	55
	U3	34.3	1.5	41.9	44.5
1900 hrs	O1	28.5	6	19.4	73.8
	O2	28.7	6	19.5	73.6
	O3	29.6	6	22.3	71
	U1	28.7	6	19.5	73.8
	U2V	28.6	5.1	19.5	72.2
	U3V	28.7	4	19.5	72

TABLE B.6: PET thermal comfort index for Point 3 for all time stamps

POINT 3		PET (deg cel)	PET (change from O1)) (deg cel)
0200 hrs	O1	18.5	
	O2	18.5	0
	O3	19	-0.5
	U1	18.5	0
	U2V	18.8	-0.3
	U3V	18.8	-0.3
0800 hrs	O1	31.6	
	O2	28.2	3.4
	O3	33.2	-1.6
	U1	28.7	2.9
	U2V	29.5	2.1
	U3V	28.8	2.8
1400 hrs	O1	36.4	
	O2	33.6	2.8
	O3	47.5	-11.1
	U1	36.7	-0.3
	U2V	36.1	0.3
	U3V	38.3	-1.9
	U2	35.2	1.2
	U3	32.9	3.5
1900 hrs	O1	21.1	
	O2	21	0.1
	O3	22.7	-1.6
	U1	21	0.1
	U2V	21.8	-0.7
	U3V	21.6	-0.5

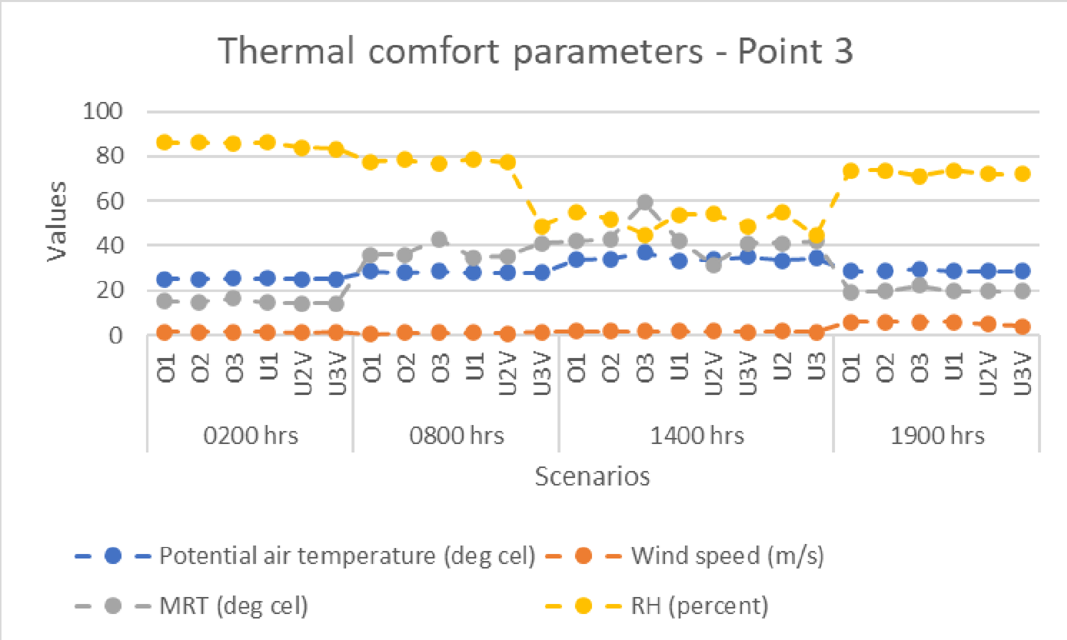

FIGURE B.5: Thermal comfort parameters for Point 3 for all time stamps

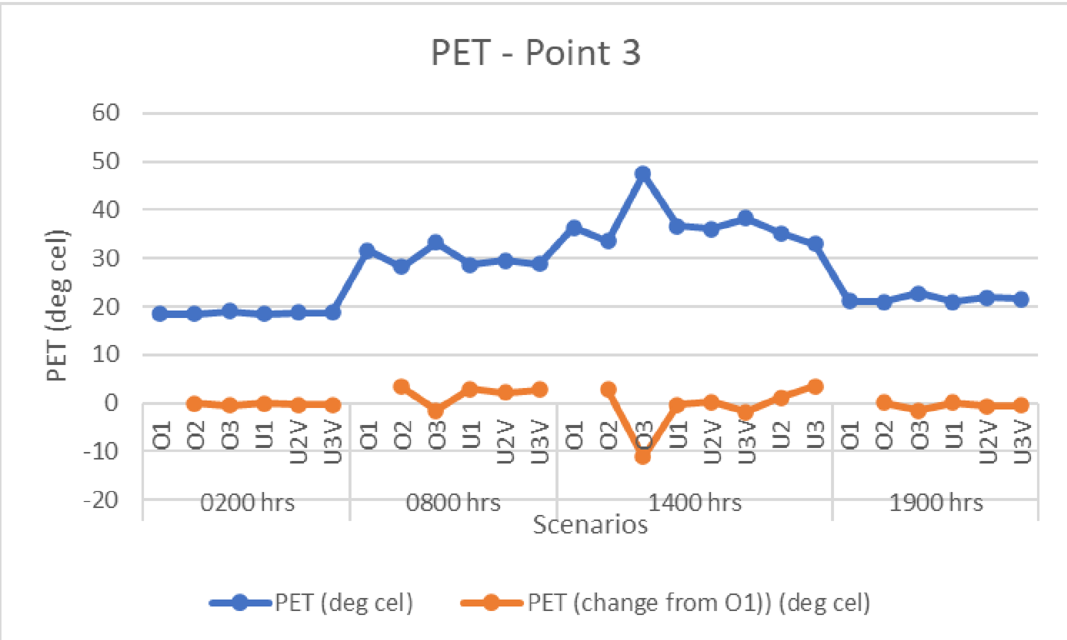

FIGURE B.6: PET for Point 3 for all time stamps

B.1.4 Point 4

TABLE B.7: Thermal comfort parameters for Point 4 for all time stamps

POINT 4		Potential air temperature (deg cel)	Wind speed (m/s)	MRT (deg cel)	RH (percent)
0200 hrs	O1	25	1.4	14.7	85.8
	O2	25	1.4	15	85.6
	O3	25.2	1.4	16.1	85.5
	U1	25.1	1.1	25	84.7
	U2V	25.4	1	24.8	81.7
	U3V	25.2	1.2	14.3	83.7
0800 hrs	O1	28.5	0.5	36.3	77.4
	O2	28.1	0.9	37	78.4
	O3	28.6	0.9	43	77
	U1	28.5	0.3	27.8	78
	U2V	28.6	0.1	23.8	77.2
	U3V	28.4	0.7	35	76.6
1400 hrs	O1	34.3	1.8	42.3	55
	O2	34.3	1.9	43	52
	O3	36.8	1.8	60	47
	U1	34.3	0.8	36.8	53
	U2V	34.1	0.6	31.6	55
	U3V	35.2	1.6	41	48.6
	U2	34.8	1.7	41	55
	U3	34.1	1.6	41	48
1900 hrs	O1	28.6	6.2	19.4	74
	O2	28.8	6	19.5	73.6
	O3	29.6	6	22.3	71.3
	U1	28.9	3	29.4	73.4
	U2V	29	2	26.9	72.8
	U3V	28.9	5.2	19.5	73

TABLE B.8: PET thermal comfort index for Point 4 for all time stamps

POINT 4		PET (deg cel)	PET (change from O1)) (deg cel)
0200 hrs	O1	18.5	
	O2	18.5	0
	O3	19	0
	U1	22.2	-0.5
	U2V	21.8	-3.7
	U3V	18.3	-3.3
0800 hrs	O1	31.6	
	O2	29.5	2.1
	O3	33.9	-2.3
	U1	27.6	4
	U2V	28.5	3.1
	U3V	29.9	1.7
1400 hrs	O1	37.3	
	O2	36.6	0.7
	O3	47.5	-10.2
	U1	34.2	3.1
	U2V	32.1	5.2
	U3V	36	1.3
	U2	37	0.3
	U3	32.9	4.4
1900 hrs	O1	21.4	
	O2	21.4	0
	O3	22.7	-1.3
	U1	24.5	-3.1
	U2V	25.8	-4.4
	U3V	21.3	0.1

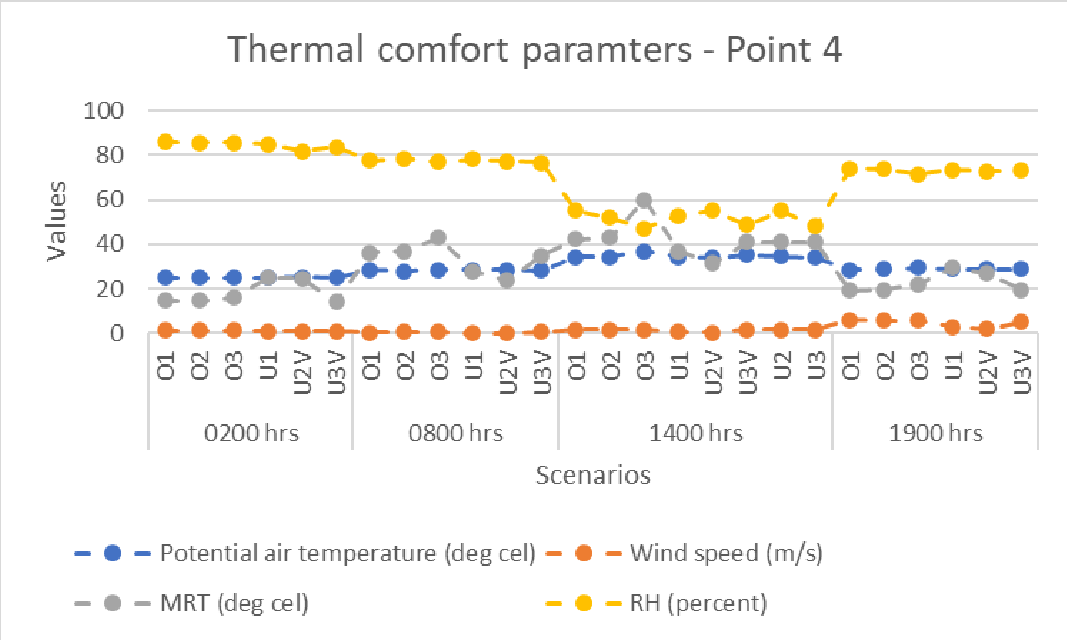

FIGURE B.7: Thermal comfort parameters for Point 4 for all time stamps

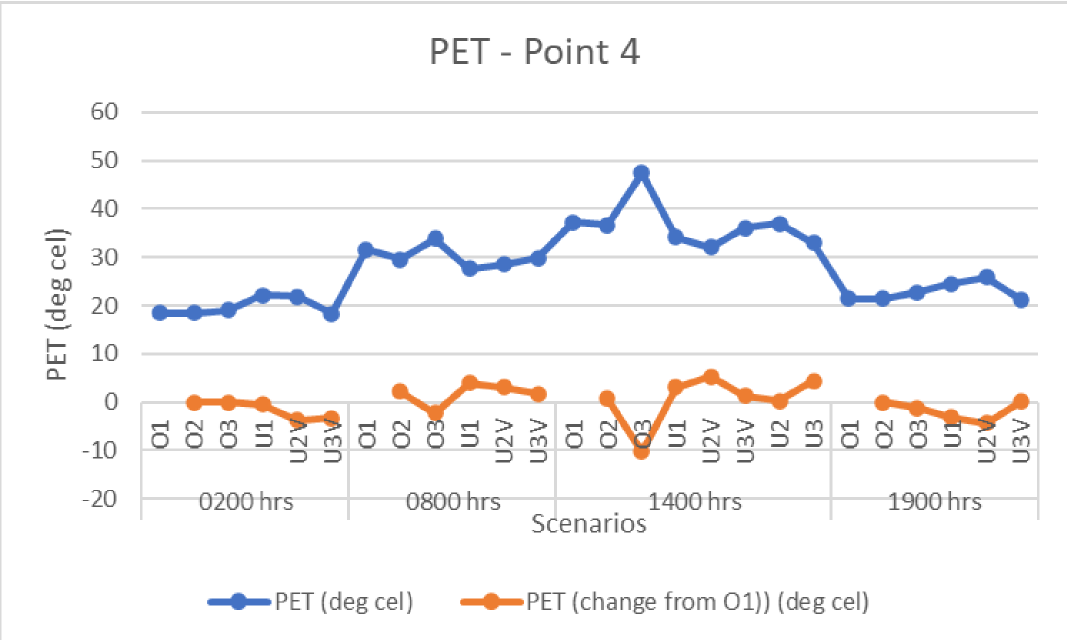

FIGURE B.8: PET for Point 4 for all time stamps

B.2 Wind comfort

B.2.1 Calm climate

Calm climate wind comfort criteria as per [88].

Table B.9: Calm climate wind comfort criteria

Class	Velocity (m/s)	Exceedance (percent) criteria	Scenario	No. of hours wind speed>threshold	Exceedance (percent)
Unfavorable	<1.5	50	O	2400	53.1
			U2V	380	34
Acceptable	>1.8	<5	O	965	52.4
			U2V	53	30
	>3.6	2	O	965	27.6
			U2V	53	4.5
	>5.3	2	O	965	18.3
			U2V	53	1.2
Intolerable	>7.6	2	O	135	4.3
			U2V	0	0.08
Danger	>15	0.05	O	7	0.08
			U2V	0	0